

O₂ Activation by Metal Surfaces: Implications for Bonding and Reactivity on Heterogeneous Catalysts

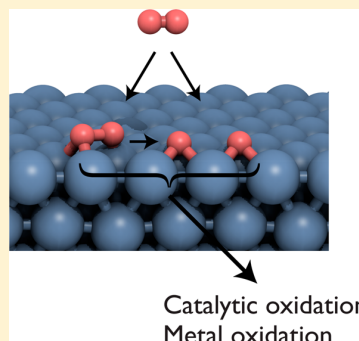
Matthew M. Montemore,^{†,‡} Matthijs A. van Spronsen,[†] Robert J. Madix,[‡] and Cynthia M. Friend^{*,†,‡,§}

[†]Department of Chemistry and Chemical Biology, Harvard University, 12 Oxford St, Cambridge, Massachusetts 02138, United States

[‡]John A. Paulson School of Engineering and Applied Sciences, Harvard University, 29 Oxford St, Cambridge, Massachusetts 02138, United States

Supporting Information

ABSTRACT: The activation of O₂ on metal surfaces is a critical process for heterogeneous catalysis and materials oxidation. Fundamental studies of well-defined metal surfaces using a variety of techniques have given crucial insight into the mechanisms, energetics, and dynamics of O₂ adsorption and dissociation. Here, trends in the activation of O₂ on transition metal surfaces are discussed, and various O₂ adsorption states are described in terms of both electronic structure and geometry. The mechanism and dynamics of O₂ dissociation are also reviewed, including the importance of the spin transition. The reactivity of O₂ and O toward reactant molecules is also briefly discussed in the context of catalysis. The reactivity of a surface toward O₂ generally correlates with the adsorption strength of O, the tendency to oxidize, and the heat of formation of the oxide. Periodic trends can be rationalized in terms of attractive and repulsive interactions with the d-band, such that inert metals tend to feature a full d band that is low energy and has a large spatial overlap with adsorbate states. More open surfaces or undercoordinated defect sites can be much more reactive than close-packed surfaces. Reactions between O and other species tend to be more prevalent than reactions between O₂ and other species, particularly on more reactive surfaces.



CONTENTS

1. Introduction	2817	5.2. Group 10 Metals (Pt, Pd, and Ni)	2831
2. Methods for Studying O ₂ Activation on Metal Surfaces	2818	5.2.1. O ₂ Adsorption on Pt Surfaces	2831
2.1. Experimental Techniques	2818	5.2.2. O ₂ Adsorption on Pd Surfaces	2831
2.1.1. Adsorption and Desorption Dynamics	2818	5.2.3. O ₂ Adsorption on Ni surfaces	2832
2.1.2. Probing Adsorbates	2818	5.3. Group 9 Metals (Ir, Rh, and Co)	2832
2.2. Computational and Theoretical Methods	2818	5.3.1. O ₂ Adsorption on Ir Surfaces	2832
3. Overview of Trends in Bonding of O ₂ and O to Metal Surfaces	2819	5.3.2. O ₂ Adsorption on Rh and Co Surfaces	2832
3.1. Fundamentals of O ₂ Adsorption	2819	5.4. Groups 4–8	2832
3.2. Trends in O ₂ Adsorption	2822	5.5. Metals Dominated by s and p Electrons	2833
3.3. Binding of Atomic Oxygen	2824	6. Mechanisms and Barriers for O ₂ Dissociation	2833
3.4. Relationship Between O ₂ and O Adsorption	2824	6.1. Group 11 Metals (Au, Ag, and Cu)	2833
4. Overview of Reactivity of O ₂ and O on Metal Surfaces	2825	6.1.1. O ₂ Dissociation on Au Surfaces	2833
4.1. Relative Reactivity of Adsorbed O ₂ and O	2826	6.1.2. O ₂ Dissociation on Ag Surfaces	2834
4.2. CO Oxidation	2826	6.1.3. O ₂ Dissociation on Cu Surfaces	2835
4.3. Selective Oxidation of Olefins	2827	6.2. Group 10 Metals (Pt, Pd, and Ni)	2835
4.4. Selective Oxidation of Alcohols	2828	6.2.1. O ₂ Dissociation on Pt Surfaces	2835
4.5. Other Oxidation Reactions	2828	6.2.2. O ₂ Dissociation on Pd Surfaces	2836
5. Molecularly Adsorbed O ₂ States on Particular Surfaces	2829	6.2.3. O ₂ Dissociation on Ni Surfaces	2836
5.1. Group 11 Metals (Au, Ag, and Cu)	2829	6.3. Group 9 Metals (Ir, Rh, and Co)	2836
5.1.1. O ₂ Adsorption on Au Surfaces	2829	6.3.1. O ₂ Dissociation on Ir Surfaces	2836
5.1.2. O ₂ Adsorption on Ag Surfaces	2829	6.3.2. O ₂ Dissociation on Rh and Co Surfaces	2837
5.1.3. O ₂ Adsorption on Cu Surfaces	2830	6.4. Groups 4–8	2837

Special Issue: Oxygen Reduction and Activation in Catalysis

Received: April 26, 2017

Published: November 8, 2017

6.5. Metals Dominated by s and p Electrons	2837
7. Effect of the Surface Geometry on O ₂ Dissociation	2837
7.1. The Case of Pt	2838
7.1.1. O ₂ on Pt Steps and Kinks	2838
7.1.2. O on Pt Steps and Kinks	2838
7.1.3. O ₂ Activation on Pt Clusters	2839
7.2. The Case of Au	2840
7.2.1. O ₂ on Au Steps and Kinks	2840
7.2.2. O on Au Steps and Kinks	2841
7.2.3. Strain Effects on Au	2841
7.2.4. O ₂ Activation on Au Clusters	2841
8. Dynamics of O ₂ Dissociation	2842
8.1. Steering and Rotational Effects	2842
8.2. Spin Dynamics	2842
8.3. Hot Atoms	2843
9. Effect of Pre-Adsorbed O on O ₂ Dissociation	2844
9.1. Repulsive Interaction with PreadSORBED O	2844
9.2. Trapping of O ₂ by Adsorbed O and O ₂	2845
9.3. Oxygen-Induced Surface Reconstruction	2845
10. Conclusions and Outlook	2846
Associated Content	2846
Supporting Information	2846
Author Information	2846
Corresponding Author	2846
ORCID	2846
Notes	2846
Biographies	2846
Acknowledgments	2847
References	2847

1. INTRODUCTION

Activation of molecular oxygen is a critical step in ubiquitous heterogeneous oxidative processes, including heterogeneous catalysis, electrocatalysis, and corrosion of metals.^{1–6} The interaction of O₂ with metal surfaces changes its chemical stability and reactivity, both of which are important for oxidative chemistry. These processes all play important roles in the global economy.

A major motivation for the investigation of O₂ activation on transition metal surfaces is understanding and predicting oxidation catalysis, which encompasses a critical set of processes in the chemical industry and emissions control. Examples of important catalytic processes that consist of oxidation by O₂ on transition metals include ethylene epoxidation,⁷ CO and hydrocarbon conversion in catalytic converters,⁸ oxidative formaldehyde production from methanol,⁹ and HCN production from methane and ammonia.¹⁰ These processes account for a substantial amount of worldwide chemical production and, therefore, are major factors in energy use and associated CO₂ production. For example, approximately 50 million tons of formaldehyde¹¹ and 28 million tons of ethylene oxide^{12,13} are produced every year (Figure 1), and the chemical industry in the United States used roughly 5 × 10¹⁸ J in 2010.¹⁴

Describing O₂ activation on metal surfaces under gaseous conditions is also a starting point for understanding key electrochemical processes, such as the oxygen reduction reaction in hydrogen fuel cells. The oxygen reduction reaction is an essential part of clean energy conversion in fuel cells and understanding bonding and bond activation in O₂ has been

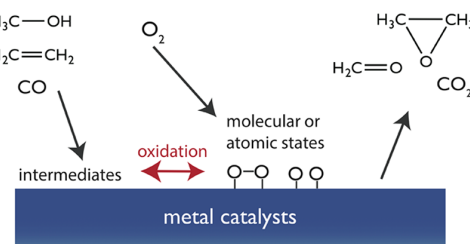


Figure 1. Schematic of a few technologically important oxidative processes where O₂ activation to adsorbed O₂ or O on metal surfaces is critical: formaldehyde synthesis from methanol (~50 million tons/yr¹¹), ethylene epoxidation (~28 million tons/yr^{12,13}), and CO oxidation (performed by catalytic converters in automobiles⁸).

used already to predict trends in the efficacy of various materials for this process.

Dioxygen activation on metal surfaces is the first stage in their oxidation; therefore, understanding O₂ activation also provides insight into both corrosion and the formation of oxide protective layers. For example, maintaining the conductivity of a material can depend critically on preventing oxidation,¹⁵ and the stability of stainless steel^{16,17} or Ti surgical implants¹⁸ depends on resistance to bulk oxidation.

The activation of O₂ in all of these processes is critical because charge transfer from metal surfaces to the stable dioxygen molecule renders it more reactive toward reactants such as CO and also lowers the barrier for O–O dissociation. With sufficient charge transfer to the O₂, dissociation to two surface-bound O atoms will occur. The extent of charge transfer to O₂ depends intimately on the electronic and geometric structure of the metal surface. Thus, a general framework for predicting the reactivity of activated molecular oxygen bound to metals is valuable. The reactivity of O atoms bound to surfaces is also key since they often react with molecules, including CO, ethylene, and methanol;¹⁹ the reactivity of adsorbed O is generally described in terms of its bond strength to the surface,²⁰ and similar species can be related using “scaling relationships”.²¹

Herein, the binding and dissociation of O₂ on metal surfaces is discussed and placed in a general framework; pure metals have received the most attention, but alloys are discussed as well. Knowledge gained from studies of well-defined, single crystal surfaces is used to establish broad trends in bonding and reactivity. Even though catalytic processes are often carried out on supported metal particles or on thin films, the functioning catalysts are often relatively large (micron scale or larger) and crystalline, rendering extended single-crystal surfaces excellent models. Single-crystal studies also benchmark modeling using atomistic theory that provides a more general understanding of bonding and bond activation. Specifically, powerful spectroscopic, imaging, and diffraction techniques probe both electronic and geometric structure that can be directly compared to theory.

Dioxygen activation at low or moderate O coverage, when the surfaces are most well-defined and metallic, is a specific focus of this paper. This overview will serve as a complement to reviews of O₂ activation in inorganic complexes where geometric and bonding characteristics are different than on extended surfaces.

Overall, this review is focused on the activation of the O–O bond on metal surfaces. Key questions include the following. (1) What are the trends in O₂ activation across metal surfaces?

(2) What are the mechanisms and associated energetics of O₂ activation on particular surfaces? By combining the results from a variety of experimental and theoretical studies, we provide a generalized picture of O₂ activation on many metal surfaces. We also discuss reactions of O and O₂ with other species on metal surfaces, as it is highly relevant to O₂ activation, but a complete, comprehensive discussion of oxidation chemistry and oxidation catalysis is outside the scope of this work. Some discussion of the surface chemistry of oxidation is available in other reviews.^{1,4,22–25} We also discuss surface and bulk oxidation of metals,^{3,26} but primarily in the context of how these relate to O₂ activation.

2. METHODS FOR STUDYING O₂ ACTIVATION ON METAL SURFACES

2.1. Experimental Techniques

2.1.1. Adsorption and Desorption Dynamics. The first step in O₂ activation is adsorption on a solid surface, either directly into a dissociated state or into a molecular precursor state. The latter entails both physisorption and chemisorption into superoxo or peroxy states.

The mechanism of adsorption can be studied experimentally by measuring the sticking probability. This adsorption probability on the surface is determined using the King-Wells technique.²⁷ At the beginning of such an experiment, an O₂ beam directed at the sample is blocked by a beam stopper, an inert surface that completely deflects the beam away from the sample. The scattered beam results in a certain partial pressure, which decreases after removing the beam stopper. This drop is due to adsorption of a fraction of the beam, now impinging on the surface of interest. The partial pressure difference and its evolution over time is measured via quadrupole mass spectrometer (QMS).

The adsorption dynamics can be further investigated by following the sticking probability as a function of the kinetic energy of the incoming O₂ molecules, surface temperature, adsorbate coverage, or incidence angle. For example, direct dissociation results in little or no dependence of the sticking probability on the surface temperature. Furthermore, if combined with calorimetry,²⁸ the energetics of adsorption can be studied.

The reverse reaction, desorption of O₂, can be studied by using temperature-programmed desorption²⁹ (TPD) techniques. In this type of measurement, a desired coverage of adsorbates is obtained by exposing the crystal to an atmosphere of the species at a certain partial pressure for a specified time. The sample is cooled to low temperatures, typically around 100 K, to block desorption. After adsorption, the setup is evacuated and the sample is heated while measuring the gas phase with a QMS to detect desorbing species. The variation in desorption rate with coverage or heating rate provides insight into the desorption kinetics.

2.1.2. Probing Adsorbates. After the initial adsorption, spectroscopic techniques are frequently used to study the adsorbates. These can be based on vibrational fingerprinting, electronic structure, diffraction, or microscopy. Although these techniques can in principle be used to study uptake or desorption, experimental restrictions usually limit the measurement focus to stably adsorbed surface species.

Vibrational spectroscopy can probe the internal vibrational modes of the adsorbate as well as the vibration of the adsorbate with respect to the surface. Therefore, it is used to determine

the adsorption state of O₂. The vibrations can be excited in several ways, such as with infrared (IR) light or with low-energy electrons. These electrons lose energy due to excitation of vibrational modes after scattering from the surface. This is the principle of high-resolution electron energy-loss spectroscopy³⁰ (HREELS). Compared to IR spectroscopy, it has the major advantage that it can be used to measure vibrations with lower wavenumbers, which is needed to detect M-O or M-O₂ bonds. On the Pt(111) surface, for example, these have wavenumbers of 480 and 380 cm⁻¹.³¹

Electron emission spectroscopy can be separated into core-level spectroscopy, such as X-ray photoelectron spectroscopy (XPS) or Auger electron spectroscopy (AES), and valence-band spectroscopy. The former can easily distinguish between molecular and atomic oxygen and yields the adsorbate coverage. The latter, ultraviolet photoelectron spectroscopy (UPS), can provide more information regarding the chemical nature of the adsorbed species, but interpretation can be difficult. X-ray absorption spectroscopy (XAS), including near edge X-ray absorption fine structure (NEXAFS) and surface-extended X-ray absorption fine structure (SEXAFS), can give information about the electronic structure of a species, and structural parameters can be determined.

Structural information on adsorbates is obtained using diffraction or microscopy. Two widely applied techniques are low-energy electron diffraction³² (LEED) and scanning tunneling microscopy^{33,34} (STM). Diffraction requires that the adsorbate overlayer has a long-range repetitive structure, whereas STM allows for imaging of individual adsorbates or disordered structures. Further, diffraction uses beams typically larger than tens of micrometers, which averages the obtained information over a large surface area, while local information is collected with STM.

2.2. Computational and Theoretical Methods

Density functional theory (DFT)³⁵ is the most widely used computational method for studying the chemical interactions between molecules and surfaces. In most of these systems, DFT affords the best compromise between accuracy and computational expense, allowing routine calculation of the structures and energies of periodic or cluster systems up to a few hundred atoms. Typical DFT calculations give equilibrium structures and their energies, and other important quantities, such as vibrational spectra and activation energies, can also be calculated.

Practical approaches to DFT involve the Kohn-Sham formalism, in which the interacting system of electrons is mapped onto a fictitious system of noninteracting electrons with the same density.³⁶ The energy of the noninteracting system can be calculated exactly, and a correction term, called the exchange-correlation functional, is used to try to account for the difference between the interacting and noninteracting systems. Various exchange-correlation functionals have been proposed and applied, falling into several classes. The simplest is the local-density approximation (LDA), which is generally quite inaccurate for chemical applications. Somewhat more sophisticated is the generalized gradient approximation (GGA), which is widely used in surface systems because of its efficiency and relative accuracy. In particular, PW91,³⁷ PBE,³⁸ and RPBE³⁹ are the most popular functionals, and have similar errors when compared to experimental adsorption energies.⁴⁰ RPBE tends to predict weaker adsorption, while PBE and PW91 give similar results (typically overbinding). The BEEF-

vdW functional⁴¹ uses an ensemble of GGA functionals, which allows error estimation. Meta-GGA functionals such as TPSS⁴² are computationally tractable for surface systems but have not gained widespread adoption as their increased complexity does not always result in improved accuracy over GGA, particularly for metals.^{43,44} However, recently developed meta-GGAs may be significantly more accurate and may gain widespread use in the future.^{45,46} Hybrid functionals, which include exact exchange as calculated in Hartree–Fock theory, are widely used in gas-phase calculations and can give significantly more accurate results than GGA functionals for molecular species.⁴⁷ However, hybrid functionals are too expensive to use routinely in surface problems, and some of them are inaccurate or exceedingly expensive for metals and/or the solid state.^{48,49} Most exchange-correlation functionals, and in particular the GGA functionals used in most surface studies, do not properly account for long-range dispersion (van der Waals) interactions.⁵⁰ Dispersion interactions are critical for understanding aspects of some systems, but for small molecules such as O₂ their effect is usually small. For strongly correlated materials, such as bulk oxides, the semiempirical Hubbard U correction⁵¹ is necessary to correct GGA functionals, but for metal surfaces this correction is rarely used. The U correction is also not generally employed for surface oxides, but the validity of this methodology is unclear. Since most computational studies of O₂-metal interactions use Kohn–Sham DFT with GGA functionals, in this work, we will generally use “DFT” to signify this methodology.

Early DFT studies of surfaces often used cluster models, but most recent studies use periodic boundary conditions such that surfaces are truly two-dimensional, which often provides a better description of an extended surface, particularly for metals. Vacuum space is inserted into the unit cell so that the surface does not interact with its periodic image in the perpendicular direction.

The accuracy of DFT is a complex subject, as it depends strongly on the quantity and system,⁵² but a few rules of thumb are helpful. In general, GGA-DFT gives good structural properties, within a few hundredths of an Å. Absolute adsorption energies typically have an error of roughly 0.2 eV,⁴⁰ but relative energies are generally more accurate, particularly for similar systems. However, GGA-DFT is known to be particularly inaccurate for gas-phase O₂, resulting in a prediction of the O–O bond that is stronger than the experimental value. When accurate O adsorption energies are needed relative to gas-phase O₂, a correction term is often added. This correction can be derived from some combination of experimental and computational quantities for gas-phase molecules.⁵³ Since this error is manifested for the O–O double bond, but not for adsorbed O, it may result in barriers higher than the experiment in some cases, as the initial state may be overstabilized relative to the transition state.

3. OVERVIEW OF TRENDS IN BONDING OF O₂ AND O TO METAL SURFACES

In this section, a broad overview of the bonding interactions of molecular and atomic oxygen with metal surfaces is provided and specific definitions for peroxy and superoxo states are articulated. The periodic trends in O₂ and O adsorption, as well as the correlation between O₂ and O adsorption energies, are also discussed. The summaries and generalities in this section are based on the body of literature that is discussed throughout the review. We refer directly to the literature when necessary,

but refer the reader to later sections for more detailed discussions of particular findings and systems.

3.1. Fundamentals of O₂ Adsorption

Understanding O₂ adsorption on metal surfaces provides crucial insight into key factors and trends in O₂ activation. Both weakly bound (physisorbed, binding energy typically less than roughly 50 meV [~5 kJ/mol, ~1 kcal/mol] per adsorbate atom) and chemically bound (chemisorbed) O₂ states have been identified on metal surfaces (Figure 2). The strength of

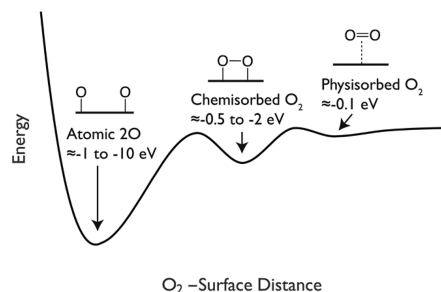


Figure 2. Schematic one-dimensional potential energy surface for an O₂ molecule approaching a surface. Rough energy values are given, relative to gas-phase O₂ far from the surface.

O₂ binding is reflected in the molecular orientation. The O–O bond axis of the more strongly bound chemisorbed states are nearly always parallel to the surface of transition metals, whereas more weakly bound physisorbed states and chemisorbed states on metals dominated by s and p electrons can be vertically oriented.^{54,55}

There is generally a significant amount of charge transfer to the O₂ from the metal surface for more strongly bound chemisorbed states. In the gas phase, the degree of charge on the dioxygen is used to define the superoxo- (O₂⁻, corresponding to an O–O bond order of 1.5) or peroxy-like state (O₂²⁻, corresponding to an O–O bond order of 1). Both the vibrational frequencies and signatures of the electronic structure are used to assign states in the gas phase (Table 1).

On surfaces, these definitions of peroxy and superoxo are less clearly defined because of the wide variation in the degree of charge transfer; hence, the spin state of the surface-bound O₂ is used to define these two types of states. This definition was adopted because measuring, calculating, or even defining charge transfer is difficult because of orbital mixing between the O₂ and the metal (Figure 3). Both gas-phase and physisorbed O₂ have a total magnetic moment of 2 μ_B (2 electrons, each with spin 1/2 and magnetic moment of 1 μ_B). A superoxo-like chemisorbed state is defined as a state that has a magnetic moment between 0 and 2 μ_B , whereas a peroxy-like state has approximately 0 magnetic moment. Since charge transfer to O₂ populates antibonding orbitals, the reactivity of a peroxy species is usually, but not always, higher than that of a superoxo species. Because measuring the spin is difficult, in practice the O–O stretching frequency is often used to make assignments. This is quite useful but can occasionally lead to ambiguity.

A molecular orbital picture provides general insight into the bonding of O₂ to metal surfaces (Figure 3). The valence orbitals of O₂ shift to new values when it adsorbs on a metal surface; these orbitals are occupied if they are below the Fermi energy of the combined system. (For a metal, the Fermi energy is the energy of the highest occupied electron state.) This shift

Table 1. Properties of Gas-Phase O₂ in Different Oxidation States

species	bond order	O–O bond energy (eV)	magnetic moment (μ_B)	$d(O–O)$ (Å)	$\nu(O–O)$ (cm ⁻¹)
O ₂	2	-5.12 ⁵⁶	2	1.207 ⁵⁶	1580 ⁵⁶
O ₂ ⁻ (superoxo)	1.5	-4.10 ⁵⁷	1	1.35 ⁵⁷	≈1100 ⁵⁸
O ₂ ²⁻ (peroxo)	1	-2.18 ^{4,59}	0	1.48 ^{4,60}	877 ^{4,61}

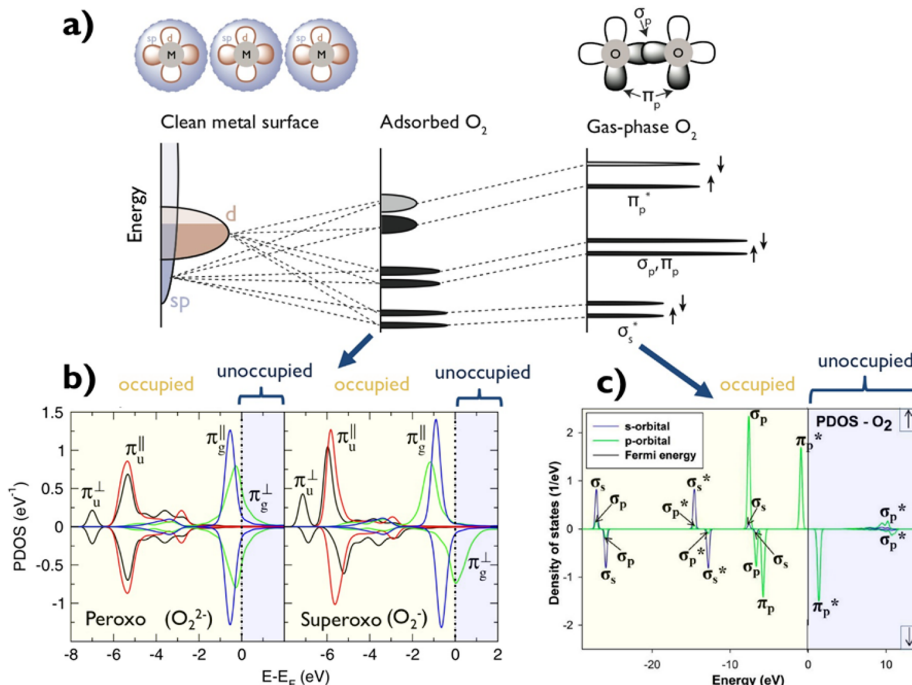
^aFor HOOH.

Figure 3. (a) Schematic molecular orbital diagram for O₂ adsorption on a transition metal surface that shows the interaction of the sp and d bands of a typical transition metal on the left that lead to shifts and broadening of O₂ molecular orbitals (MOs) resulting from interaction with the surface (“adsorbed O₂”). As a reference, the MOs of gas-phase O₂ are shown on the right. Filled states are fully shaded. The filling of the π_p^* orbital that is shaded gray depends on whether the chemisorbed state is peroxo or superoxo. (b) Density of states (DOS) for O₂ adsorbed on Ag(110), with the left panel corresponding to a peroxo-like (O₂²⁻) state and the right panel corresponding to a superoxo-like (O₂⁻) state. Adapted with permission from ref 62. Copyright 2010 American Physical Society. (c) DOS and molecular orbital diagram for gas-phase O₂. The peaks have a finite width, likely due to some broadening used in the projection. Reprinted with permission under a Creative Commons License.⁶³

is typically dominated by interaction with s and p electrons of the metal, as the d electrons in a transition metal are localized near the atoms and O₂ does not adsorb as closely to the surface as a radical species.

The spin state of the adsorbed O₂ depends on the occupancy of the π_p^* orbitals (Figure 3, panels a and b). Gas-phase O₂ has a pair of half-occupied π_p^* orbitals, resulting in a triplet spin state, which is magnetic. The spin-up and spin-down states are split. If these orbitals are completely occupied upon adsorption to a metal surface, the magnetic moment of the O₂ will be zero and, thus, assigned as a peroxo state. The spin splitting will also disappear if the π_p^* states are fully occupied. If these orbitals are only partly occupied then O₂ will still have a magnetic moment, the spin states will be split, and, by our definition, the O₂ will be in a superoxo state.

The effect of increasing charge transfer to O₂ is illustrated by comparing adsorption on clean Pt(111) and on Pt(111) with 1/9 monolayer (ML) of adsorbed Na. The Na decreases the work function (the Fermi energy relative to the vacuum energy), reflecting the charge donation from Na to the surface.⁶⁴ Hence, there is more charge donation to superoxo

O₂ species adsorbed on the surface (Figure 4), resulting in a lower spin-state, a weaker O–O bond, and a stronger O₂–Pt bond. This shows that shifts in the energy of the highest occupied orbitals in the metal relative to the metal surface’s vacuum level (work function) can be used as a qualitative guide to understanding changes in O₂ adsorption for different surfaces.

The difference between a superoxo and a peroxo species is further illustrated by the charge density difference plot for two different states of O₂ on Pt(111), which have different adsorption sites and different oxidation states (Figure 5). The peroxo state has increased charge depletion from the O–O bond.

Comparing the bonding state of O₂ chemisorbed on different metal surfaces or at different sites is less straightforward than the shift in work function described above. On different surfaces, the O₂ molecular orbitals are generally shifted to different values due to variations in their interaction with the electronic structure of the surface. Therefore, the work function alone is not sufficient to determine whether a surface will produce superoxo or peroxo species, as demonstrated by the

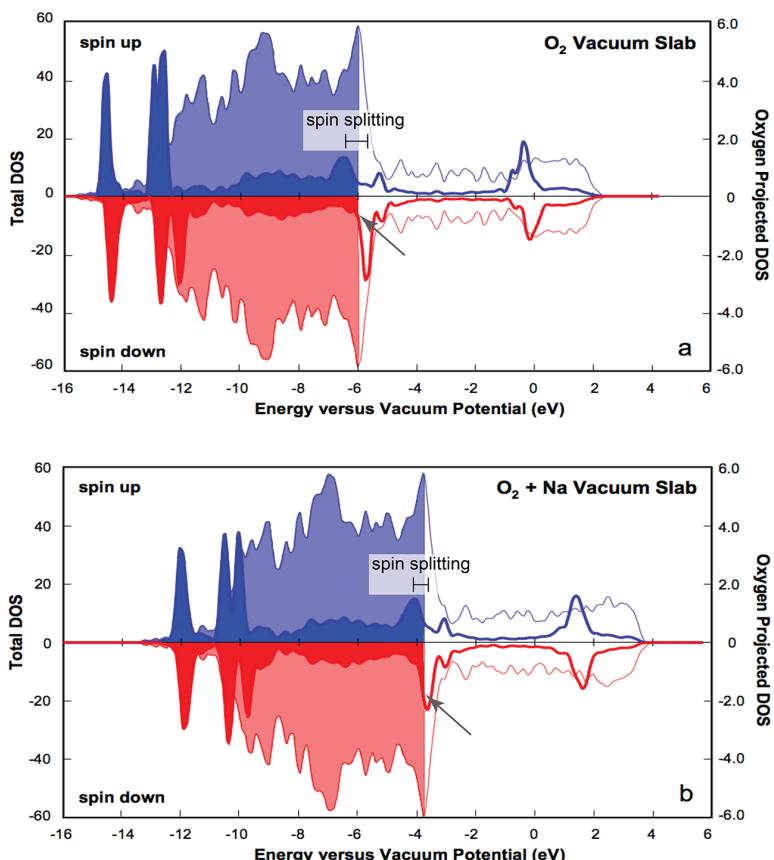
$O_2/Pt(111)$ without and with co-adsorbed Na

Figure 4. Illustration of the change in the degree of charge transfer to O_2 due to the shift in the highest occupied states (Fermi level) using the case of Pt(111) with and without coadsorbed Na. The top panel is a superoxo-like (O_2^-) species formed on clean Pt(111). The bottom panel is a more peroxy-like (O_2^{2-}) species formed on Na-covered Pt(111). The increased occupation of O_2 antibonding states is indicated by the arrows and by the reduced spin splitting (see markers). Total (light) and O-projected (dark) DOS plots are shown. Occupied states are filled in color; unoccupied states are depicted by lines. Adapted with permission from ref 64. Copyright 2008 Royal Society of Chemistry.

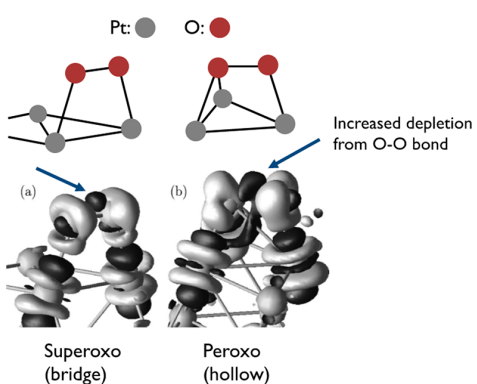


Figure 5. O_2 states on Pt(111): (a) superoxo (bridge site) and (b) peroxy (fcc hollow site). The light isosurface represents excess electron density, while the dark isosurface represents electron depletion. The difference in bond depletion in the O–O region is indicated by the arrows. The schematics above are to aid in understanding the geometry of the structures. Reprinted with permission from ref 65. Copyright 2000 American Physical Society.

coexistence of these species on different surfaces. The strength of interaction is primarily determined by the orbital energies of the surface atoms and their coupling to the electronic states of oxygen. This is determined by the composition and geometry of the surface (e.g., the surface facet, steps, kinks, etc.). Additionally, dynamic and kinetic effects need to be evaluated, because these effects will determine the experimentally observed species.

Chemisorption of O can be considered the first step in the bulk oxidation of metals, which occurs when the O_2 chemical potential is sufficiently high. As the chemical potential increases, the O coverage will increase, followed by formation of oxide structures. Therefore, saturation coverages necessarily refer to the maximum coverage at a particular set of conditions.^{66–69} Bulk oxidation can be preceded by the formation of a single oxide layer, forming the interface between the metallic bulk and the O_2 gas phase. For example, Pt and Pd can form different surface oxides prior to bulk oxidation, both in O_2 and under oxidative reaction conditions. However, the thermodynamically predicted phases are not necessarily identical to those observed experimentally. This can be the case if the O_2 dissociation rate decreases strongly with increasing coverage (see section 9.1), which leads to a kinetic

limitation to form structures with higher O coverage. This state is usually described as the saturation coverage and typically refers to the highest obtainable O coverage under the low-pressure conditions of UHV experiments. An example is the saturation coverage of Pt(111), which is 0.25 ML.^{70,71} Higher coverage can be obtained at sufficiently high pressure⁷² or when stronger oxidants are used, such as NO₂, this does not involve O₂ dissociation.⁶⁸

3.2. Trends in O₂ Adsorption

There are clear periodic trends in the binding of O₂ to late transition metal surfaces such that the lower-right section of the d block is the most inert with respect to O₂ adsorption. This is reflected in the degree of charge transfer to the O₂ for various transition metals (Figure 6a). For example, O₂ is extremely

a) States observed experimentally				b) DFT Adsorption Energies for O ₂ (eV)		
Fe	Co	Ni	Cu	Co	Ni	Cu
O	O	O	O ₂ ⁻ O	-2.26	-1.61±0.18	-0.75±0.22
Ru	Rh	Pd	Ag	-1.95	-0.97±0.40	-0.15±0.02
Os	Ir	Pt	Au	-1.21±0.09	-0.68±0.09	0.01±0.12

Figure 6. Sections of the periodic table showing (a) states observed when exposing the metal to O₂ under ultrahigh vacuum (UHV) conditions at low coverage and at temperatures below room temperature (all surface facets are included). Physisorbed (O₂⁰), superoxo (O₂⁻), peroxy (O₂²⁻), and atomic (O) species are indicated. (b) DFT adsorption energies for O₂ on the close-packed fcc(111) or hcp(0001) surface. The data, averages taken from the literature, are given in Table 2 to Table 4.

weakly bound on Au surfaces indicative of essentially no charge transfer. Indeed, the binding of O₂ to Au is most likely entirely due to dispersion forces given that the experimental desorption temperatures are between 37 and 55 K, whereas the desorption from condensed multilayers occurs at 34 K.⁷³ These desorption temperatures correspond to an adsorption energy of -0.06 to -0.11 eV,⁷³ which is comparable to the enthalpy of sublimation of O₂ of 0.09 eV.⁷⁴ Depending on the facet, Ag, Pt, and Pd surfaces can support both superoxo and peroxy species. On Ir and Ru, only peroxy species have been identified. On even more reactive metals, such as Rh, Co, and Fe, O₂ adsorbed states have not been observed, presumably because the dissociation barriers are so low that the dissociation occurs quickly, even at low temperature. The lower-right section of the periodic table interacts weakly with O₂ because the d-band is full and because the d orbitals are low in energy and large in spatial extent. This results in little attractive, covalent interaction and strong Pauli repulsion.

The experimental trends are mirrored by the adsorption energies of O₂ as calculated by DFT (Figure 6b). O₂ is bound most weakly to transition metals near the lower-right corner of the d block, such that its adsorption energy on Au is essentially 0, indicating no charge transfer. The reactivity then increases for metals further up and to the left. These are the same trends as explained for atomic O below in terms of interactions with the d-band and lone-pair repulsion. On the left side of the d block, O₂ often dissociates with little or no barrier, and therefore few data are available on its molecular adsorption

energy. However, if O₂ also behaves similarly to O on these metals, the lower-left section of the transition metals is the most reactive toward O₂.

On the (111) facets of the late transition metals, such as Ag, Pd, and Pt, the bridge site and hollow site are often the most stable sites and have fairly similar adsorption energies (see section 5 for more detail).^{65,75,76} When in the bridge site, O₂ is typically in a superoxo state, while in the hollow site it is typically in a peroxy state. On the more reactive surface Ir(111), adsorption in either site results in a peroxy species.⁷⁷ Adsorption in either of the two 3-fold hollow sites, fcc (no metal atom in the second layer below the site) and hcp (contains a metal atom in the second layer below the site), results in very similar O₂ properties.

The frequency of the O–O stretch in adsorbed O₂ gives important information about the degree of charge transfer since the vibrational energy is sensitive to the O–O bond dissociation potential. First, as anticipated, the O–O stretch frequency decreases on average with increasing O–O distance in the adsorbed molecule in DFT calculations (Figure 7a). The

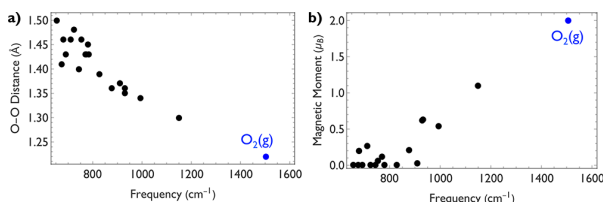


Figure 7. Correlations between the O–O stretching frequency and (a) O–O distance; and (b) magnetic moment, for O₂ adsorbed on a variety of transition metal surfaces calculated with DFT, as well as gas-phase O₂.⁷⁸ The data are average values from the literature and are given in Table 2 to Table 4.

frequency also decreases with decreasing magnetic moment in the adsorbed O₂ (Figure 7b). These correlations support the notion of using the frequency to assign a state as peroxy (below roughly 900 cm⁻¹) or superoxo (above roughly 900 cm⁻¹), although the delineation is not a clear line. However, the frequency and oxidation state do not cleanly predict adsorption energies across surfaces. Analysis of all available data (see Table 2 to Table 4) suggests that the DFT frequencies available in the literature are generally within ~50–100 cm⁻¹ of the experimental frequencies, and some of the discrepancies may be due to coverage effects.

One of the challenges in comparing the theoretical and experimental data is that adsorbed O usually passivates surfaces toward further O₂ activation, and indeed on more reactive surfaces adsorbed O is necessary in order to stabilize O₂ enough for it to be observed experimentally. The end result is that O₂ is in an environment that is different than the bare metal surface (e.g., there are adsorbate–adsorbate interactions and differences in the surface electronic structure due to adsorbed O or surface oxides). Therefore, it can be important to distinguish between surfaces where only molecular O₂ is observed at low temperatures, such as Pt(111) or Ag(110), and those where significant amounts of dissociation occur at low temperatures, such that the adsorbed O allows the formation of adsorbed molecular O₂, such as Rh(111).

The sticking probability of O₂ generally decreases with increasing coverage due to higher degree of occupied adsorption sites. For several metals, such as the Pt-group

Table 2. Properties of Adsorbed O₂ on Group 11 Metal Surfaces^a

ox state	magnetic moment (μ_B)	$\nu(\text{O}-\text{O})$ (cm ⁻¹)	$d(\text{O}-\text{O})$ (Å)	O ₂ ads energy (eV)	notes/ref
Cu(111)					
peroxyo	0	655 ± 13	1.50 ± 0.00	-0.85 ± 0.03	bridge-hollow ^{b,222,223}
peroxyo	-	610	-	-	dominant at low coverage. exptl ^{c,224}
peroxyo	0.00 ± 0.00	779 ± 9	1.45 ± 0.01	-0.75 ± 0.22	3-fold hollow ^{b,222,223,225,226}
peroxyo	-	834 ± 16	-	-	dominant at high coverage. exptl ^{c,224,227}
peroxyo	0.00 ± 0.00	724 ± 26	1.48 ± 0.01	-0.60 ± 0.13	bridge-hollow-bridge ^{b,214,223,225,226}
Cu(110)					
peroxyo	0.00 ± 0.00	-	1.54 ± 0.01	-1.58 ± 0.08	4-fold hollow ^{b,228}
Cu(100)					
	-	631	-	-	exptl ^{c,229}
	-	-	1.52	-	exptl ^{d,230}
Ag(111)					
superoxo	1.10 ± 0.16	1149	1.30 ± 0.00	-0.15 ± 0.02	2-fold bridge ^{b,117,214,231,232}
peroxyo	0.10 ± 0.14	-	1.35	-0.08 ± 0.39	3-fold hollow ^{b,232,233}
peroxyo	-	685 ± 21	-	-	exptl ^{c,206,212}
Ag(110)					
peroxyo	0.12 ± 0.21	770 ± 31	1.43 ± 0.01	-0.41 ± 0.15	4-fold hollow, [001] ^{b,234–239}
peroxyo	-	665 ± 29	-	-	exptl ^{c,240,241}
peroxyo	0.06 ± 0.10	753 ± 16	1.46 ± 0.01	-0.44 ± 0.14	4-fold hollow, [1̄10] ^{b,231,234–239}
peroxyo	-	-	1.47	-	O–O along [1̄10] exptl ^{d,242}
peroxyo	-	637 ± 7	-	-	exptl ^{c,240,243,244}
Ag(100)					
	-	782	1.43	-0.68	4-fold hollow ^{b,245}
	-	678 ± 0	-	-	exptl ^{c,246,247}
	-	637 ± 0	-	-	exptl ^{c,246,247}
Au(111)					
physisorbed	2.00 ± 0.01	1163 ± 126	1.26 ± 0.04	0.01 ± 0.12	2-fold bridge ^{b,78,117,231,233,248,249}
Au(110)					
	-	-	1.3	-0.19	2-fold bridge, not reconstructed ^{b,231}
Au(100)					
	-	775 ± 43	1.43 ± 0.00	-0.13 ± 0.08	4-fold hollow, not reconstructed ^{b,78,248}

^aExperimental (exptl) data are marked; others are computational. Methods are given below. ^bDFT(PBE/PW91). ^cEELS. ^dXAS.

metals, repulsive interactions between adsorbed O atoms lead to saturation coverages well below 1 ML for typical surface science experiments (low pressure and temperature). The decrease in sticking probability with increasing coverage is less pronounced (or absent) at lower surface temperatures or for incoming O₂ with a lower kinetic energy. Under these conditions, a transiently physisorbed O₂ molecule has a sufficiently long lifetime to find an appropriate chemisorption or dissociation site.

Conversely, preadsorbed O and O₂ raise the O₂ adsorption and dissociation rate in a few cases. Several dynamical arguments have been proposed, such as very low mass mismatch leading to optimal sticking onto adsorbed O₂ islands. Adsorbed O can also direct physisorbed O₂ to suitable sites for chemisorption. Preadsorbed O and O₂ may themselves provide sites with enhanced binding or lower dissociation barriers. Finally, surface reconstructions induced by preadsorbed O can lead to a surface with a higher reactivity toward O₂. The effects of preadsorbed O are discussed further in section 9.

Another factor in determining the degree of O₂ activation is the coordination number of the metal atoms on the surface. Specifically, sites with lower coordination numbers are generally more reactive (i.e., stronger adsorption and lower dissociation barriers) toward O₂ than more coordinated sites. Indeed, coordination number, or generalizations thereof, can be used to quantitatively predict DFT-calculated adsorption energies for

some oxygen-containing species.^{79,80} This applies to both flat surfaces, where reactivity often, but certainly not always, increases as (111) < (100) < (110), and for steps and kinks. However, there can be exceptions. For example, reconstructions can passivate surfaces, or a particular arrangement of surface atoms may allow more overlap with the orbitals of O₂ for purely geometric reasons. In other words, a particular arrangement may allow better overlap with orbitals on both O atoms simultaneously. In general, steps and kinks on late transition metals stabilize the adsorbed O₂ states and the dissociation transition state similarly, resulting in a small change in the activation energy but an increase in the branching ratio toward dissociation versus desorption. Additionally, there are conflicting experimental results on the effects of steps on Pt surfaces. We discuss these issues in more detail in section 7.

Overall, O₂ can behave very differently on different transition metal surfaces, from very weakly interacting [e.g., Au or, to a lesser extent, Ag(111)] to forming strongly bound O₂ states that are stable at low temperatures [e.g., Ag(110)] to very facile dissociation such that O₂ is very difficult or impossible to observe at low coverage (e.g., Co surfaces). These trends primarily reflect differences in the electronic structure of the transition metals, which have been more clearly delineated in the case of adsorbed O. Specific systems are discussed in section 5.

3.3. Binding of Atomic Oxygen

The interaction of atomic O with a metal surface is largely controlled by the interaction of the metal states with the p orbitals in the oxygen atom; the s orbitals in O have a relatively small effect.⁸¹ Conceptually, the O-surface interaction can be divided into covalent (attractive) and Pauli repulsion (repulsive) parts. A qualitative picture of O binding to transition metal surfaces is provided by the d-band model,⁸² which relates adsorption energies primarily to interactions between renormalized adsorbate states and the d electrons of the surface. The bonding of atomic O to metal surfaces has been discussed previously;⁸² however, a brief overview is given here.

The p orbitals in O are shifted and broadened by their interaction with the sp states in the metal (Figure 8). The

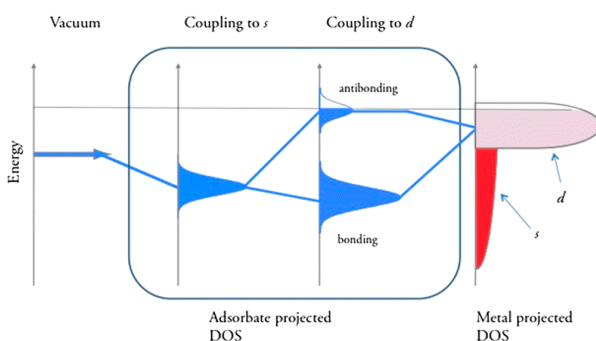


Figure 8. Schematic showing the O adsorbate state (left) interacting with the bands in a metal surface (right). The adsorbate state is renormalized by the sp bands (middle left) and then splits with the d bands (middle right). Reproduced from ref 84. Copyright 2014 Springer Nature.

broadened p orbitals are split into metal-O bonding and antibonding states by the interaction with the d band. The filling of the metal-O antibonding states depends on the energy of the d band relative to the Fermi energy: a deep d band will result in the antibonding states being mostly filled (weak adsorption), while a high-energy d band will result in the antibonding states being mostly unfilled (strong adsorption). Generally, the average energy of the d electrons, known as the d-band center, is used to characterize the energy of the entire d band. When considering a subset of fairly similar surfaces, such as PtCo alloys or pure 3d metals, the d-band center often suffices to predict the DFT-calculated O adsorption energy (Figure 9).^{82,83}

The d-band center does not yield accurate predictions when considering a broad range of surfaces (Figure 10, where the right panel shows OH, which correlates well with O).^{85,86} The matrix coupling element (essentially, the strength of interaction) between the adsorbate states and the metal d states, V_{ad} , also affects adsorption energies, a larger coupling element leads to both stronger covalent interaction (which is attractive) and stronger Pauli repulsion (which is repulsive).^{82,85} For O on late transition metals, the repulsion dominates, which explains why Au adsorbs O more weakly than Ag, despite the deeper d-band of Ag (Figure 11).

The DFT-calculated adsorption energy of O (and other adsorbates that are radicals in the gas phase) can be quantitatively predicted on a transition metal surface as^{85,87}

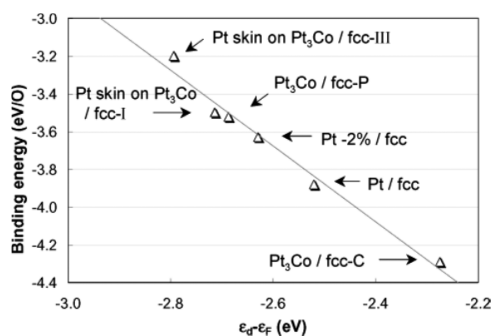


Figure 9. Binding energy of O on a variety of Pt alloy surfaces linearly scales with the d-band center, enabling prediction of O adsorption energies on a set of similar surfaces. Reprinted from ref 83. Copyright 2004 American Chemical Society.

$$E_{ads} = b_1 \epsilon_a + b_2 \epsilon_d + b_3 n_p + a_1 V_{ad}^2 f + a_2 V_{ad}^2 \quad (1)$$

where ϵ_a is the energy of the highest occupied molecular orbital (HOMO) of the adsorbate, ϵ_d is the d-band center of the metal, n_p is the number of p electrons in the metal, and f is the d-band filling. The a_i are adsorbate-dependent fitting parameters and the b_i are universal fitting parameters. Since O has lone pair electrons (or, equivalently, has a high-energy HOMO), a_1 is positive, making its term repulsive, and $a_2 = -0.67a_1$, such that its term is attractive.⁸⁷ This framework allows us to understand trends in O adsorption. When moving left on the periodic table, the d-band center typically increases relative to the Fermi energy, resulting in stronger adsorption. An increased number of p electrons results in stronger adsorption, although this effect is smaller and harder to correlate with periodic trends. Moving down the periodic table generally increases V_{ad} as it roughly scales with the size of the metal atom. For metals with a mostly full d shell, increasing V_{ad} results in weaker adsorption, while for metals with a mostly empty d shell increasing V_{ad} results in stronger adsorption. Therefore, the lower-right section of the d-block is the most inert with respect to O adsorption, while the lower-left section is the most reactive. These trends are supported by experimental formation enthalpies of bulk oxides. Of those compiled in refs 88 and 89, HfO₂ is the most exothermic (followed by ZrO₂) and Au₂O₃ is the least exothermic (followed by Ag₂O). Similar trends are also found in experimental estimates of O adsorption energies on transition metals.^{90,91}

Oxygen adsorption can therefore be understood based on the energetics of the electrons in the surface, the filling of the d-band, and the coupling between the metal states and the adsorbate states. O typically withdraws electrons from the surface, which affects the metal atoms around it and has implications for its interactions with other adsorbates; this can have crucial implications for ordering and reactivity.^{53,92,93}

3.4. Relationship Between O₂ and O Adsorption

The binding strength and degree of charge transfer to adsorbed O₂ and O follow similar periodic trends. Indeed, correlations between the O and O₂ adsorption energies, known as a scaling relation,^{21,94} have been found in several studies of metal surfaces (Figure 11).

The linear correlation of the O₂ and O binding energies breaks down on Pt alloy surfaces,⁸⁶ probably because O₂-Pt interactions are dominated by Pauli repulsion, as shown previously for Pt-OH interactions.⁹⁸ Therefore, the correlation

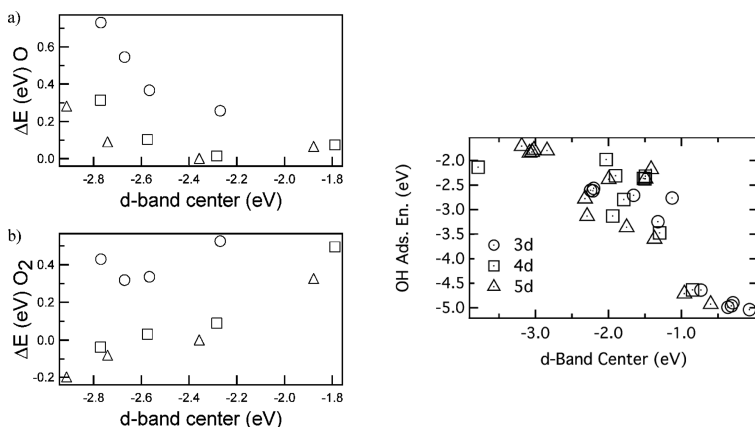


Figure 10. (Left) The moderate correlation between the d-band center and the DFT-calculated adsorption energies of O (top) and O_2 (bottom) does not accurately predict adsorption energies for model Pt alloys where the second layer is replaced with another transition metal (○ denote substitution by 3d metals, □ for 4d metals, and △ for 5d metals). Reproduced from ref 86. Copyright 2007 American Chemical Society. (Right) The correlation (moderate but not predictive) between the d-band center and the DFT-calculated OH adsorption energies on a variety of monometallic and alloy transition metal surfaces. Reproduced from ref 85. Copyright 2014 American Chemical Society.

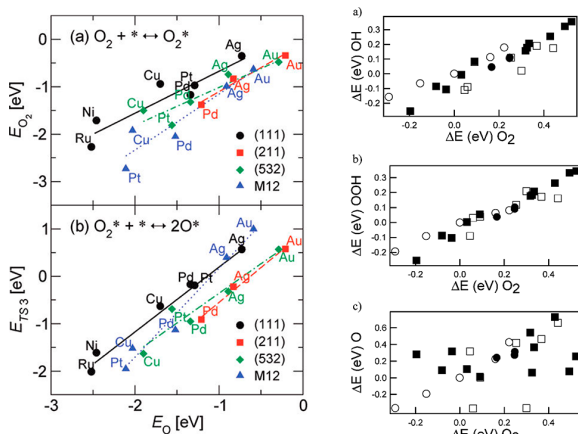


Figure 11. (Left) (a) Scaling relation (linear correlation) between DFT-calculated O and O_2 adsorption energies and (b) correlation between the O adsorption energy and the adsorption energy of the O_2 dissociation transition state. Reproduced from ref 97. Copyright 2009 American Chemical Society. (Right) Scaling relations for DFT-calculated adsorption energies on Pt(111) alloys for (a) OH vs O_2 and (b) OOH vs O_2 , as well as (c) the broken scaling relation for O vs O_2 . ○ are for strained Pt surfaces, □ are for Pt pseudomorphic overlayers, ■ are for Pt surfaces with another metal replacing the second layer, and ● are for a Pt overlayer on a Pt_xM alloy. Reproduced from ref 86. Copyright 2007 American Chemical Society.

between the adsorption energies of O and O_2 will not necessarily hold on other noble metal alloys. This suggests an opportunity to tune the reactivity of O_2 by designing specific alloys.

Overall, metals with a low O_2 dissociation barrier tend to adsorb O_2 and O strongly and oxidize easily. This is clear based on the ease with which early transition metals dissociate O_2 and form both surface and bulk oxides. This is consistent with both scaling relations and Brönsted–Evans–Polanyi (BEP) relationships, which state that a more exothermic reaction step tends to have a lower barrier.

4. OVERVIEW OF REACTIVITY OF O_2 AND O ON METAL SURFACES

An important aspect of oxidative heterogeneous catalysis is understanding and predicting reactivity of both molecular and atomic oxygen bound to metal surfaces with reactant molecules. Selective oxidation (e.g., olefin epoxidation or methanol conversion to formaldehyde) is catalyzed by Ag.^{7,9,13} Combustion is catalyzed by Group 10 transition metals; for example, oxidized Pd is used for methane combustion.⁹⁹ A broad range of metals can catalyze CO oxidation, although commercial catalysts are primarily comprised of Group 9–10 metals (e.g., Pd, Rh, and Pt). These reactions have been reviewed previously;^{1,23} thus, reactivity in the context of heterogeneous catalysis is only briefly discussed here. The discussion is further limited to thermal reactions at the gas-solid interface.

On the basis of the studies we reviewed below, a few trends are apparent. Inert metals tend to be more selective for oxidation and can require O in order to be reactive at all. O often acts by abstracting H in an acid–base reaction, and the selectivity typically decreases with O coverage. More reactive metals tend to be less selective, and O may be less involved in bond scission, although it can have other effects, such as clean-off reactions. On these reactive metals, O can passivate the surface, and the selectivity can increase as O coverage increases.

The correlation between the binding strength of O_2 and O adsorbed on monometallic surfaces suggests that their reactivity will follow periodic trends. On one hand, increased charge transfer to adsorbed O_2 would be expected to increase its reactivity because of the weakening of the O–O bond. The reactivity observed will also depend, however, on the bonding in the transition state for a specific reaction. Therefore, there is the possibility that the oxidation state of the surface-bound O_2 would affect reactivity, although this has not been systematically investigated.

The degree of charge transfer also affects the kinetics of O_2 dissociation; thus, it has only been possible to isolate and investigate the reactivity of O_2 on a few surfaces: Ag, Au alloys (primarily PdAu and AgAu), and Pt. Even so, only reactions with low barriers are possible because the O_2 is only stable on these surfaces at low (<300 K) temperature.

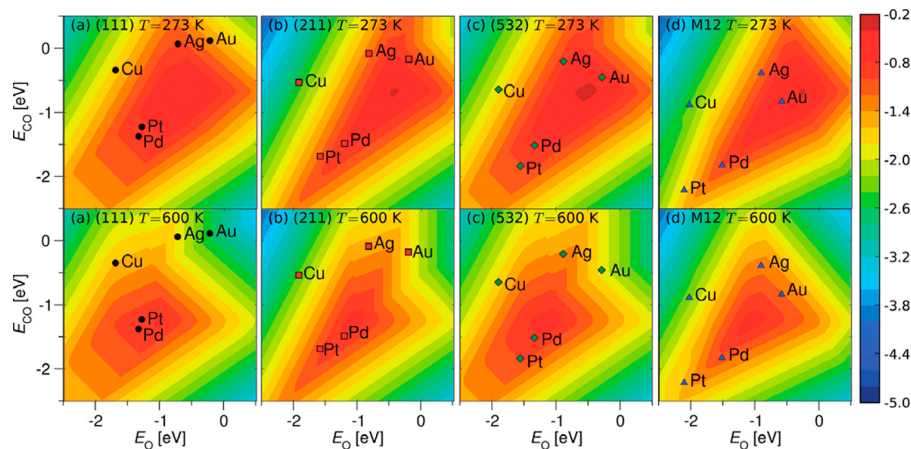


Figure 12. Estimates of the reaction rate for CO oxidation are plotted on a logarithmic color scale as a function of the adsorption energies of O and CO (red is high activity; blue is low). The so-called Sabatier activity is calculated using mean-field microkinetic models using DFT energetics by assuming optimal coverage for all intermediates. For the top row, $T = 273\text{ K}$, $p(\text{O}_2) = 0.21\text{ bar}$, $p(\text{CO}) = 0.01\text{ bar}$; for the bottom row, $T = 600\text{ K}$, $p(\text{O}_2) = 0.33\text{ bar}$, $p(\text{CO}) = 0.67\text{ bar}$. Reproduced from ref 97. Copyright 2009 American Chemical Society.

Even though adsorbed O_2 species are only isolable under ultrahigh vacuum conditions at very low temperature, they will have finite lifetimes on catalytic surfaces at higher pressures and temperatures. For example, the lifetime of O_2 on the Pt(111) surface is on the order of 10 ns at 400 K ($E_{\text{des}} = E_a = 0.41\text{ eV}$, $\nu_{\text{des}} = 10^{13}$, and $\nu_{\text{dis}} = 10^{12}$).^{100,101} For the earlier transition metals, the dissociation barrier is close to 0 and rapid dissociation reactions will most likely predominate. At elevated pressures, however, competitive adsorption, of for example CO, can lower the dissociation rate by blocking the necessary sites for O_2 dissociation.¹⁰² This could effectively enhance the lifetime of O_2 adsorbed on the surface.

The reactions of adsorbed O with various small molecules, including CO, methanol, formaldehyde, olefins, and ammonia, have been widely investigated and are qualitatively described in terms of the Sabatier principle, which suggests that intermediate binding strength leads to the optimal catalyst. Using scaling relationships for both adsorbates and transition states, the catalytic activity of a surface can often be predicted in terms of one or two adsorption energies, and the optimal catalyst has moderately strong adsorption energies for these key intermediate(s).^{94,103} Essentially, the stronger the metal-O bond, the less reactive the oxygen is toward an incoming molecule, such as CO or ethylene. Hence, weakly bound adsorbed O will be most reactive.^{97,104} In the context of catalysis, there must be sufficient bonding (charge transfer) to the O_2 by the metal for dissociation to atomic O but not too strong of a metal-O bond to be reactive, resulting in a so-called “volcano plot” (Figure 12).

There is clearly a significant opportunity to design alloy catalysts that break the linear correlation between O_2 and O bonding, as illustrated by the example of the Pt-based alloys described above. If O_2 dissociation can be enhanced on less reactive metals without correspondingly increasing the metal-O bond strength, the rate of oxidation of incoming molecules can, in principle, be increased. For example, DFT calculations show that scaling relations can be broken on very inhomogeneous alloys^{94,105} and indeed spillover has been observed in IrAu alloys from the Ir active sites to the Au sites.¹⁰⁶ This spillover is presumably driven by some combination of entropy and repulsive interactions between O atoms. In order to fully realize

the use of alloys to further optimize reactivity, it is necessary to synthesize appropriate alloys that retain active configurations under reaction conditions. The few examples of alloy configurations that can potentially change reactivity suggest there is a fertile area of research in the modeling, synthesis, and testing of new alloy catalyst materials.

4.1. Relative Reactivity of Adsorbed O_2 and O

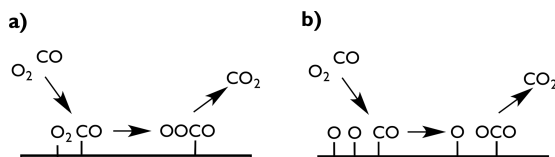
The reactivity of O_2 has only been investigated on a few surfaces on which a molecular state can be isolated at low temperature, as discussed above. Specifically, a few reactions have been studied on Ag, Pt, and alloys of Pd/Au(111). Hence, only reactions with relatively low barriers can be observed on model systems because desorption and dissociation to atomic O dominate at elevated temperature. Under operating catalytic conditions, it is conceivable that O_2 species have sufficiently long lifetimes to react with other molecules present; however, this has been a subject of controversy in the literature. Therefore, it is important to consider patterns of reactivity for O_2 on surfaces because of potential relevance to catalysis and also because peroxy and related species are often important in biological oxidations.¹⁰⁷ It appears that the reactivity between O_2 and another species is primarily controlled by adsorption energies, as is common in catalysis, but this has not been systematically studied. The relative reactivity of peroxy and superoxo species has also not been systematically clarified.

4.2. CO Oxidation

Oxidation of CO to CO_2 is one of the most widely investigated reactions on surfaces because of its simplicity and the fact that it is a key technology in pollution control. Mechanistically, an important question is whether CO reacts directly with adsorbed O_2 to form OCOO or whether O_2 first dissociates, and CO reacts with adsorbed O (Scheme 1). The reaction of CO with atomic O is well-known; however, the CO reaction with surface-bound O₂ has also been reported.

In fact, CO reacts with O_2 bound to transition metal surfaces in most of the few cases that are experimentally accessible. For example, CO_2 is produced from CO reaction with O_2 on Ag surfaces. On Ag(110), O_2 reacts with CO between 95 to 100 K to produce CO_2 .^{108–110} Likewise, CO reacts with O_2 on Pt(111) below 200 K to produce CO_2 .¹¹⁸ On AuPd(111)

Scheme 1. Two Possible Pathways for CO Oxidation on a Surface: (a) an Associative Mechanism and (b) a Dissociative Mechanism



alloys, DFT studies indicate that CO oxidation by O_2 will also proceed on Au-rich surfaces (Figure 13).¹¹¹ The exception is

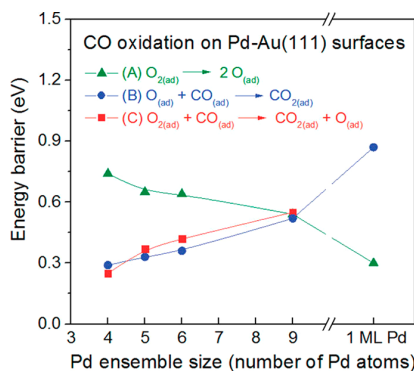


Figure 13. Energy barriers for various CO oxidation mechanisms on a Au(111) surface with various amounts of Pd, calculated using DFT. Reprinted from ref 111. Copyright 2015 American Chemical Society.

Pd(111) for which experimental studies at low temperatures show that CO does not react with O_2 .^{112–114} This may reflect the fact that Pd has a higher affinity for O than Pt does.

While O_2 can react with CO on the few surfaces investigated, the oxidation of CO on transition metal surfaces is generally dominated by reaction of adsorbed CO and adsorbed O in a so-called Langmuir–Hinshelwood mechanism.¹¹⁵ The barrier for this reaction correlates with the adsorption energy of the initial state (adsorbed O and CO), such that the barrier is low on inert surfaces and generally higher on more reactive surfaces.¹⁰⁴

On Ag, atomic O is reactive toward CO, and two O species have been distinguished.^{110,116} DFT calculations indicate that CO oxidation by atomic O on Ag(111) has a very low barrier for reaction of 0.20 eV.¹¹⁷ On Pt(111), CO is readily oxidized by O,^{118,119} with a calculated barrier of roughly 0.75 eV.¹⁰⁴ The reaction with O is generally thought to dominate for both Pt(111) and Pt(110) under catalytically relevant conditions.^{120,121} Recent work suggests that Pt(111) in its most active state is metallic,¹²² although oxidation of the surface under O_2 -rich conditions has been reported.⁶⁹ On Pd(111), experimental studies at low temperatures show that CO reacts with O, even though it does not with O_2 .^{112–114} On Pd, formation of a surface or bulk oxide can decrease activity compared to the metal surface,^{123,124} but a large body of recent work suggests that certain Pd oxides can be more active than the metallic state.^{69,125–127}

The relative contributions of CO oxidation by adsorbed O versus O_2 on Pd/Au(111) alloys are predicted by DFT studies to depend on the distribution of Pd on the surface. The barrier for O_2 dissociation decreases with increasing Pd on the surface so that the reaction of CO and atomic O predominate on Pd-rich surfaces (Figure 13).¹¹¹ At the same time, the barrier for

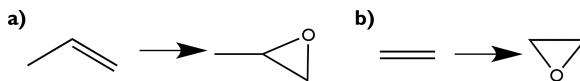
CO reaction with either atomic O or adsorbed O_2 increases with increasing Pd ensemble size, indicative of the stronger metal–O bonding to the surface. Experimental results indicate that isolated Pd atoms do not bind O_2 at 77 K. Ensembles of Pd atoms, identified in IR spectra by their ability to bind CO bridged between Pd atoms, bind O_2 predominantly molecularly. A small fraction dissociates upon heating above 180 K and then readily reacts with CO. Adsorbed molecular O_2 does not react but is displaced by adsorbing CO.¹¹¹ AuPd nanoparticles supported on TiO₂ are active for CO oxidation under elevated pressures, possibly by adsorbate-induced segregation of Pd thus forming these Pd ensembles *in situ*.¹²⁸

Consistent with the expectation that weakly bound O will be highly reactive, preadsorbed O on Au(111), Au(110), and Au(310) readily oxidizes CO to CO_2 .^{117,129,130,569} DFT calculations on stepped and kinked Au surfaces suggest that O₂ can react with CO with a fairly low barrier of 0.09–0.56 eV,^{131,132} but the weak bonding of O₂ and corresponding lack of dissociation apparently prevent this from occurring at appreciable rates, as pure nanostructured gold is not active for CO oxidation.¹³³ The barrier for CO oxidation by O is approximately 0 on the stepped, kinked Au surface.

4.3. Selective Oxidation of Olefins

Selective oxidation of olefins is a major industrial process and, therefore, widely investigated and the subject of several reviews.^{7,23,134} Modified silver is the commercial catalyst for production of ethylene oxide from ethylene and O₂. Selective oxidation of larger olefins (e.g., propene) is more challenging because of the fact that the acidic, allylic hydrogen in these olefins is subject to attack by oxygen (Scheme 2). Hence, there is interest in development of new catalysts for selective oxidation of olefins with acidic C–H bonds.

Scheme 2. Reaction Schemes for (a) Propene Epoxidation, a Case Where the Olefin Has Allylic Hydrogens, and (b) Ethylene Epoxidation



Atomic oxygen is active for olefin epoxidation on Ag and Au surfaces. For example, adsorbed O on Ag(110) leads to epoxidation of the olefin norbornene on Ag(110),¹³⁵ which was used as a proxy for ethylene oxidation. Ethylene itself does not react with atomic oxygen under ultrahigh vacuum conditions because the barrier for desorption of ethylene is lower than the barrier for O addition across the C=C bond. The mechanism often proceeds through formation of an oxametallacycle, although an additional direct mechanism has been proposed for ethylene epoxidation based on DFT studies.^{136,137} While early work suggested that O₂ may be the oxidizing species for ethylene epoxidation on Ag, it has been shown that the active species is actually O.^{138–142} Promoters, such as K and Cl, can strongly affect the activity and selectivity and can be necessary for reaction.^{143,144} The effects of these promoters can also give insight into how to tune selectivity.¹⁴⁵

DFT studies suggest that a surface tends to be a selective catalyst for epoxidation of olefins without allylic hydrogens (e.g., ethylene) if its affinity for carbon-bound species is weak relative to its affinity for oxygen-bound species.^{85,146} This difference in affinity controls whether the oxametallacycle intermediate forms ethylene oxide or acrolein (which typically

combusts before detection); this branching is thought to determine selectivity.^{146–148} Because Cu–C bonds are weak relative to Cu–O bonds, this picture suggests that Cu should be most selective, followed by Ag and then Au. This predicted trend is in agreement with model studies of styrene epoxidation on single crystals, which find extremely high selectivity on Cu, lower selectivity on Ag, and somewhat lower selectivity on Au.^{85,147,149–152} However, Cu oxidizes under reaction conditions, and the oxidized material is less selective. On the basis of experimental correlations, it has also been suggested that the electronic structure of O determines selectivity: electrophilic O leads to epoxidation, while nucleophilic O leads to nonselective oxidation.^{140,153–155} The exact correspondence between this design paradigm and the mechanism has not been elucidated. For Ag(111), chemisorbed O is more selective than O from the surface oxide.¹⁵⁶

For olefins with allylic hydrogens (e.g., propene), selective surfaces favor oxametallacycle formation while nonselective surfaces favor scission of allylic C–H bonds.^{157–159} The reactivity of allylic C–H bonds with atomic O fits the general paradigm of describing oxidation in terms of Brønsted acid–base reactions. While few studies have systematically compared several surfaces for propene epoxidation, it has been suggested that low basicity O atoms should have improved selectivity.¹⁶⁰ Cu(111) has been shown to be selective for the epoxidation of propene and other more complex alkenes,^{159–162} but as for ethylene epoxidation, the surface becomes nonselective when it is oxidized, which is an impediment to the development of practical catalysts. There is somewhat different reactivity of O toward allylic H on Au and Ag surfaces,²³ but single-crystal studies show that both metals produce little or no propene oxide.^{140,163–165} However, by deuterating the methyl hydrogens in propene, some propene oxide can be produced on O/Au(111), showing that even a small decrease in the C–H bond scission rate can allow epoxidation.¹⁶⁴ The lack of propene oxide in single-crystal studies somewhat contrasts with the ability of supported Au catalysts to produce propene oxide in the presence of O₂ and H₂.¹⁶⁶ On Ag(110), O can perform more complex chemistry on alkenes that have additional functionality, including cycloaddition and selective dehydrogenation.^{167–169}

More reactive surfaces, such as Pd and Pt, tend to oxidize olefins to CO₂ or CO and H₂O.^{170–172} On these surfaces, C–H bond scission can be facile even in the absence of O, which may cause them to be nonselective.

4.4. Selective Oxidation of Alcohols

There are indications that O₂ can react directly with alcohols on metal surfaces. On AgAu alloys, DFT studies show that coadsorption of methanol stabilizes adsorbed O₂ by hydrogen bonding. Furthermore, the coadsorption complex leads to facile O₂ activation by H transfer from methanol, forming a hydroperoxyl species, OOH. The barrier for this pathway is 0.55 eV lower than direct dissociation of O₂. However, there is a lower barrier for desorption of O₂ and methanol than for donation of H to O₂, and therefore this reaction may be improbable at low temperature.¹⁷³ On Cl-modified Ag(111)¹⁷⁴ and Pt(111),^{175,176} O₂ was proposed as the species responsible for oxidizing methanol to formate, and it has been suggested that O does not oxidize methanol to formate on Pt(111).¹⁷⁷ However, most work focuses on the interaction between O and alcohols, which is thought to be more relevant for catalysis.²³

Both with and without adsorbed O, alcohols tend to first undergo O–H scission followed by β -hydrogen elimination, and the latter is often the rate-determining step.^{178,179} This is likely a consequence of the tendency for O–metal bonds to be stronger than C–metal bonds⁸⁵ and may reflect the propensity of alcohol O–H bonds to have a higher acidity than C–H bonds. As metals become more reactive, the product of alcohol oxidation tends to switch from coupling products to aldehydes to decomposition products.^{23,180–184} Stabilizing methoxy (particularly with respect to decomposition) can result in formaldehyde formation.¹⁸⁵

On noble metals such as Cu, Ag, and Au, adsorbed O acts as a Brønsted base, and reactants can donate H to the O, or to adsorbed OH or alkoxides.^{173,178,186–189} O can therefore greatly increase the surface reactivity toward alcohols.^{190–193} For example, on Au surfaces, adsorbed O is necessary to break the O–H bond and initiate the reaction, and Au surfaces without O are inert toward alcohols.¹⁸¹ Increased amounts of O reduce the selectivity on Ag and Au,^{194,195} and above ~0.5 ML O, the activity of Cu is reduced.^{191,192,196} At high temperature (580–900 K) and pressure, Ag surfaces restructure and a strongly bound O species is formed; this species is likely responsible for methanol oxidation under industrial reaction conditions.¹⁹⁷ More weakly bound O may be more reactive; for example, O/Ag(110) is more reactive for dehydrogenation of ethoxy than O/Cu(110).¹⁹³ On Ag(111), the Brønsted acidity of surface species correlates with their gas-phase acidity.¹⁹⁸

On more reactive metals, donation of H directly to the metal surface can have a similar or lower barrier than donation to an oxygenate; therefore, oxygenate Brønsted bases are less critical for initiating or facilitating reactions.^{188,189} However, O can still act as a hydrogen scavenger, nucleophile, or Brønsted base and can affect the electronic structure of the surface.^{190,199,200} For example, on Pd(111), 1,2-propanediol forms an alkoxide with or without adsorbed O, but the presence of O increases the amount of decomposition and affects activation barriers.¹⁹⁹ On Pt(111), methanol decomposition proceeds through two routes, both of which proceed through a methoxy intermediate. The methoxy can be dehydrogenated to CO, or the C–O bond in methoxy can break to form C, which can poison the surface at millibar pressures. Adding O to the surface increases the overall decomposition rate significantly, perhaps by cleaning off the adsorbed C.²⁰¹ At lower pressures, O can stabilize methoxy against decomposition.²⁰²

On quite reactive metals such as Rh or Mo, adsorbed O tends to passivate the surface and make it more selective,^{203–205} which is the opposite behavior as inert surfaces. For example, O coverages above 0.5 ML inhibit ethanol decomposition on Mo(110) and improve selectivity to ethylene and H₂.²⁰⁴ On these more reactive metals, the surface is apparently so reactive that O is less reactive by comparison. Further, since the O is more strongly bound, it may be less reactive than on more inert metal surfaces. Qualitatively, the O may prefer to form a stronger bond to the surface over bonding with an H atom from a reactant.

4.5. Other Oxidation Reactions

Ag is a useful testbed for the reactivity of O₂ and O because of the stability of O₂ on Ag surfaces. For example, O₂ can react with ammonia on Ag(111), where the active O₂ state is a transient precursor to the chemisorbed peroxy state.²⁰⁶ On Ag(110), O₂ can oxidize SO₂ or CO.¹⁰⁸ However, on Ag(110) O₂ does not react with ethylene, cyclohexene, or acetonitrile,

although these species do react with adsorbed O.^{169,207,208} Adsorbed O on Ag(110) can also react with the olefin norbornene,¹³⁵ 1,3-butadiene,¹⁶⁷ allyl alcohol,²⁰⁹ π -allyl,²¹⁰ and CO₂.²¹¹ It has been suggested that O₂ on Ag(110) is reactive only toward species that are good π electron acceptors.²⁰⁷ O₂ can break the O–H bond in water on Ag(111) or Cu(111)²¹² but not on Ag(110).²¹³

DFT calculations on close-packed surfaces suggest that the dissociative mechanism for O₂ hydrogenation is more favorable for the more reactive metals Rh, Ir, Ni, and Cu, but the associative mechanism is more favorable for the more inert metals Pd, Pt, Ag, and Au.²¹⁴ This is qualitatively similar to CO oxidation on AuPd surfaces, where more inert surfaces favor associative mechanisms but more reactive surfaces favor dissociative mechanisms due to a lower barrier for dissociating O₂.¹¹¹

Importantly, if O₂ dissociation can be induced, reaction with O on inert surfaces is typically facile, due to the weak binding of O. Indeed, on Au surfaces, O can oxidize a variety of species, such as alcohols, amines, and alkenes,^{151,178,183,184,187} while O₂ desorbs before interacting with other species. The inertness of the surface also results in high selectivity toward many reactions.

Studies have also been performed on metals not traditionally used in catalysis, showing that O₂ and O can both be reactive on these surfaces. At 80 K, CO₂ forms a complex with O₂ on Mg(0001) that is quite reactive and forms carbonate.²¹⁵ Adsorbed O atoms can break O–H bonds in water and methanol on Zn(0001) and can also react with formic acid.²¹⁶ O₂ can react with pyridine on Zn(0001), such that pyridine induces O₂ dissociation.²¹⁷

In some cases, oxidation occurs not by O₂ itself but by recently dissociated, transient, hot O atoms.^{6,218} For example, ammonia oxidation on Cu or Mg surfaces around room temperature occurs through this mechanism.^{219–221}

5. MOLECULARLY ADSORBED O₂ STATES ON PARTICULAR SURFACES

In this section, we discuss molecularly adsorbed O₂ states on particular metal surfaces. We discuss the main features of the adsorbed states in the text and give data from many studies in a series of tables. For simplicity, in each table we give mean values plus/minus a standard deviation, which involves grouping studies of the same state using somewhat different methodologies (e.g., different coverages or computational parameters.) The full tables are available in the *Supporting Information*. We assign the oxidation state where reasonably possible. Since the RPBE functional tends to give fairly different adsorption energies from the PBE and PW91 functionals, we group it separately.

5.1. Group 11 Metals (Au, Ag, and Cu)

5.1.1. O₂ Adsorption on Au Surfaces. Few experimental studies examine adsorbed O₂ on Au surfaces, as it desorbs at a low temperature. On Au(110), O₂ desorbs below 55 K.⁷³ The O₂/Au(110) state has been characterized using UPS and NEXAFS, and these suggest that O₂ is physisorbed. The UP spectrum for the Au atoms in the presence of O₂ is very similar to its spectrum in the presence of other gases, including noble gases, suggesting that the Au is largely unaffected by the presence of O₂. Exposure of Au(111) to an oxygen plasma apparently results in formation of an adsorbed O₂ state that exists on the surface at 77 K and can be desorbed using a beam

of Kr or CO, while exposure to ozone does not generate this species.^{250,251} The origin and nature of this species is unclear, although it may be due to the adsorption of vibrationally or electronically excited O₂ in the plasma jet.

In agreement with the experimental studies, DFT studies show an adsorption energy near 0 (Table 2). Although these studies generally ignore dispersion interactions, the total interaction is still expected to be very weak. Some DFT studies examine unreconstructed Au(110) or Au(100) surfaces, which show somewhat stronger binding. However, these surfaces reconstruct under most conditions (such as vacuum), and therefore these studies are likely to overestimate the binding under most conditions.

5.1.2. O₂ Adsorption on Ag Surfaces. It is generally believed that intact O₂ on Ag(111) can exist in both physisorbed and chemisorbed states. However, there have been some inconsistencies and controversies regarding both of these states. While it seems fairly clear that both states exist, their precise character and importance are less clear. This may be related to the inertness of Ag(111), as established in molecular beam studies. These experiments are consistent with weak interaction of O₂ on Ag(111) in that direct-inelastic scattering along with transient trapping-desorption, ion formation, molecular chemisorption, and dissociative chemisorption have been observed, and the probability for dissociation is generally very low.^{252–260} The inertness and low sticking probability of Ag(111) leads to the possibility that defects and coadsorbates can have a significant influence on measurements.

Many studies have invoked a physisorbed O₂ state on Ag(111), and this state has been used to rationalize or fit TPD data and molecular beam data.^{261,262} Indeed, low-temperature studies have observed a physisorbed O₂ state at 20–25 K on Ag(111) using EELS and UPS.^{253,263} However, molecular dynamics (MD) studies based on a DFT-derived potential energy surface reproduce the experimental trends in sticking coefficient that have been used to justify the importance of the physisorbed state in the dynamics of O₂–Ag(111) interactions. Since this DFT-derived potential energy surface does not feature a physisorbed state due to the lack of dispersion interactions in the functional, this calls into question the importance of the physisorbed state.

Chemisorbed O₂ states have been observed on Ag(111) as well. One study found that dosing at 300 K and at pressures above 10^{−2} Torr results in both adsorbed atomic O and chemisorbed O₂; the intact O₂ desorbed at 380 K.²⁶⁴ However, this state was not observed in another study, which instead found a chemisorbed O₂ state by dosing at 150 K and desorbed at 217 K.²⁶¹ Only a small fraction of this O₂ state dissociated. Other studies have observed that the chemisorbed state desorbs by 210 K²⁰⁶ or dissociates by 300 K.²⁶⁵ The chemisorbed state has also been used to rationalize molecular beam data.²⁶² Further experimental characterization of this state has proven difficult.^{252,257,262} A weakly bound O₂ state has been observed using EELS, XPS, and TPD, and the O₂ has been assigned to both peroxy and superoxo-like states.^{206,212,261,264,266} DFT studies have identified a superoxo state of O₂ bound to the bridge site (Figure 14).^{214,231,232} The large discrepancy between the frequencies from EELS and DFT (Table 2) suggests that the experiments may be observing a different state from that found in DFT, either due to a defect or coadsorbate in the experiments, as suggested previously.^{267–270} Alternatively, the discrepancy may be due to a large, qualitative

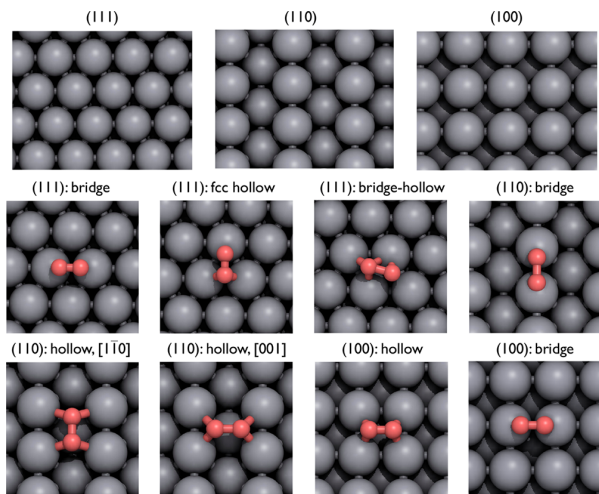


Figure 14. Surface structures of low-index planes of fcc metals and O_2 adsorption sites that are most commonly identified as the lowest energy states on these surfaces. On the (111) facet, the bridge (also called tbt), fcc hollow (fbh), and bridge-hollow (bhf) are shown; the hcp hollow (thb) is identical to the fcc hollow except that it has a metal atom in the second layer directly below the O_2 . On the (110) facet, the bridge and the 4-fold hollow with the O–O axis in the $[1\bar{1}0]$ or $[001]$ directions are shown. On the (100) surface, the 4-fold hollow and the bridge are shown.

error in how the adsorbed O_2 is treated in GGA-DFT. A study employing Raman spectroscopy at higher pressure has found an O–O stretching frequency of 990 cm^{-1} , different from both the UHV and DFT results.¹⁵⁷

Below 160 K, O_2 can be observed in the 4-fold hollow site on Ag(110), in two nearly degenerate configurations (Figure 14): one with the molecular axis in the $[1\bar{1}0]$ direction (parallel to the trough in which it lies) and one with the axis perpendicular to the trough (the $[001]$ direction).^{271,272} These two configurations have somewhat different vibrational frequencies, with both DFT and EELS indicating that the $[001]$ species has a higher frequency (Table 2). Most studies suggest that both of these are peroxy species. However, a DFT study that used a + U correction on the p states of O_2 was able to reproduce the experimental inelastic electron tunneling scattering spectrum, while the spectrum was incorrectly predicted without the + U correction.⁶² When including this correction, the $[001]$ configuration is a superoxo state, while the $[1\bar{1}0]$ configuration is a peroxy state (Figure 3b). This is not inconsistent with experimental studies identifying the O_2 as a peroxy species based on its electronic structure, as they have generally found the O–O axis to be in the $[1\bar{1}0]$ direction.²⁴² The O_2 species are fairly mobile, with a diffusion barrier of $0.22 \pm 0.05\text{ eV}$.²⁷³ There are small O_2 – O_2 repulsive interactions (0.02 – 0.04 eV) for nearest neighbors, and attractive interactions of a similar magnitude for second nearest-neighbor or diagonal interactions.

The literature is somewhat inconsistent on how the two species are formed. An EELS study claimed that heating a physisorbed O_2 layer (originally dosed at 40 K) results in purely the $[001]$ state, while O_2 dosed at a higher temperature results in population of both states.²⁴⁰ However, it has also been claimed that heating physisorbed O_2 results in the formation of both states, while direct chemisorption from the gas-phase²⁷⁴ results in mostly $[1\bar{1}0]$ oriented molecules.²³⁵ A physisorbed

state has been observed at about 30 degrees with respect to the surface and is thought to lie in the $[001]$ direction.^{240,275,276}

O_2 can chemisorb on the Ag(100) surface at low temperatures (e.g., 60 K),^{246,277} and EELS spectra suggest that there are two peroxy species in different sites (Table 2). The O_2 can be stabilized to a higher temperature by coadsorbing sodium.²⁷⁸ At room temperature, less than 0.5% of adsorbed O_2 molecules dissociate, and they may be dissociating at kink sites.²⁷⁹ The O_2 is thought to reside in the 4-fold hollow, based on STM, tight-binding calculations, and DFT calculations (Figure 14). Using Raman spectroscopy, a study at higher pressure assigned a frequency of 957 cm^{-1} to the O–O stretch, significantly higher than the DFT and UHV results.¹⁵⁷

5.1.3. O_2 Adsorption on Cu Surfaces. In the range of 100–300 K, chemisorbed O_2 (alongside adsorbed O) has been observed on Cu(111) using EELS and photoelectron spectroscopy.^{224,265,280} The amount of O_2 present decreases upon heating, with most (but not all) disappearing upon annealing to 170 K²²⁴ and very little remaining at 300 K. Recent DFT results show that the lowest energy states are the fcc hollow site and bridge-hollow site.^{223,281} These sites have respectively been calculated to have stretching frequencies of approximately 770 and 650 – 660 cm^{-1} , in reasonable agreement with the experimental values of 820 – 870 and 610 cm^{-1} . The remaining discrepancy may be due to coverage effects (e.g., the presence of adsorbed O in the experiment) or may be due to an inaccuracy in the DFT calculations. Although an earlier DFT study suggested that superoxo species may be present (in the bridge site),²²⁶ more recent work indicates that only peroxy species are present and the two observed EELS species are peroxy species in two sites.²²³ Assuming that the DFT assignments are correct, EELS indicates that the bridge-hollow site is dominant at low coverage, and the fcc hollow is dominant at high coverage.²²⁴

Adsorbed O_2 has proven difficult to observe on Cu(110). Upon exposure of Cu(110) to O_2 at 80–100 K, some studies observe no chemisorbed O_2 , suggesting that all O_2 dissociates.²⁸² However, other studies, including some that dose at 100 K, indicate that a small fraction of the adsorbed O_2 does not dissociate.^{265,283} An STM study with the surface at 4 K but the incident O_2 at 300 K observed both O_2 molecules and O atoms in the 4-fold hollow site.²⁸³ DFT calculations suggest that O_2 adsorbs in the 4-fold hollow, and the dissociation barrier is approximately 0 if the O–O axis is along the $[001]$ direction, but it is 0.12 eV if the O–O axis is along the $[1\bar{1}0]$ direction.²²⁸ This is generally consistent with the experimental results, except that STM seems to indicate preferential dissociation along the $[1\bar{1}0]$ direction.²⁸³ The vibrational frequency from EELS (660 cm^{-1}) and the magnetic moment from DFT (0) both suggest that the chemisorbed O_2 is in a peroxy state. The chemisorbed molecular O_2 dissociates completely at 150 K,²⁸⁴ and O_2 dosed at higher temperatures adsorbs dissociatively.^{287,288}

Adsorbed O_2 has been observed alongside O on Cu(100) upon dosing at 100 K,^{229,265,285} and it is completely dissociated at 250–300 K. Physisorbed O_2 has also been observed, with an O–O distance of 1.21 \AA (identical to the gas-phase).²³⁰ The chemisorbed O_2 has been shown to be fairly flat, with an angle of about 30° , using XAS.²³⁰ Adsorption is exclusively dissociative at higher temperatures.²⁸⁷

Table 3. Properties of Adsorbed O₂ on Group 10 Metal Surfaces^a

ox state	magnetic moment (μ_B)	$\nu(O-O)$ (cm ⁻¹)	$d(O-O)$ (Å)	O ₂ ads energy (eV)	notes/ref
Ni(111)					
peroxy	0.20 ± 0.05	679 ± 17	1.46 ± 0.01	-1.61 ± 0.24	3-fold hollow ^{b,65,214,223,233}
peroxy	0.26 ± 0.04	711 ± 16	1.46 ± 0.01	-1.01 ± 0.01	3-fold hollow ^{c,289}
Ni(100)	—	—	1.24	—	exptl ^{d,290}
Pd(111)					
superoxo	0.54 ± 0.34	993 ± 47	1.34 ± 0.02	-0.82 ± 0.18	2-fold bridge ^{b,65,75,291,292}
superoxo	—	1004 ± 32	—	—	ν increases with coverage. exptl ^{e,293–297}
peroxy	0.03 ± 0.05	909 ± 27	1.37 ± 0.02	-0.97 ± 0.40	3-fold hollow ^{b,65,214,233,298}
peroxy	—	832 ± 19	—	—	ν increases with coverage. exptl ^{e,293–297}
peroxy	—	622 ± 21	—	—	exptl ^{e,293–297}
Pd(100)	—	726	—	—	exptl ^{e,299}
—	0	—	—	-0.76	4-fold hollow ^{b,300}
Pt(111)					
superoxo	0.63 ± 0.24	931 ± 76	1.36 ± 0.02	-0.63 ± 0.15	2-fold bridge ^{b,64,65,214,301–303}
superoxo	0.62	930	1.35	-0.22	2-fold bridge ^{c,289}
superoxo	—	871 ± 3	—	—	exptl ^{e,310,304–306}
peroxy	0.00 ± 0.00	743 ± 75	1.40 ± 0.03	-0.68 ± 0.09	3-fold hollow ^{b,65,83,233,301–303}
peroxy	—	698 ± 10	—	—	exptl ^{e,310,304–306}
peroxy	0	827	1.39	-0.17	3-fold hollow ^{c,289}
peroxy	—	—	1.39 ± 0.06	—	exptl ^{d,242,307,308}
Pt(110)					
peroxy	0.21	877	1.36	-1.45	2-fold bridge, reconstructed ^{b,309}
peroxy	—	850 ± 14	—	—	exptl ^{e,310,311}
peroxy	—	—	1.38 ± 0.01	-1.58 ± 0.01	2-fold bridge, unreconstructed ^{b,312,313}
superoxo	—	1250	—	—	exptl ^{e,310}
peroxy	—	930	—	—	exptl ^{e,310}
Pt(100)	—	—	1.37	-1.02	2-fold bridge, unreconstructed ^{b,312}
peroxy	0	—	—	-0.75	4-fold hollow, unreconstructed ^{b,300}

^aExperimental (Exptl) data are marked; others are computational. Methods are given below. ^bDFT(PBE/PW91). ^cDFT(RPBE). ^dXAS. ^eEELS.

5.2. Group 10 Metals (Pt, Pd, and Ni)

5.2.1. O₂ Adsorption on Pt Surfaces. Both superoxo and peroxo O₂ chemisorption states have been observed in many studies on Pt(111), using both experimental and computational techniques (Table 3). The superoxo species lies in the bridge site and has a magnetic moment of approximately 0.6 μ_B , while the peroxo state lies in the fcc hollow site and has no magnetic moment. Both species lie nearly parallel to the surface, although the fcc hollow state is at a slight angle.³¹⁴ The species are nearly degenerate, with the energy difference likely depending on coverage. Experimental work using a molecular beam showed that for high incident kinetic energies only the peroxo state is populated at low coverage, while the superoxo state also appears at higher coverage.³⁰⁵ The superoxo state can be converted to the peroxo state using X-ray radiation or heating.³⁰⁷ A physisorbed state has also been observed, in which the O₂ lies parallel to the surface, although in multilayers O₂ lies perpendicular to the surface.³⁰⁸ The physisorbed species acts as a precursor to molecular chemisorption^{315,316} and is converted to a chemisorbed species around 30 K.³¹⁷ The barrier for this transformation has been calculated to be 0.05 eV using DFT.³¹⁸ Upon heating the physisorbed state, the superoxo species appears first, which is converted to the peroxo species around 135 K.³⁰⁷

Many studies have observed O₂ on Pt(110), which exhibits a missing row (1 × 2) reconstruction, at temperatures below 133 K.^{310,311,319–323} At low coverage (<1/2 ML), O₂ appears to

adsorb in the bridge site between two top-layer Pt atoms, with the axis along the Pt row. (An early study identified the bottom of the trough as the adsorption site, based on a mistaken assumption concerning the site preference of Xe.)^{309,320} At higher coverage, another O₂ state appears, which is likely adsorbed on the (111) microfacets. These states are thought to be peroxo, but this is not clear.^{309,310} At even higher coverage, a superoxo state appears. The O₂ does not induce a structural change on either the (1 × 2) or (1 × 1) structures.³²⁴

Pt(100) has received much less attention than Pt(111) or Pt(110). Adsorbed O₂ states have been observed using DFT; they occupy the bridge site with a low barrier for dissociation.^{313,325,326} These DFT studies focus on the unreconstructed surface, even though Pt(100) undergoes a hexagonal reconstruction. However, since adsorbed O can reconstruct the Pt(100) surface to a (3 × 1) or (1 × 1) structure, the unreconstructed surface may be the most relevant under some conditions.³²⁷

5.2.2. O₂ Adsorption on Pd Surfaces. Below 110 to 160 K, O₂ adsorbs molecularly on Pd(111),^{295,296,328–330} and EELS measurements indicate the presence of three species, two of which are peroxo and one of which is superoxo. DFT calculations generally predict the hollow site is the most stable for adsorbed O₂,^{214,233,298} and this has been identified with one of the peroxo states (~850 cm⁻¹) based on DFT and STM.^{75,329} STM measurements at 25 K suggest that O₂ resides primarily in the fcc hollow site, with some occupation of the

Table 4. Properties of Adsorbed O₂ on Group 9 Metal Surfaces^a

ox state	magnetic moment (μ_B)	$\nu(O-O)$ (cm ⁻¹)	$d(O-O)$ (Å)	O ₂ ads energy (eV)	notes/ref
Co(0001)					
Rh(111)	0.46	—	1.5	-2.26	3-fold hollow ^{b,233}
peroxo	0.00 ± 0.00	675	1.41 ± 0.04	-1.73 ± 0.26	3-fold hollow ^{b,214,233,344}
superoxide	1	—	1.32	-1.95	2-fold bridge ^{b,344}
Ir(111)					
peroxo	0.00 ± 0.00	691 ± 17	1.43 ± 0.01	-1.17 ± 0.14	2-fold bridge ^{b,77,214}
—	—	805	—	—	high O coverage, exptl. ^{c,345}
peroxo	0.00 ± 0.00	513	1.46 ± 0.03	-1.21 ± 0.05	3-fold hollow ^{b,77,233}
—	—	740	—	—	high O coverage, exptl. ^{c,345}
Ir(100)	—	—	1.38	-2.1	2-fold bridge ^{b,346}

^aExperimental (exptl) data are marked; others are computational. Methods are given below. ^bDFT(PBE/PW91). ^cEELS.

hcp hollow site.³²⁹ The bridge site is also quite stable,²⁹² and this has been identified with the superoxo state (~1010 cm⁻¹), similar to the case for Pt(111). The weaker adsorption in the bridge site predicted with DFT is consistent with the lower temperature desorption peak associated with this state.²⁹⁶ The EELS peaks shift to higher wavenumber as coverage increases.²⁹⁴

The second peroxo state observed in EELS, with an O–O stretching frequency of 600 to 650 cm⁻¹, has not been identified in DFT or STM, although it has been speculated to be associated with O₂ islands or coadsorbed H.^{75,329} This state can be generated by heating the hollow-site O₂²⁹⁴ or by waiting,²⁹⁶ and the activation energy for this conversion is estimated to be 0.3 to 0.5 eV, depending on the coverage. A physisorbed O₂ state has also been observed, which can act as a precursor to the chemisorbed state.^{294,331,332}

Below 160 K, molecularly adsorbed O₂ can be observed on Pd(110) alongside O³³³ while exposure at 200 K or heating to 160 K results purely in dissociation.³³⁴ Most O₂ dissociates even at 80 K,³³⁴ and at 110 K coadsorbed O is necessary to keep some O₂ in the molecular state. On the basis of DFT calculations, the most stable O₂ adsorption site is the bridge site (Figure 14).

At higher O coverages and low temperatures (below 90 K), adsorbed O₂ can be observed on Pd(100).^{299,335,336} This state has a stretching frequency of 726 cm⁻¹, which is likely indicative of a peroxo species. DFT calculations suggest that the adsorbed O₂ lies in the hollow site.³⁰⁰

5.2.3. O₂ Adsorption on Ni surfaces. While dissociation is thought to proceed through a molecular precursor,³³⁷ O₂ dissociation apparently has a very low activation energy on Ni surfaces, such that observing this precursor has proven quite difficult. On Ni(111) surfaces partially covered with Ag, molecular O₂ can be observed at 100 K, although it dissociates below 250 K.³³⁸ DFT studies have observed molecular O₂ on Ni(111) with a low dissociation barrier (Table 3). It is likely that the magnetic surface induces some magnetism on the adsorbed O₂, complicating the determination of its oxidation state. Molecular O₂ has been observed on Ni(100) at 80 K and high exposure, but its short O–O bond (1.24 Å) and vertical orientation suggest that it is weakly interacting with the surface and may even be physisorbed.²⁹⁰ Work function measurements on Ni(111) and Ni(100) indicate the presence of an O₂ state that is stable until 25 K, but the character of this state is unclear.³³⁹ Other studies on Ni(111), Ni(110), and Ni(100) at 8–147 K show only dissociative adsorption, unless the surface

is oxidized, in which case physisorption can be observed.^{265,340–343} This discrepancy in whether O₂ is observed may be due a residual gas layer on the surface for some low-temperature experiments.³⁴⁰

5.3. Group 9 Metals (Ir, Rh, and Co)

5.3.1. O₂ Adsorption on Ir Surfaces. At 68 K and high coverage, some chemisorbed O₂ has been observed on Ir(111) using EELS (Table 4).³⁴⁵ Chemisorbed O₂ states have also been identified using DFT, with the lowest energy state in the bridge site, and a state 0.10 eV higher in the fcc hollow site.⁷⁷ The DFT calculations show a magnetic moment of 0, indicating a peroxo species. The experimental and theoretical frequencies are not in close agreement, which may be partly due to the high O coverage in the experiment. Above 180 K, all adsorption is dissociative.³⁴⁷

On Ir(110), molecular O₂ can form below 100 K.³⁴⁸ Experimental results suggest that chemisorption can occur through a physisorbed precursor or directly from the gas phase.^{348–352} The energetics of the physisorbed and chemisorbed states have been mapped out in detail.³⁵² The effective activation barrier for O₂ chemisorption from the gas phase is 0.22 eV, and the dissociation barrier from the chemisorbed state is 0.11 eV lower than the desorption energy. Somewhat unusually among the late transition metals, on this surface the presence of oxygen³⁵² or a surface oxide³⁵³ apparently has little effect on O₂ dissociation. Adsorbed O can also lift the missing row reconstruction on Ir(110).³⁵³ On Ir(100), DFT calculations predict that O₂ can stably reside in the bridge site, although it dissociates spontaneously when placed in some other configurations.³⁴⁶

5.3.2. O₂ Adsorption on Rh and Co Surfaces. Although kinetic studies suggest O₂ dissociation on Rh(111) is precursor mediated, O₂ dosed at 40 K results in complete dissociation.³⁵⁴ DFT studies have identified O₂ adsorbed states, with the peroxo state in the hollow sites nearly degenerate with a superoxo state in the bridge site.³⁴⁴ Experimental studies have not identified an O₂ adsorbed state on Co surfaces, but DFT calculations show a stable O₂ adsorbed state (Table 4).²³³

5.4. Groups 4–8

On most metals from groups 4 through 8, O₂ adsorption is purely dissociative until the O coverage is high, at which point O₂ can physisorb or chemisorb at low temperatures. Presumably, adsorbed O or a surface oxide passivates the surface enough for O₂ to be stable. For example, on Ru(0001) even at 100 K only dissociative adsorption has been observed at

Table 5. Properties of Adsorbed O₂ on Metal Surfaces from Groups 4–8^a

ox state	magnetic moment (μ_B)	$\nu(O-O)$ (cm ⁻¹)	$d(O-O)$ (Å)	O ₂ ads energy (eV)	notes/ref
Ru(0001)					
peroxo	0	—	1.48	-1.36	fcc hollow ^{b,302}
peroxo	0	—	1.42	-0.96	bridge ^{b,302}
—	—	790	—	—	only at high O coverage ^{c,355}

^aExperimental (exptl) data are marked; others are computational. Methods are given below. ^bDFT(PBE/PW91). ^cEELS.

Table 6. Properties of Adsorbed O₂ on Metal Surfaces Dominated by s and p Electrons^a

ox state	magnetic moment (μ_B)	$d(O-O)$ (Å)	O ₂ ads energy (eV)	notes/ref
Be(0001)				
superoxo	0.8	1.47	-1.12	3-fold hollow ^{b,365}
Ba(110)				
—	—	1.48	-4.09	off-center hollow site ^{b,366}
Pb(111)				
—	—	1.44 ± 0.02	-1.07 ± 0.01	3-fold hollow ^{b,367,368}
—	—	1.45 ± 0.03	-1.08	bridge-hollow-bridge site ^{b,367,368}

^aExperimental (exptl) data are marked; others are computational. Methods are given below. ^bDFT(PBE/PW91).

lower coverages,³⁵⁶ while chemisorbed O₂ has been observed at higher O coverages (Table 5).³⁵⁵ DFT calculations have identified a stable peroxo O₂ state on Ru(0001), which presumably has a low dissociation barrier and is thus difficult to observe experimentally.³⁰² At a temperature of 5 K, physisorbed and weakly chemisorbed O₂ species have been observed on W(111) but only after the adsorbed O state is saturated.³⁵⁷ O₂ states on W(112) have been observed at 100 K, after the O coverage is high enough.³⁵⁸ Physisorbed O₂, with a desorption barrier of 0.08 eV, has been observed on W(110) at high O coverage.³⁵⁹ On Re(0001), a peroxo species has been observed experimentally at 50 K alongside O.³⁶⁰ On Ti(0001), a small amount of molecular O₂ has been observed at room temperature, alongside adsorbed O.³⁶¹ O₂ dissociates easily on Cr(110),³⁶² although at 100 K a superoxo state has been observed alongside O.^{363,364}

5.5. Metals Dominated by s and p Electrons

Most metals outside of the d block are quite reactive toward O₂, and hence O₂ states are not often observed (Table 6). Adsorbed O₂ states have been studied using DFT on Pb(111) and Ba(110). On Pb(111), thin films of 3 to 11 layers have O₂ adsorption energies that vary by up to 0.2 eV, due to quantum size effects, and the experimental oxidation rate also varies based on the thickness.^{367,369,370} On Mg(0001), O₂ adsorption is dissociative at 80 K, but molecular O₂ can be stabilized by coadsorption of CO₂.²¹⁵ No barrier for O₂ dissociation on Mg(0001) is found by DFT calculations, but this may be a failing of the adiabatic method.³⁶⁵ Chemisorbed O₂ can form on Zn(0001), which is likely stabilized by adsorbed O or a surface oxide.³⁷¹ On Be(0001), a chemisorbed O₂ state in the hcp hollow has been observed in DFT.³⁶⁵ Notably, while O₂ is nearly always quite parallel to transition metal surfaces, for simple metals it can prefer to lie perpendicular to the surface.

6. MECHANISMS AND BARRIERS FOR O₂ DISSOCIATION

In this section, we focus on O₂ dissociation on various surfaces, again giving averaged results (plus/minus a standard deviation) in tables while providing a general overview in the text. Full tables are available in the Supporting Information.

6.1. Group 11 Metals (Au, Ag, and Cu)

6.1.1. O₂ Dissociation on Au Surfaces. Au is the most inert metal with respect to oxygen, such that O₂ dissociation has not been observed on pure, unsupported, metallic Au, even on highly stepped surfaces,³⁸² except at temperatures above 970 K and pressures of 1 bar.^{383,384} DFT calculations show that the O₂ activation barrier is much higher than the desorption energy, even at steps and kinks.³⁸⁵ Early reports of O₂ dissociation on Au surfaces are likely due to contaminants.^{386–391} Some Au catalysts can perform oxidation reactions using O₂, but the O₂ activation is thought to be due to the Au-support interface,^{392–394} or the presence of basic conditions, aqueous conditions, and/or coadsorbates. For example, H₂,³⁹⁵ water,^{394,396,397} and OH^{188,189} have all been shown to aid in O₂ dissociation on Au catalysts. Small nanoclusters may also be able to activate O₂.^{398–400} Field-ion microscopy experiments have shown that a Au tip can change in response to an O₂ atmosphere, and it was proposed that a surface oxide was formed.⁴⁰¹ However, several later studies show negligible O₂ dissociation or catalytic activity for nanostructured Au, even for Au nanoparticles on non-oxide supports.^{133,402–404} Recently, experimental and computational work have suggested that twinning sites on nanostructured Au may be able to catalyze CO oxidation by O₂.⁴⁰⁵

Since pure Au is generally quite inert, it is selective but not very active. By doping Au with more reactive metals in the right concentrations, it is possible to create a catalyst that retains high selectivity but is much more active. Generally, a significant ensemble size of the dopant species is necessary for the surface to behave significantly differently than pure Au with respect to O₂ activation. This may be due to the large number of surface atoms involved in O₂ activation and the tendency for Au atoms to passivate most dopants.

Several studies have examined the interaction of O₂ with AuPd alloys as well as CO oxidation on these alloys, in order to understand the effectiveness of AuPd alloys for catalyzing oxidation reactions.^{189,406} DFT studies on PdAu(111) surfaces consistently show that large Pd ensemble sizes are needed in order for the O₂ barrier to become lowered significantly from pure Au.^{111,291,407} For example, 1 or 2 Pd atoms in Au(111) have a high O₂ dissociation barrier of roughly 1.2 eV, and more than 6 Pd atoms are needed before the dissociation barrier is

lower than the desorption energy.¹¹¹ This is in agreement with experimental work, where TPDs of AuPd(111) surfaces show no O₂ dissociation for Au coverages over 0.6 ML,⁴⁰⁸ and CO oxidation requires contiguous Pd sites.⁴⁰⁹ On the basis of DFT results, O₂ dissociation has a significantly lower barrier on AuPd(100),^{410,411} but these studies examine an unreconstructed surface, and it is unclear whether the alloy surfaces form a hexagonal reconstruction as does Au(100). DFT studies also consistently show that any CO oxidation that occurs on small AuPd ensembles likely undergoes the OCOO mechanism.^{412–415} However, O₂ desorption appears to be more facile than OCOO formation in most of these cases. Indeed, TPD experiments on AuPd(111) show that only O₂ that dissociates contributes to CO oxidation, while molecular O₂ does not react with CO.⁴⁰⁸ For larger Pd ensembles, the O₂ dissociation pathway becomes more favorable than the OCOO pathway. Therefore, while the OCOO mechanism cannot be completely ruled out for AuPd catalysts in reaction conditions, the O₂ dissociation mechanism is likely the dominant pathway, as it appears to be under UHV conditions.

AgAu alloys have also attracted significant attention, due to the high catalytic performance of AgAu alloys such as nanoporous Au.^{416–419} This work shows that adding Ag into Au alloys increases their reactivity. However, in most configurations, a significant amount of Ag is necessary in order to significantly reduce the O₂ dissociation barrier.^{231,420} Similarly, even a surface coverage of 0.5 ML Au on a Ag(110) surface prevents almost all O₂ dissociation.²³⁷ Since nanoporous Au is usually just 1–3% Ag, it was initially unclear if surface structures with a high local concentration of Ag form. Further, the activation energy for O₂ dissociation on nanoporous Au has been measured to be 0.22 eV,⁴²¹ significantly lower than most DFT results on AgAu surfaces. It has been proposed that O₂ activation on nanoporous Au occurs through O₂ interaction with methanol¹⁷³ or CO.¹³² While these mechanisms cannot be ruled out, experimental evidence suggests that nanoporous Au can dissociate O₂ in the absence of other species, as exposing nanoporous Au to O₂ results in a strongly bound oxygen species.⁴²¹ A possible resolution to this issue has been suggested using DFT-based thermodynamic modeling of AgAu surfaces in O₂ atmospheres.⁴²² These results suggest that, under oxidation reaction conditions, AgAu bimetallic steps form. These bimetallic steps have a low activation energy for O₂, in qualitative agreement with the experimental results.

O₂ dissociation has been studied on the Au(111) surface doped with a variety of transition metal atoms using DFT.⁴⁰⁷ All dopant atoms decreased the barrier for O₂ dissociation, from a value of 1.90 eV on pure Au(111) to 0.38 eV for Ni-doped Au(111). On Au(111) surfaces doped with Ir, spillover of O atoms from the Ir active sites to Au sites has been observed.¹⁰⁶ Similarly, spillover has been observed on Au surfaces with Ca impurities.⁴²³

6.1.2. O₂ Dissociation on Ag Surfaces. The reactivity of Ag(111) toward O₂ has been somewhat controversial, with different studies giving initial sticking coefficients that vary from <10⁻⁸ to 10⁻³.^{211,254,260–262,268,269,381,424,425} This disagreement persists even for studies with similar conditions: for molecular beams with incident energies of 0.1 to 0.8 eV, sticking coefficients of 3 × 10⁻⁴ and <6 × 10⁻⁷ have been reported by separate groups.^{257,268,269,381} At low impact energy and room temperature, little or no dissociation is observed, while at higher temperatures dissociation can be induced.^{257,381} The

barrier has been estimated as 0.73 eV³⁸¹ or 0.36 eV,²⁶¹ again showing large variation between different experiments. Some studies observe both direct and precursor-mediated dissociative sticking, both of which are strongly activated processes.³⁸¹ The barrier for O₂ dissociation has been calculated to be roughly 1 eV using DFT (Table 7). Molecular dynamics studies based on

Table 7. O₂ Adsorption Energies and Dissociation Barriers on Group 11 Metals^a

	O ₂ ads energy (eV)	O ₂ dissociation barrier (eV)	notes/ref
Cu(111)			
−0.87 ± 0.13	0.09 ± 0.10	3-fold hollow site ^{b,222,223}	
−0.85 ± 0.03	0.13 ± 0.03	bridge-hollow ^{b,222,223,281}	
−0.53 ± 0.04	0.22 ± 0.02	bridge-hollow-bridge ^{b,214,225,226}	
−	0.13	exptl ^{c,372}	
Cu(110)			
−1.58 ± 0.08	0.04 ± 0.07	4-fold hollow site ^{c,228,373}	
−	0.03	exptl ^{d,374}	
−	0.17	exptl ^{e,375}	
Cu(100)			
−	0.51	2-fold bridge, unreconstructed ^{b,376}	
−	0.11	exptl ^{c,377}	
−	0.12 ± 0.07	exptl ^{e,378,379}	
Ag(111)			
−0.12 ± 0.03	1.15 ± 0.08	2-fold bridge ^{b,214,231,232,380}	
−0.08 ± 0.39	1.00 ± 0.14	3-fold hollow ^{b,232}	
−0.4	0.54 ± 0.26	exptl ^{f,261,381}	
Ag(110)			
−0.39 ± 0.16	0.43 ± 0.06	4-fold hollow, [001] ^{b,236–239}	
−0.44 ± 0.14	0.52 ± 0.09	4-fold hollow, [1̄10] ^{b,231,235–239}	
−0.4	0.34	exptl ^{f,261}	
Au(111)			
−0.04 ± 0.06	2.16 ± 0.31	2-fold bridge slightly preferred ^{b,214,231,233}	
Au(110)			
−0.19	0.85	2-fold bridge, unreconstructed ^{b,231}	
Au(100)			
−0.22	0.44	4-fold hollow, unreconstructed ^{b,248}	

^aExperimental (exptl) data are marked; others are computational. Methods are given below. ^bDFT(PBE/PW91). ^cEllipsometry.

^dMolecular beam. ^eWork function measurements. ^fTPD.

a DFT-derived potential energy surface also demonstrate that flat Ag(111) is quite inert, with no direct dissociation observed until the incident energy is above 1.2 eV.²⁶⁷ However, DFT studies show that subsurface O can somewhat reduce the barrier for O₂ dissociation²³² and that the stepped (211) surface has a dramatically lower barrier of 0.09 eV.⁴²² Similarly, experimental studies show that coadsorbates such as OH and H₂O can promote O₂ dissociation.^{212,257} Overall, the literature suggests that flat, clean Ag(111) is quite inert toward O₂ with a low sticking coefficient, but that steps, defects, and coadsorbates can dramatically change its reactivity. As remarked previously,^{267–269} defects and contaminants are the most likely explanation for the variations in experimental results.

Ag(110) is more reactive toward O₂ than either Ag(100) or Ag(111) and has consequently received somewhat more attention with regard to O₂ dissociation. Direct dissociation can occur at high initial translational energies but not at low initial translational energies,²³⁸ such that dissociation under

most conditions is likely precursor-mediated. Chemisorbed O₂ dissociates on Ag(110) at around 180 K.^{240,241,426}

However, there has been some controversy concerning the reactivity of the two O₂ adsorbed states, [001] and [1̄10]. STM studies showed that the tip induces dissociation in the [1̄10] state and either rotation or dissociation in the [001] state, depending on the tunneling direction.²⁷² However, a later STM study suggested that thermal dissociation occurs only in the [001] direction.⁴²⁶ This was resolved by a DFT study, which compared dissociation and rotation barriers at various electric field strengths and showed that the [1̄10] state should dissociate in the presence of a field while the [001] state should dissociate in the absence of a field.²³⁹ However, it has also been suggested that O₂ dissociation results in hot O atoms, which displace other O₂ molecules.^{427,428} This mechanism suggests that the [1̄10] state is dissociating, as hot atom motion seems more likely along the [1̄10] direction, which is along the troughs between Ag atoms. Further, an EELS study has shown evidence that the [1̄10] state dissociates O₂.²⁴⁰ Therefore, it is possible that both the [001] and [1̄10] states dissociate O₂ with nonzero probabilities, and that these probabilities depend on the conditions. A DFT study also suggested that the vibrational coupling to phonons in the Ag surface may cause dissociation in the [001] direction to be preferred.²³⁶ If so, the relative reactivity of the two species may depend on temperature. Further, the coverage of both O₂ and O may affect the relative dissociation rate of the two states, as the energetic differences are small. In some experimental work, subsurface O was found to be present.²⁴²

After dissociation, at low temperatures adsorbed atomic O is present, but at higher temperatures an added-row reconstruction forms.⁴²⁹ Unlike Ag(111), there is evidence that O₂ does not interact with water on Ag(110), which may make this surface less sensitive to contaminants.²¹³

O₂ dissociation on the Ag(100) surface has a significant barrier: MD studies based on DFT only observe dissociation for incident energies above 1.05 eV, although singlet O₂ can dissociate for energies as low as 50 meV.⁴³⁰ The experimental results show similar low sticking at low incident energies, which increases at higher energies.⁴³¹ The sticking decreases dramatically with coverage. Additionally, the dissociated O can induce a missing row reconstruction.⁴³²

6.1.3. O₂ Dissociation on Cu Surfaces. O₂ dissociation on Cu(111) is generally precursor mediated. Some adsorbed O₂ dissociates at 100 K, and by 300 K nearly all of the O₂ has dissociated,²⁶⁵ such that dosing at 300 K results in only dissociation.⁴³³ Measurements of the apparent activation energy suggest it is low, in the range of 0.09 to 0.17 eV.³⁷² DFT calculations generally give activation barriers in the same range (Table 7). As the surface oxidizes, the activation barrier is predicted to increase.³⁷³

The results of molecular beam experiments for O₂ on Cu(110) suggest that there are two dissociation channels. The first is a trapping mechanism, likely into a physisorbed state, and the other is activated dissociative chemisorption (which could be direct or through a short-lived chemisorbed state).^{434,435} DFT calculations suggest that O₂ precursors can exist on the surface, in agreement with low-temperature experimental studies, although dissociation is complete by 45 K.⁴³⁶ The DFT calculations also show no barrier for dissociation from some O₂ configurations. The activation barrier has been experimentally estimated as 0.03 to 0.17 eV, and DFT calculations are in agreement (Table 7). On the basis

of STM studies, the dissociation of O₂ in the hollow site can occur in both the [1̄10] and [001] directions, with a preference for the [1̄10] direction.²⁸³

Cu(100) appears to be quite reactive toward O₂ dissociation,^{229,437} although the literature is somewhat inconsistent as to whether this is intrinsic to the flat surface or is due to defects. Two experimental studies have shown that the activation energy is higher at higher temperature, with the increase occurring at 300 K³⁷⁸ or 473 K,³⁷⁷ and no barrier at low temperature.³⁷⁷ A direct dissociation mechanism has been proposed based on molecular beam studies.⁴³⁸ However, some experimental and computational work has suggested that defects are important for O₂ dissociation on this surface.^{376,439,440} DFT-calculated elbow plots (2D cuts through the potential energy surface) have indicated a barrier of 0.51 eV on the flat surface, compared to no barrier at vacancies and a barrier of 0.12 eV at steps.³⁷⁶ Since experiments suggest that O₂ dissociates easily on Cu(100), it was suggested that vacancies dominate the experimental behavior. Ab initio MD simulations show that O₂ adsorbs molecularly at low incoming energies but dissociates at higher incoming energies.⁴⁴¹ However, recent DFT studies have found no barrier for O₂ dissociation even on the flat Cu(100) surface.³⁷³

6.2. Group 10 Metals (Pt, Pd, and Ni)

6.2.1. O₂ Dissociation on Pt Surfaces. Dosing O₂ on Pt(111) under UHV conditions results in dissociation around 150 K.³⁰⁷ No dissociation is observed at 100 K.^{447,448} Both experimental and theoretical work strongly suggest that O₂ dissociation occurs solely through a molecular precursor and not through a direct dissociation route,^{305,449} although this may change at higher coverage.⁴⁵⁰ The peroxy state appears to have a somewhat lower dissociation barrier than the superoxo state (Table 8). For CO oxidation, DFT calculations indicate that the O₂ dissociation barrier is much lower than the OCOO formation barrier,²⁸⁹ suggesting that CO oxidation involves O₂ direct dissociation. The dissociation barrier depends on the coverage: at low coverage, the barrier is significantly lower than at higher coverage.

On the basis of molecular beam studies, the sticking probability for O₂ on Pt(111) at low coverage is generally around 0.02 to 0.1.^{70,71,451} Adsorption may occur through a weakly bound state, and molecules that do not stick often do not accommodate with the surface.⁴⁵² The sticking probability decreases with increasing coverage, decreases as the temperature is increased from 300 to 600 K, and increases on steps.^{70,71,451} Scattering experiments indicate that there is some formation of negative O₂ ions, with a similar probability as Ag(111) of about 0.15.²⁵⁹

O₂ dissociation is thought to be precursor mediated on Pt(110),⁴⁵³ consistent with the clear identification of an adsorbed O₂ species at low temperatures. Dissociation begins around 125 K and is complete by 200–220 K, such that adsorption at higher temperatures is dissociative.^{310,319,453,454} Short-lived O₂ species can interact directly with adsorbed C, suggesting that O₂ dissociation can be mediated by coadsorbates.^{19,455} Under strongly oxidizing conditions, a surface oxide can form.^{66,456,457}

DFT calculations suggest that unreconstructed Pt(100) is quite reactive toward O₂ dissociation. On the hexagonal reconstruction, which is the most stable surface structure in vacuum, O₂ dissociation is a direct, activated process, in contrast to the unreconstructed structure.^{458,459}

Table 8. O₂ Adsorption Energies and Dissociation Barriers on Group 10 Metals^a

O ₂ ads energy (eV)	O ₂ dissociation barrier (eV)	notes/ref
Ni(111)		
-1.75 ± 0.17	0.15 ± 0.11	3-fold hollow ^{b,65,223,233}
-1	0.08	3-fold hollow ^{c,289}
-	0.085	exptl ^{d,337}
-	0.013	exptl ^{e,339}
Pd(111)		
-0.82 ± 0.18	0.62 ± 0.28	2-fold bridge ^{b,65,75,291,292}
-0.97 ± 0.40	0.48 ± 0.38	3-fold hollow ^{b,65,214,233,298}
-	0.32	exptl ^{f,294}
Pd(110)		
-1.3	-	2-fold bridge ^{b,442}
-	0.17	direct dissociation ^{b,442}
Pd(100)		
-0.76	0.12	2-fold bridge ^{b,300}
Pt(111)		
-0.63 ± 0.11	0.63 ± 0.16	2-fold bridge ^{b,64,65,83,214,303,314,318,443,444}
-0.16 ± 0.08	0.67 ± 0.33	2-fold bridge ^{c,289,444}
-0.63 ± 0.10	0.55 ± 0.28	3-fold hollow ^{b,65,233,303,314,445,446}
-0.1	0.6	3-fold hollow ^{c,444}
-0.37 ± 0.02	0.32 ± 0.03	exptl ^{f,306}
Pt(100)		
-1.10 ± 0.00	0.14 ± 0.01	2-fold bridge ^{b,325,326}
-0.75	0	4-fold hollow ^{b,300}

^aExperimental (exptl) data are marked; others are computational. Methods are given below. ^bDFT(PBE/PW91). ^cDFT(RPBE). ^dMolecular beam. ^eWork function measurements. ^fEELS/TPD.

6.2.2. O₂ Dissociation on Pd Surfaces. O₂ can dissociate on Pd(111) directly with a high barrier or through a precursor state with a low barrier.⁷⁵ At low incident energies, the chemisorbed precursor is accessed from a physisorbed state,^{331,332} but at higher energies, direct O₂ chemisorption can occur.²⁹⁴

Dissociation of adsorbed O₂ begins at roughly 100 K,^{294,329} while desorption occurs around 150 K.²⁹⁴ TPD studies suggest that O₂ in the fcc hollow site may not dissociate, while the unidentified peroxy species may dissociate.²⁹⁶ At higher temperatures and pressures (470 K and 10⁻⁴ Pa), a surface oxide can form.⁴⁶⁰

A monolayer of Pd on Ru(0001) is more inert than Pd(111).⁴⁶¹ This was attributed to both compressive strain and charge transfer. However, most studies of bimetallics suggest that orbital overlap is a more relevant and useful concept than charge transfer, where increased overlap between an atom and its neighbors tends to passivate the atom.^{79,462,463}

At low incident energy, O₂ dissociates on Pd(110) through a precursor-trapping mechanism,^{442,464} but at higher incident energy direct, activated dissociation can also occur.⁴⁴² DFT calculations suggest that direct dissociation occurs with a barrier of 0.17 eV.

Unlike most other late transition metals, direct dissociation is possible on Pd(100) at a low beam energy (56 meV) and a low temperature (100 K),^{335,465} although the process is still precursor mediated at even lower beam energies. Both DFT calculations and experimental work suggest that phonons are important in the dissociation process.^{335,466} The dissociation barrier is thought to be low.⁴⁶⁷ Surface oxide formation is facile and has been characterized by several studies.^{468,469}

6.2.3. O₂ Dissociation on Ni Surfaces. O₂ dissociation is quite facile on Ni surfaces, with roughly 10% of molecules dissociating on Ni(111) at room temperature⁴⁷⁰ and 70–100% dissociating on rough surfaces or at higher incident kinetic energy.^{337,470} The process is thought to be precursor-mediated.^{337,339} Recent molecular beam work has given an effective barrier of 1 eV for dissociation directly from the gas-phase,^{471,472} but the dissociation barrier from the precursor is much lower. It has been shown experimentally that O₂ molecules with their spin antiparallel to the spin of the Ni(111) surface have a greater sticking probability than those with parallel spins, showing that the magnetic character of the surface has some effect on dissociation.⁴⁷³ On Ni(100), eight adjacent metal atoms are the minimum ensemble for O₂ dissociation, corresponding to two hollow sites.⁴⁷⁴

A consistent picture has emerged for the interaction of O₂ with Ni surfaces at various coverages: at low coverage, dissociative chemisorption occurs, followed by 2D oxide formation, and finally bulk oxide formation (depending on the conditions).^{343,471,475–480} This overall process appears to be similar on other metals, but the moderate reactivity of Ni allows it to be easily studied in more detail. Some oxidation of Ni(111) can occur even at 100 K.⁴⁸¹ Once the surface has significantly oxidized, O₂ can physisorb on the surface. The transition from chemisorbed O atoms to an oxidized surface does not occur for very cold Ni(111) surfaces, even at high incident O₂ energies, suggesting thermal motion is necessary.⁴⁷⁸

6.3. Group 9 Metals (Ir, Rh, and Co)

6.3.1. O₂ Dissociation on Ir Surfaces. Molecular beam studies suggest that O₂ dissociation on Ir(111) may proceed through a molecular state.³⁴⁵ A precursor for adsorption has also been postulated.⁴⁸² From the bridge site, the lowest energy O₂ adsorption site identified in DFT, the dissociation barrier has been calculated at 0.06 eV (Table 9). On Ir(110),

Table 9. O₂ Adsorption Energies and Dissociation Barriers on Group 9 Metals^a

O ₂ ads energy (eV)	O ₂ dissociation barrier (eV)	notes/ref
Co(0001)		
-2.26	0.04	3-fold hollow site ^{b,233}
Rh(111)		
-1.86 ± 0.17	0.20 ± 0.04	3-fold hollow site ^{b,233,344}
Ir(111)		
-1.27	0.06	2-fold bridge site ^{b,77}
-1.24	0.71	3-fold hollow site ^{b,233}
Ir(110)		
-	0.35	exptl ^{c,348}
Ir(100)		
-2.1	0.26	2-fold bridge site ^{b,346}
-1.14	0	4-fold hollow site ^{b,300}

^aExperimental (exptl) data are marked; others are computational. Methods are given below. ^bDFT(PBE/PW91). ^cEELS/TPD.

dissociation also appears to be mediated by a chemisorbed O₂ precursor and is an activated process, with a barrier that lies 0.07 to 0.11 eV below the energy of the gas-phase O₂ reference.^{351,352} The dissociated O is strongly bound, with a desorption barrier of roughly 2 to 3 eV, depending on the coverage.³⁴⁸ On unreconstructed Ir(100), DFT calculations show a barrier of 0.26 eV from the most stable bridge site, although spontaneous dissociation was observed from some other sites.³⁴⁶ This surface reconstructs under vacuum

conditions, and the reconstructed surface is much less reactive, with a sticking coefficient 2.5 to 5 times lower and a finite activation barrier.^{483,484} However, adsorbed O can lift the reconstruction, which can make the surface more reactive as the O coverage increases.⁴⁸³

On Ir(111) at 300 K, O can diffuse into the subsurface.³⁴⁷ In the range of 575 to 875 K, and between 10^{-6} and 100 mbar, exposing Ir(111) to O₂ can result in chemisorbed O, an O–Ir–O trilayer, a multilayer oxide, or bulklike IrO₂.⁴⁸⁵

6.3.2. O₂ Dissociation on Rh and Co Surfaces. Experimentally, Rh(111) is quite reactive toward O₂.^{354,447} An O₂ dissociation barrier of 0.22 eV has been calculated, which drops to 0 at 1/4 ML O coverage and increases again as O coverage is further increased.⁴⁸⁶ However, this barrier was not calculated from the most stable adsorption site at low coverage. Since experiments show that O₂ dissociates even at 40 K,³⁵⁴ either the experiment probes O₂ dissociation which is promoted by adsorbed O or the barrier from the more stable adsorbed state is lower.

On Co(0001), the O₂ dissociation barrier has been calculated to be very low, 0.03 eV.²³³ Even dosing O₂ at 100 K results in some oxidation of the surface,⁴⁸⁷ and the surface O cannot be reduced by CO.⁴⁸⁸ Similarly, Co(1̄120) dissociates O₂ at 100 K,⁴⁸⁹ and in general Co oxidizes quite easily.

6.4. Groups 4–8

Metals in groups 4 through 8 tend to be very reactive toward O₂. On Ti(0001), no barrier was found for O₂ dissociation using DFT,⁴⁹² and it is likely that O₂ dissociation is barrierless on many of these metals. On Nb(110), even at 20 K O₂ dissociates and begins to form a surface oxide, similar to its behavior at 80 and 300 K, again suggesting very low barriers for O₂ activation.⁴⁹³ On Re(0001), O₂ adsorbs dissociatively at 150 K, without oxidizing the surface, and the O is so strongly bound that it is unaffected by annealing in H₂.⁴⁹⁴ There is a high sticking probability for O₂ on W(110) even at low temperature, suggesting a low dissociation barrier.⁴⁹⁵ On this surface, a precursor state plays a role at low incident energies, but above 0.1 eV, the precursor state has little effect.⁴⁹⁶ W adsorbs O₂ just as well as O (unlike Au or Be), again suggesting that the barrier for O₂ dissociation is quite low.⁴⁹⁷ However, W does not form an oxide as easily as some other metals. Ru(0001) is quite reactive toward O₂, and covering 95% of the surface with Pd only decreases the reactivity by a small amount.⁴⁶¹

The oxidation of these surfaces typically starts with O₂ activation, and the formation of O chemisorbed on the surface, followed quickly by the formation of a surface and then bulk oxide.^{498–500} Surface oxidation of Ti(0001) occurs at 90 K,⁵⁰¹ Re forms a surface oxide at room temperature,⁵⁰² and Fe oxidizes very quickly at room temperature.^{503,504} On these more reactive metals, research therefore typically focuses on the oxidation kinetics (i.e., the growth of the oxide layer) not on O₂ activation per se.⁵⁰⁴ The formation of a thin oxide at the surface can play an important role in protecting the material from further corrosion.⁵⁰⁵ More inert metals undergo formation of surface and bulk oxides at higher temperatures and pressures, which may not be reached in typical UHV studies of well-defined surfaces.

6.5. Metals Dominated by s and p Electrons

Simple metals appear to be quite reactive for O₂ dissociation. On Al(111), O₂ adsorption is purely dissociative at 30 K, until high O coverage when physisorption can occur.⁵⁰⁶ STM studies show that the dissociated O atoms are far apart, which was

initially interpreted as a signature of a hot-atom mechanism but has subsequently been interpreted as an indication that one O atom is ejected to the gas-phase.⁵⁰⁷ It appears that ejection of O atoms to the gas phase during dissociation has not been reported on any metals other than Al, although most metals outside of the d block have not been carefully studied with STM. We discuss Al(111) in more detail in section 8.2, in the context of dynamics. On Mg(0001), all O₂ dissociates even at 80 K.²¹⁵ On Ba(110), DFT calculations suggest that there is no barrier for O₂ dissociation.³⁶⁶ A low activation energy of around 0.25 eV has been calculated on both Be(0001) and Pb(111) (Table 10).^{54,365,368,370} Be and Zn oxidize easily at or below room temperature,^{497,508–512} and O₂ dissociation on Zn proceeds through a trapping-mediated mechanism.²¹⁷

Table 10. O₂ Adsorption Energies and Dissociation Barriers on Metals Dominated by s and p Electrons^a

	O ₂ ads energy (eV)	O ₂ dissociation barrier (eV)	notes/ref
Be(0001)			
–		0.25	3-fold hollow site ^{b,54}
–		0.23	bridge-hollow-bridge site ^{b,365}
Al(111)			
–		0.19	O ₂ vertical to surface ^{c,55}
Pb(111)			
–1.12		0.25	3-fold hollow site ^{b,370}
–		0.31	bridge-hollow-bridge site ^{b,368}

^aExperimental (exptl) data are marked; others are computational. Methods are given below. ^bDFT(PBE/PW91). ^cEmbedded wave function.

Lanthanides and actinides are also quite reactive toward O₂. In DFT, relaxing O₂ on U or Pu surfaces results in spontaneous dissociation in nearly all sites, suggesting a dissociation barrier near 0.^{513,514} Hence, it is not surprising that U, Pu, Th, and Gd oxidize easily, even at low temperatures (e.g., 77 K).^{515–521}

7. EFFECT OF THE SURFACE GEOMETRY ON O₂ DISSOCIATION

The effect of steps on the adsorption and dissociation of O₂ was reviewed by Vattuone and Rocca in 2008.⁵²² This review showed that studies have focused on the vicinal surfaces of Pt, Ag, and, to a lesser extent, Cu. Since the publication of that review, most papers regarding the effect of surface defects on O₂ dissociation have been focused on Pt. The interest in Pt stems largely from its high activity for the oxygen reduction reaction (ORR),⁵²³ in which the activation of O₂ is an important step. Furthermore, the discovery of Au nanoparticles as active, low-temperature oxidation catalysts⁵²⁴ dramatically increased the number of publications aimed at delineating the role of low-coordinated atoms on the activity. More recently, it was found that bulk Au in the form of a spongelike nanoporous material can act as a selective oxidation catalyst.⁴¹⁶ This nanoporous Au has a high surface area with many vicinal surfaces or defects. Therefore, this section will concentrate on the recent literature aimed at understanding surface corrugation using Pt as well as Au model catalysts, including both extended surfaces and support-free particles/clusters.

7.1. The Case of Pt

7.1.1. O₂ on Pt Steps and Kinks. For the adsorption of O₂ on Pt, the presence of steps as well as the kinetic energy of the incoming O₂ molecule are important. Below a kinetic energy of 0.1 eV, the reactivity toward dissociation does not depend on the precise atomic configuration of the step. The (111) step in the Pt(553) surface was studied by Juurlink and co-workers using supersonic molecular beams⁵²⁵ and compared to similar studies performed on the (100) steps of the Pt(533)⁵²⁵ surface and the Pt(110)-(1 × 2) surface.⁴⁵³ For all three surfaces, the sticking coefficients were much higher than for the Pt(111) surface. This was explained by a step-induced increased rate of converting physisorbed O₂ into chemisorbed O₂ as well as direct adsorption of O₂ into a chemisorbed state. The latter mechanism was both proposed to be nonactivated⁵²⁶ and activated.⁵²⁵

For all four surfaces, the dependence of the sticking coefficient on the kinetic energy follows the same trend (Figure 15). Up to 0.15–0.20 eV, it decreases with increasing

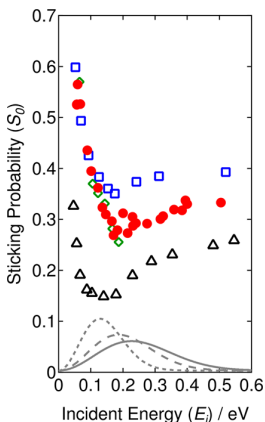


Figure 15. Variation of the O₂ sticking probability with kinetic energy, for Pt(553) (red ●),⁵²⁶ Pt(533) (blue □),⁵²⁵ Pt(110)-(1 × 2) (green ◇),⁴⁵³ and Pt(111) (black △).⁵²⁷ Surface temperature of 200 K and normal incidence angle. Gray lines represent Maxwell distributions for 298 (dotted), 623 (dashed), and 923 K (solid line) with arbitrary intensity. Figure reproduced from ref 526. Copyright 2015 American Institute of Physics.

kinetic energy, which was attributed to decreased sticking in the physisorbed state. At higher energy, it increases gradually with increasing kinetic energy, hinting at an activated adsorption pathway. This process could be activated by direct adsorption into the chemisorbed states on terrace⁵²⁶ or step sites.⁵²⁵ However, at higher kinetic energy, the reactivity of the (111) steps was much lower than that of the (100) steps. In fact, the sticking coefficient of the Pt(553) surface was intermediate between those of the Pt(533) and the Pt(111) surfaces.

Diametrically opposite results were reported by King and co-workers:⁵²⁸ the highest O₂ sticking coefficient was found for the Pt(111) surface and decreased for the Pt(211) and Pt(411) surfaces at 300 K while dosing O₂ with a supersonic molecular beam at a normal translation energy of 0.09 eV. The corresponding heat of adsorption, as measured with microcalorimetry,^{528,529} showed, on the other hand, the highest value for the Pt(211) surface (2.7 eV), while the Pt(411) and the Pt(111) surface had almost the same value (2.3 and 2.1 eV, respectively). Under these circumstances, O₂ adsorbs dis-

sociatively and these results seem to indicate that O₂ dissociation is most exothermic on the stepped surface but not faster.

DFT studies show that dissociation of O₂ is facile on the kinked steps of the Pt(321) surface with a barrier of 0.47 eV.⁵³⁰ This barrier is relatively low due to a strong stabilization of the transition state by two kink sites. Since the barrier is only 0.05 eV lower than for Pt(111), the enhanced activity of Pt(321) is mostly related to the stabilization of the initial state, by about 0.8 eV. The most stable adsorption sites for O₂ are the bridge sites involving a kink. DFT calculations also show that strong adsorption leads to energetic adsorbates that are unable to dissipate their kinetic energy fully and are less hindered to cross the dissociation barrier.⁵³⁰ Similar stabilization was found for the (111) steps in the Pt(331) and the Pt(221) surfaces.⁵³¹

DFT calculations suggest that, similarly to the kinks, the enhanced activity of steps cannot be explained by a difference in activation energy. Instead, it is related to a stabilization of the molecular precursor state, by 0.8 eV on Pt(211) as compared to Pt(111).^{444,532} This stabilization leads to a decrease in desorption rate with respect to the reaction rate and hence to an increased lifetime of this state. Furthermore, stronger adsorption results in a precursor state with more kinetic energy to overcome the reaction barrier. Because the transition state was stabilized by a similar amount, the activation energy (0.6 eV) for the Pt(111) surface was equal to that for the Pt(211) surface. Recently, low (0.19 and 0.16 eV) barriers were found for the (111) steps in the Pt(331) and the Pt(221) surfaces.⁵³¹ However, these DFT calculations cannot explain why the (111) steps of Pt(553) are lower in activity than the (100) steps of Pt(533).^{525,526} These DFT calculations further reveal that O₂ is adsorbed to the bridge site between two step atoms with the molecular axis parallel to the step.

7.1.2. O on Pt Steps and Kinks. Typically, experiments have focused on the difference between the (111) and (100) steps; however, the terrace width can be equally important.⁵³³ The terrace width of the (211) and the (533) surface differs by a single atom (i.e., 3 vs 4 atoms wide), but both have (100) step planes. The small difference in terrace width had a significant influence on the desorption behavior of O. The O saturation coverage on these surfaces suggests a 1:1 ratio of Pt_{step} and O_{step}.^{525,533} The higher step coverage on the (211) surface leads to a new feature in the TPD spectra. Similar desorption features were observed for the Pt(533) surface but were related to irreversible O₂ adsorption, either via faceting or roughening, growth of oxide clusters, or formation of subsurface O.⁵³⁴ A 1200 K anneal between consecutive desorption measurements eliminated this feature and resulted in reproducible TPD experiments.

Under UHV conditions, a saturation O coverage of 0.33 ± 0.04 ML has been reported on Pt(322) and Pt(553), which is higher than the 0.25 ML coverage under similar conditions on Pt(111).⁵³⁵ The suggested structure involves (2 × 2)-O on terraces in conjunction with half of the step atoms covered with O. A higher exposure of the Pt(332) surface to 500 langmuir (L) at 310 K resulted in a coverage of 0.42 ML.⁵³⁶ Aided by DFT, a structure was proposed in which the (111) steps form a one-dimensional (1D) PtO₂ structure. A distinct XPS Pt 4f_{7/2} core-level shift was assigned to the Pt atoms that were coordinated to 4 O atoms. Similar oxide rows were argued to form on the (100) steps of the Pt(755) surface after exposure to 1 to 10 Torr at room temperature.⁵³⁷

The (100) steps of the Pt(533) surface bind adsorbed O more strongly than the (111) steps of the Pt(553) surface, based on the desorption temperatures, but the terrace regions of the two surfaces behave identically.⁵³⁸ Theoretical studies focusing on the low-coverage limit showed that the (111) and (100) steps bind O differently. For the (111) step, the fcc site closest to the step gives the strongest O bonding.^{535,539,540} For the (100) step, on the other hand, the bridge site on the top edge of the step is calculated to be the most stable.^{535,539,541,542} The (100) steps bind O more strongly, and both steps bind O more strongly than the most stable site on Pt(111), the fcc site. This stabilization was found to be 0.15–0.22 eV for the (111) steps in the Pt(553) and Pt(332) surfaces.^{535,539,540} For the (100) steps, this was calculated to be 0.23–0.32 eV on the Pt(322), Pt(533), and the Pt(211) surfaces.^{535,539,541,542}

DFT calculations indicate that step doubling in the Pt(211) surface increases the O adsorption energy by 0.07 eV compared to the pristine Pt(211) surface and by 0.30 eV compared to the Pt(111) surface^{541,543} but does not influence the adsorption geometry. Further faceting continues to increase the binding energy of O. The binding is 0.47 eV stronger on the facet edge of the 4(111) × 4(100) Pt nanorod, compared to the Pt(111) surface.⁵⁴⁴ The calculations predict that it binds O similarly to the (100) steps in vicinal (111) surfaces. The most stable binding site was the bridge site between two Pt atoms in the edge. The adsorption sites next to the facet edge showed slightly decreased binding capabilities. Molecular O₂ prefers the same binding site with its molecular axis parallel to the facet edge. The binding enhancement compared to the extended (111) surface is 0.97 eV.

The adsorption sites on the (111) terraces of vicinal Pt surfaces show weaker O bonding than the fcc site in the extended Pt(111) surface based on DFT studies. This can be related to the strain relief in the (111) surface, which is easier for the smaller (111) terraces and leads to a contraction of the surface atomic lattice.⁵⁴⁵ For example, this leads to a 2.5% compression for the lattice constant in the Pt(332) and the Pt(322) surfaces.^{540,542} This stabilizes the (111) terrace with respect to the extended (111) surface and, therefore, decreases its ability to bind O. Comparing calculations for the fcc sites on a (111) terrace with those for the extended Pt(111) surface, this leads to ~0.2 eV weaker adsorption of O on the Pt(553)/Pt(533) surfaces,⁵³⁹ ~0.1 eV for the Pt(211) surface,⁵⁴¹ and 0.05 to 0.1 eV for the Pt(332) surface.⁵⁴⁰ For the kinked Pt(321) surface, O binds to the fcc-type sites next to the kink. The most stable sites include both a bridge and a fcc hollow site.⁵³⁰

DFT studies also indicate that steps and kinks decrease the diffusion length of adsorbed O.^{530,541} Diffusion barriers on the (100)-stepped Pt(211) surface were determined to be higher both parallel (by 0.15 eV) and perpendicular (by 0.78 eV) to the step.⁵⁴¹ The latter value is for ascending the step from the lower terrace; diffusion in the reverse direction has a barrier that is higher by 0.3 eV. For the kinked Pt(321) surface, diffusion around the kink site is facile, but it becomes much harder to move farther away from the most stable adsorption site.⁵³⁰

7.1.3. O₂ Activation on Pt Clusters. Small ($2n$ with $n = 1\text{--}6$) clusters of Pt and Pd are energetically inclined to dissociate O₂ based on DFT studies.^{546,547} Compared to the extended Pt(111) surface, the binding of O is increased by 0.5 eV per O atom.⁵⁴⁶ The adsorption geometry is different from that on the extended surface, as the clusters prefer to bridge O

between two Pt atoms. For Pd, only clusters of 8–12 atoms show enhanced binding to O compared to the Pd(111) surface. For these Pd clusters, DFT predicts that O binds to hollow sites instead of to bridge sites as on Pt clusters. For both metals, total oxidation to PtO and PdO was found to be exothermic for all small clusters.

Two different adsorption geometries of both O₂ and O on the Pt₄ and Pt₁₀ clusters were proposed based on DFT calculations.^{546,547} In one study, the tetragonal-shaped cluster strongly deforms upon adsorption, even becoming flat for the Pt₄ cluster.⁵⁴⁶ In the other DFT study, the tetragonal shape remains largely intact.⁵⁴⁷

Although thermodynamically favorable, O₂ dissociation might be kinetically limited on the smallest clusters. For the flat Pt₅ cluster, the calculated barrier is 0.66 eV, higher than for the extended Pt(111) surface.⁵⁴⁸ This barrier is lowered by substituting one Pt atom for Pd, which changes the structure from a flat disc to a trigonal bipyramidal.⁵⁴⁸ For tetragonally shaped clusters, a lower barrier of 0.17 eV was calculated for Pt₄, while O₂ dissociation on Pt₁₀ was barrierless.⁵⁴⁷ The reactivity of the latter was related to the flexibility of the cluster to adapt its geometry to the dissociating O₂ molecule.

The smaller particles have a stronger tendency to oxidize than bulk Pt, as predicted by DFT.⁵⁴⁹ Furthermore, complete oxidation to Pt_xO_{2x} is preferred over Pt_xO_x formation. Oxidation of small gas-phase Pt clusters was confirmed experimentally by their IR signatures, although the clusters were found to only dissociate one or two O₂ molecules per cluster.⁵⁵⁰ Furthermore, dissociative adsorption generally leads to strong structural changes in the clusters.

The truncated octahedral clusters, Pt₃₈,⁵⁵¹ Pt₇₉,⁵⁵¹ and Pt₁₁₆,⁵⁵² show enhanced binding to O₂ in DFT calculations and have low barriers for dissociation. The most favorable O₂ adsorption site on the Pt₃₈ cluster is the edge between the (111) and (100) facets with an adsorption energy of -2.01 eV. For the larger Pt₇₉ and Pt₁₁₆ clusters, smaller adsorption energies were found. For the Pt₇₉ cluster, both the edges between adjacent (111) facets and those between the (111) and (100) facets showed a calculated binding energy of -1.8 eV, whereas O₂ on Pt₁₁₆ has a clear preference for the (111) × (111) facet edges. To all adsorption sites, O₂ binds with its axis parallel to the surface of the cluster.

O₂ dissociation has been calculated to be barrierless for both the Pt₃₈ and Pt₇₉ clusters.⁵⁵¹ The most favorable pathways do not include the most stable adsorption sites. Therefore, diffusion of O₂ to the fcc or hcp adsorption sites near the facet edges is likely the first step in dissociation. For the smaller cluster, the fcc site near the (111) × (111) facet edge has no barrier, while the hcp site near the (111) × (100) facet edge has a calculated barrier of 0.04 eV. For the larger cluster, the pathways via the fcc and hcp adsorption sites near the (111) × (111) facet edge provide the lowest dissociation barriers. The pathway via the hcp site near the (111) × (100) edge has a much higher calculated barrier of 0.2 eV. The difference in reactivity was correlated with the ease with which the Pt atoms involved in the transition states are distorted. Although relatively high, this barrier is still more than a factor of two lower than that calculated for the extended Pt(111) surface. Similarly, very modest barriers were found for the Pt₁₁₆ cluster.⁵⁵²

The smaller Pt₃₈ cluster shows quite different O-adsorption behavior from the extended Pt surfaces or the larger clusters. Calculations show that the truncated octahedral Pt₃₈⁵⁵¹ binds O

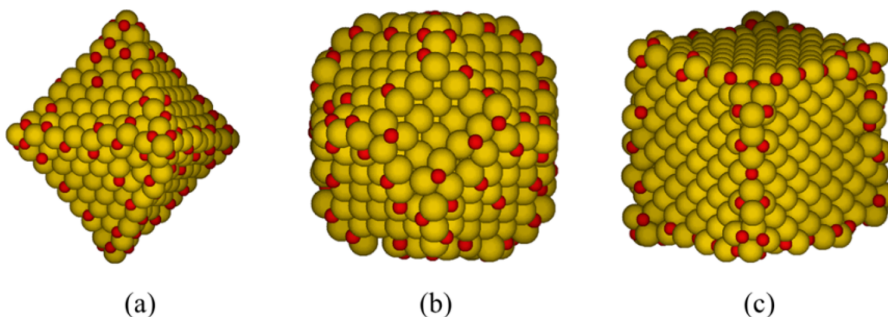


Figure 16. O₂ adsorption ($T = 500$ K and $p_{O_2} = 10^{-15}$ atm) on differently shaped Pt nanoparticles with edge lengths of ~ 2.3 nm. From left to right: octahedron (Pt₄₈₉), cuboctohedron (Pt₆₉₅), and cubic (Pt₈₆₄). Reprinted from ref 554. Copyright 2016 American Chemical Society.

stronger via hcp sites next to the (111) \times (100) facet edge, instead of the bridge on the edge. The latter binds O less strongly by ~ 0.1 eV and equally strongly as the fcc site next to the (111) \times (111) facet edge.

Compared to the smallest clusters, the calculated binding energy of O is 0.1–0.2 eV lower for larger clusters and is more similar in nature to the extended, vicinal surfaces. For the cuboctohedron Pt₅₅⁵⁵³ and the truncated octahedrons, Pt₇₉,⁵⁵¹ Pt₁₁₆,⁵⁵² and Pt₂₀₁,⁵⁵³ the bridge sites on the (111) \times (100) facet edges is preferred, although for the Pt₂₀₁ particle, the preference is not that pronounced. This cluster binds O almost equally as strongly via the fcc site next to the (111) \times (111) edge.

The O₂ pressure required to fully oxidize Pt nanoparticles increases with increasing size. Spherical particles between 1.0 nm, Pt₄₃, and 3.0 nm, Pt₉₃₅, were studied using reactive force fields.⁵⁵⁴ The smallest particles are predicted to oxidize at 10^{-20} atm, while the 3 nm particles do not oxidize to the same extent up to the highest considered pressure of 10^{-1} atm. Furthermore, the shape has a profound effect on the adsorption capabilities of the Pt nanoparticles (Figure 16). The octahedron-shaped particles were found to adsorb O more strongly than cubic, which can be related to a strong preference of O to adsorb to (111) facets over (100) facets. However, all particles may be limited in their catalytic activity by strongly bound O at steps, which may poison these sites for chemical reactions.

For Pt nanotubes, which have sparked interest as active ORR catalysts, the calculated O adsorption strength is dependent on the radius of curvature.^{555,556} The Pt nanotubes, essentially a wrapped up sheet of a single layer of Pt(111), bind O more strongly compared to the extended Pt(111) surface by 0.06–0.44 eV if their diameter is less than 0.5 nm. For wider nanotubes, O adsorption is weaker than on the Pt(111) surface. Generally, the nanotubes show a smaller decrease in adsorption energy with increasing coverage compared to the Pt(111) surface. For all nanotubes, adsorbed O prefers 3-fold hollow sites and the adsorption results in strong deformation of the nanotubes, based on DFT calculations.

7.2. The Case of Au

7.2.1. O₂ on Au Steps and Kinks. Vicinal Au surfaces show increased interaction with O₂. The Au(310) surface, with 3-atom-wide (100) terraces and (110) steps, binds O₂ with a calculated adsorption energy of -0.19 eV. However, on the related Au(210) surface, calculations do not show a stable adsorbed O₂ state.⁵⁵⁷ Comparable O₂ adsorption energies to the Au(310) surface were found for the kinked steps of the

Au(321) surface.³⁸⁵ On the basis of DFT calculations, the (111) steps of the Au(997) surface bind O₂ with -0.12 eV, while the adsorption to the (111) terrace atoms was almost 0. The (100) steps of the Au(211) surface bind O₂ almost equally as strong as the (111) steps.^{558,559}

Surprisingly strong adsorption of O₂ has been predicted by DFT for a diatomic row of Au atoms on the Au(100) surface.⁵⁶⁰ With a calculated binding energy of -0.52 eV, O₂ binds to the 4-fold hollow site on the row with its axis parallel to the surface. After adsorption, the calculated O–O binding length is increased by 0.2 Å. Similar binding energies were predicted for a wire of Au atoms on the Au(111) surface.⁵⁶¹

In addition to steps, adatoms bind O₂ more strongly than flat terraces. Although this is expected, the magnitude of the increased interaction is extraordinary. For Au/Au(111), O₂ binds end-on, and an adsorption energy of 0.38 eV was calculated.⁵⁶¹ For small adatom clusters of 2 and 3 atoms on the Au(111) surface, adsorption energies of 0.63 and 0.30 eV, respectively, were calculated. The binding geometry changes and a 4-membered ring forms that involves 2 Au atoms. For adatoms on the Au(100) surface, different theoretical values for O₂ were found of -0.1 ⁵⁶⁰ and -0.25 eV.⁵⁵⁷ These calculations suggest that rough, low-indexed Au surfaces may bind O₂, but this notion is still pending experimental verification.

Surface defects increase the reactivity of Au toward O₂. Of these defects, the (100) steps are the most reactive, based on DFT.⁵⁶² These particular steps were determined to be more reactive than the (111) steps, kinked steps, and adatoms. The transition state for O₂ dissociation on all of these defects is distinctly different from that on the Au(111) surface, as the O atoms do not share a Au atom. The calculated barriers for the (100) and the (111) steps were 0.93 – 0.95 eV^{559,562} and 1.16 eV,⁵⁶² respectively. These were 1.1 – 1.3 eV lower than for the Au(111) surface. For the Au(997) surface, the calculated barrier is lowered from 2.55 for the (111) terraces to 1.74 eV for the (111) steps.⁵⁶³ O₂ dissociation on the Au(321) surface is exothermic, and a barrier of 1.0 eV was reported for the kinked steps.³⁸⁵

For the diatomic rows on the Au(100) surface, the calculated O₂ dissociation barrier of 0.50 eV is slightly (0.02 eV) lower than the adsorption energy. Although dissociation is endothermic by 0.14 eV with respect to adsorbed O₂, it is exothermic with respect to gas-phase O₂.

Although theory has predicted that steps lower the O₂ dissociation barrier, dissociative adsorption has not been observed experimentally on single crystals. No O was detected after exposing the Au(211) surface to 1 – 700 Torr O₂ at 300 – 450 K.³⁸² Similarly, exposure under UHV at a lower sample

temperature, down to 85 K, did not produce any O. Additional surface roughening by ion sputtering had no effect. In agreement, the highly corrugated Au(310) surface, (100) terraces with (110) steps, did not dissociate O₂ at 80 K after exposing several hundreds L O₂.⁵⁶⁴ Similarly, the stepped Au(311) did not dissociate O₂ (1×10^{-4} mbar, 300–350 K).⁵⁵⁷

Conflicting results have been reported for O₂ dissociation on polycrystalline Au surfaces, which might be related to (small) amounts of bulk impurities. After treating (10^{-5} – 10^{-4} Torr O₂ and 300–1000 K) a polycrystalline Au foil, no O was detected using AES.^{565,566} At higher pressures, roughly above 1 Torr, O₂ dissociated on polycrystalline foil, provided that the temperature was at least 350 K.³⁹⁰

7.2.2. O on Au Steps and Kinks. The presence of defects increases the adsorption energy of O on Au, but DFT predicts that it does not scale with coordination number or the energy of the d-band center.⁵⁶² Bonding between O and Au has mainly an ionic character, the strength of which scales with the electron density around the Fermi level. With decreasing coordination, the electron density in the s/p orbitals near the Fermi level decreases, but the d band shifts up. These two trends compensate to some extent, leading to the strongest binding to the (100) steps, which is, by 0.31 eV (PBE)⁵⁶² and 0.16 eV (PW91)⁵⁵⁸ stronger than adsorption to the Au(111) surface. Bonding to (111) steps is less strong, by 0.18 eV. For the Au(997) surface, a 0.1 eV difference in calculated adsorption energy was found between the (111) steps and the (100) terraces.⁵⁶³ Similar results were obtained for the Au(310) surface and the rows on the Au(100) surface.⁵⁶⁰

On the basis of DFT calculations, kinks in the (100) and (111) steps slightly destabilize adsorbed O with respect to the flat Au(111) surface. Even weaker is the binding of O to Au/Au(111), almost 1 eV weaker than to the most stable site in the Au(111) surface.⁵⁶²

To study the O/Au interaction experimentally, O can be deposited in several ways that do not involve the dissociation of O₂. For example, the reaction between NO₂ and H₂O,⁵⁶⁷ O₃ decomposition,⁵⁶⁸ or electron irradiation of adsorbed H₂O,⁵⁶⁹ can be used (among others). The nature of the deposited O can be strongly influenced by the technique used to populate the surface with O. This is illustrated by the difference in peak desorption temperatures for O₂ recombination observed on Au(111). Temperatures of 517 K (heating rate $\beta = 3.5$ K/s)⁵⁶⁷ and 560–590 K ($\beta = 1$ K/s)⁵⁶⁸ were reported. This makes it slightly more difficult to compare different studies focusing on O/Au.

Koel and co-workers inferred stronger bonding of O to steps, based on a high-temperature shoulder at 540 K ($\beta = 3$ K/s) observed with TPD for the Au(211) surface.³⁸² A similar feature was not observed for the Au(111) surface, after similar O₃ exposure.⁵⁷⁰ Furthermore, changes in the LEED patterns suggested a transition from monatomic to double-height steps. These changes were observed for the smallest coverage and provided another indication of preferential adsorption of O to steps. The O coverage on the Au(211) surface saturated at 0.90 ± 0.04 ML, as calibrated with AES.

For the Au(997) surface, higher-temperature (468–533 K, $\beta = 3.0$ K/s) features were reported⁵⁷¹ which were not reported for the Au(111) surface.⁵⁶⁷ This comparison is complicated by the fact that O was generated by thermal decomposition of NO₂ for the former surface and by the reaction between NO₂ and H₂O for the latter surface. These two procedures are not guaranteed to lead to the same type of O overlayers.

No enhanced binding to steps, on the other hand, was concluded based on a direct comparison between the Au(311) and the Au(111) surfaces. The stepped Au(311) surface binds O similarly to Au(111).⁵⁶⁸ The Au(311) surface consists of alternating (100) and (111) facets. For both surfaces, O₃ dissociation led to O₂ desorption at comparable temperatures. For the Au(311) surface, XPS measurements indicated that the saturation coverage under these conditions was half of that obtained for the Au(111) surface. On the basis of similar desorption temperatures and the decreased saturation coverage, it was proposed that O binds solely to the (111) facets.

7.2.3. Strain Effects on Au. Activation of O₂ was found from DFT calculations to increase significantly after expanding the lattice constant in the Au(211) and the Au(111) surfaces.^{558,559} This expansion was used to model the tensile stress that oxide supports can exert on Au nanoparticles. This may partially explain the origin of the activity of Au nanoparticles for CO oxidation. The surfaces expanded by 10% bind O₂ ~0.1 eV more strongly, while binding O 0.3–0.4 eV stronger. The calculated barrier for the expanded Au(211) surface was 0.5 eV lower,⁵⁵⁹ close to that obtained for the diatomic rows/Au(100).⁵⁶⁰

Finally, direct comparison of the energies obtained with DFT using different exchange-correlation functionals warrants caution. For example, the RPBE functional predicts binding energies 0.5 eV smaller (weaker) on average than PBE/PW91, while yielding larger barriers by 0.3 eV.

7.2.4. O₂ Activation on Au Clusters. Adsorption of O₂ onto small, unsupported Au_n^q (with $n = 1$ –55 and $q = -1, 0, 1$) clusters has been extensively studied using DFT.^{248,399,572}–⁶⁰² Although the adsorption strength as well as the geometry depend on the calculation details, such as the employed exchange-correlation functional, several trends can be extracted.

For the smallest clusters, odd-numbered Au_n clusters bind O₂ more strongly than even-numbered Au_n clusters. For $n = 1$ –25, an enhancement of ~0.4 eV was calculated.⁵⁷² This difference can be related to the unpaired electron in the HOMO of odd-numbered clusters. The unpaired electron allows for easier charge transfer from the Au cluster to the adsorbed O₂. Another proposed explanation is that differences in cluster shape determine the shape of the HOMO and thereby the possible overlap with the LUMO of O₂.⁵⁷³ Finally, an uneven distribution of electron density, which could closely depend on the cluster shape, can provide sites with enhanced O₂ binding.⁵⁹¹ Adsorption of a second O₂ molecule per cluster was found to be energetically less favorable, based on DFT calculations.⁵⁹³

Two adsorption geometries have been found for O₂ in these DFT studies. Binding of O₂ via two Au atoms in a bridging mode (η^2 -O₂) results in more elongated O–O bonds, compared to binding of O₂ end-on atop a single Au atom (η^1 -O₂). The accumulation of charge is larger for η^2 -O₂ than for η^1 -O₂. In some studies, a clear preference for η^2 -O₂ was found for odd-numbered clusters.^{573,574} Adsorption via η^2 -O₂ requires a structural transformation of the cluster to a less-stable isomer. The associated barrier for this transformation is lowered by η^1 -O₂ adsorption.⁵⁷⁴

Anionic Au_n clusters bind O₂ more strongly on average compared to their noncharged counterparts. For $n = 1$ –25, an enhancement of ~0.3 eV was found in the calculated binding energy.⁵⁷² For these clusters, charge transfer to the adsorbate is more facile. Also on anionic clusters, the binding strength

oscillates with increasing n with the even-numbered clusters binding more strongly.

For larger clusters, roughly $n > 20–25$, the overall calculated binding energy decreases with increasing cluster size⁵⁷³ and the preference for odd/even clusters becomes less important.^{573,581} In larger particles, some of the Au atoms are no longer in the surface, forming an inner core. The surface was found to be negatively charged, draining electron density from the core,^{585,591,592} which is proposed to be an important factor in the O₂ binding.^{591,592}

Although O₂ dissociation is calculated to be mostly exothermic (except for Au₂^{-588,590} and perhaps Au _{n} with $n = 1, 3, 5, 7$ ⁶⁰⁰), the associated barriers are very large (1.5–3.2 eV) for small Au clusters.^{588,590,599–602} This barrier is lowered to some extent by negatively charging the clusters while positive charging results in the opposite.^{599,602} The high barrier can be explained by the need to break Au–Au bonds, in addition to stretching the O–O bond, to reach the transition state.⁵⁹⁴

The exact shape of the cluster influences the height of the barrier and the energy difference between the initial and final states. For the Au₁₃ cluster, dissociation of O₂ was studied on three different 3D clusters (although the most stable structure for Au₁₃ is a planar disc). Barriers between 0.18–1.8 eV were calculated, and the exothermicity differed by ~ 3 eV, shifting the reaction from exothermic to endothermic.^{594,598,599} O₂ adsorbed on the 4-fold hollow site of the (100) facet seems particularly reactive.²⁴⁸

The calculated barriers for O₂ dissociation on particles between $n = 25$ and $n = 147$ were determined to be much lower (0.4–0.5 eV) and independent of cluster size.^{399,599} This is remarkable, because differences in adsorption strength and elongation of the O–O bond do not significantly influence the reactivity of adsorbed O₂. However, the energy of the transition state with respect to gas-phase O₂ is not constant in this size range. Especially for the Au₃₈ cluster, the calculated energy of the transition state is lower than that of the bare cluster with gas-phase O₂ (i.e., adsorbed O₂ experiences a lower barrier for dissociation than for desorption).⁵⁹⁹ However, several DFT studies report conflicting results. For example, O₂ dissociation on Au₅₅ (cuboctahedral shape) was found to exhibit a much higher barrier of 1.31 eV.⁵⁸⁵ Additionally, the reaction is almost thermoneutral. Furthermore, O₂ dissociation was also proposed to be endothermic for the neutral pyramidal Au₂₀ cluster.⁵⁸²

For small Au _{n} clusters ($n = 1–8$), the calculated strength of O adsorption shows similar oscillatory behavior as observed for O₂ adsorption.⁶⁰³ Strongest bonding is predicted for neutral clusters with odd n and for charged clusters with an even n . The average binding energy is the highest for anionic clusters, followed by neutral clusters. In the case of O adsorption, however, the calculated binding strength does not correlate with the amount of charge transfer from the cluster to the adsorbed O. Furthermore, adsorption of O leads to strong deformation of the clusters and even Au–Au bond breaking.

Adsorption of O on Au₁₃ and Au₂₉ proceeds via a bridge site between two 5-fold coordinated Au atoms.^{248,595} For the larger Au₃₈ adsorption to the 3-fold hollow site close to the (111) \times (111) facet edge was found.⁵⁸⁴

8. DYNAMICS OF O₂ DISSOCIATION

Dynamical studies of molecule–surface interactions can give insight into how an ensemble of incoming molecules at various energies and orientations will interact with a surface.⁶⁰⁴ Experimentally, these studies generally consist of impinging a

molecular beam on a surface and measuring the sticking probability as a function of various parameters, including the incident energy, the temperature of the surface, and the angle of incidence. Computational studies of dynamics usually involve a large number of DFT calculations and interpolation between them to create a potential energy surface; classical or quasi-classical trajectories are then run on this potential energy surface.⁶⁰⁵

8.1. Steering and Rotational Effects

Steering effects have been demonstrated in several O₂/metal systems, where the potential energy surface tends to guide the incoming O₂ to a particular incoming configuration. Experimentally, a decrease in the dissociation probability as the incident kinetic energy increases is often taken as a signature of steering effects, and this can be difficult to distinguish from precursor-mediated dissociation.^{606,607} However, DFT studies have also suggested that steering can be important for O₂/metal interactions.⁶⁰⁸ These steering effects have been suggested to affect the reactivity of O₂ on Pd(100),^{465,608} Cu(100),⁶⁰⁹ Pt(111),⁶⁰⁷ and Cu(110).²²⁸ In general, steering seems to increase reactivity by guiding the incoming O₂ into states more favorable for strong adsorption and dissociation. On Ag(110), DFT-based dynamic studies show a negligible probability for direct dissociation at low incident energies, even if they are greater than the barrier, because the incoming trajectories have a very low probability of finding the low-energy dissociation pathway.²³⁸ Therefore, the lack of steering contributes to the low dissociative adsorption probability.

The rotational state of the incoming molecule can also affect reactivity. Increased rotational energy increases sticking of O₂ on Al(111).⁶¹⁰ For O₂ on Pt(111), high rotational energies can suppress steering.⁶¹¹ However, for O₂ on Ni(111), the rotational energy has a negligible effect on sticking.³³⁷ On Cu surfaces, rotational excitations hinder dissociation, while vibrational excitations facilitate it.⁶¹² The lattice recoil can also play a role in O₂ adsorption.⁶¹³

8.2. Spin Dynamics

O₂ has a triplet spin configuration in the gas phase, in contrast to most other small molecules that are used in important catalytic processes. This raises questions about the importance of the spin state and resultant magnetism for reactivity. In particular, O₂ is known to have limited reactivity with singlet species in the gas-phase, due to the spin-selection rule: spin must be conserved in a chemical reaction. The spin-selection rule is not necessarily obeyed in systems where spins can rotate due to spin–orbit coupling. Since gas-phase O₂ has nonzero spin ($s = 1$; $m_z = 2 \mu_B$), but adsorbed O generally has zero spin, the system must change spin states as the reaction proceeds. Therefore, this reaction is spin forbidden and would not occur if not for spin–orbit coupling. Thus, in any particular system, there are two questions about the role of the spin state of O₂. First, does the necessity of changing spin states inhibit the reaction? Second, do the spin state or magnetic moment of O₂ affect the energetics of the reaction?

The question of whether the necessity of a spin transition has an effect on the reactivity has been studied in some cases, without a clear resolution. The Landau–Zener formula is the formalism most often used for studying transitions between adiabatic states during chemical reactions.⁶¹⁴ In the case of O₂ dissociation, the O₂ changes from the triplet adiabatic state to the singlet adiabatic state along the reaction pathway. The probability of hopping from one adiabatic state to another

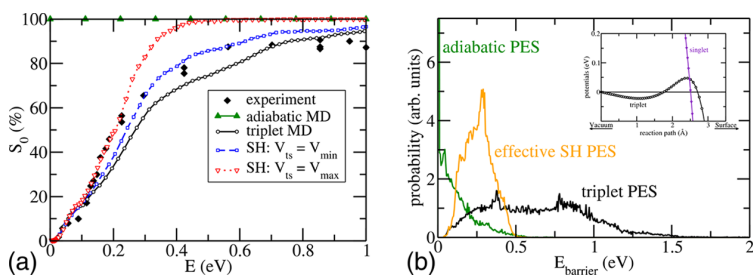


Figure 17. (a) The experimental sticking curve, compared to adiabatic molecular dynamics (MD), MD where the system always stays in the triplet state, and MD using surface hopping (SH) with two possible couplings between the triplet and singlet states. (b) Histograms of barriers from MD on each potential energy surface (PES). Reprinted with permission from ref 620. Copyright 2010 American Physical Society.

depends on several factors, most importantly the Hamiltonian matrix coupling element between the two states, which is based on spin–orbit coupling. This coupling element is difficult to calculate, and high-level wave function methods are usually employed. Since these methods are prohibitively expensive for surface calculations, it is necessary to use some kind of estimate in order to apply the Landau–Zener formalism.⁶¹⁵

Some studies have suggested that the spin transition plays an important role in inhibiting O₂ dissociation on Al(111). Experimental studies show that the sticking coefficient is low at low incident kinetic energies,⁶¹⁶ while ground-state DFT finds no barrier to dissociation, which should result in a high sticking coefficient. To resolve this issue, it has been proposed that O₂ stays in the triplet state as it approaches the surface, even in regions where the singlet is the ground state, due to a low probability for the spin transition. Indeed, running molecular dynamics on a potential energy surface where O₂ stays in the triplet state results in a sticking curve similar to the experiment,^{617,618} and a similar phenomenon has been proposed for Mg(0001).⁶¹⁹ Surface-hopping calculations, which allow the system to switch between potential energy surfaces, also show similar results to the experiment (Figure 17).⁶²⁰ However, nonadiabatic charge transfer has also been suggested as the reason for the discrepancy between computation and experiment, and semiempirical calculations that account for this charge transfer have also been shown to result in qualitative agreement with the experiment.⁶²¹ Rotational effects have also been shown to inhibit O₂ dissociation on Al(111).^{55,610,622,623} Recent work has suggested that errors in GGA-DFT are responsible for the discrepancy, and indeed, a barrier for dissociation was found when an embedding scheme with a correlated wave function method was used instead of DFT (Figure 18).⁶²⁴ These wave function calculations showed an abrupt charge transfer, along with a change in the O₂ spin state, at the transition state. This was in contrast to GGA-DFT, which showed a smoother charge transfer process. At this stage, it is unclear whether nonadiabatic effects, and in particular the spin transition, are important in this system, although an experimental test of this question has been proposed.⁶²⁵

Since Ag has a low density of states at the Fermi level, which may contribute to a slow spin transition, a theoretical study attempted to determine whether the spin transition contributes to the inertness of Ag(111) with respect to O₂ activation.²⁶⁷ This study compared a calculated sticking curve based on ground-state DFT to experimental sticking curves and came to the conclusion that the spin transition likely does not play a role.

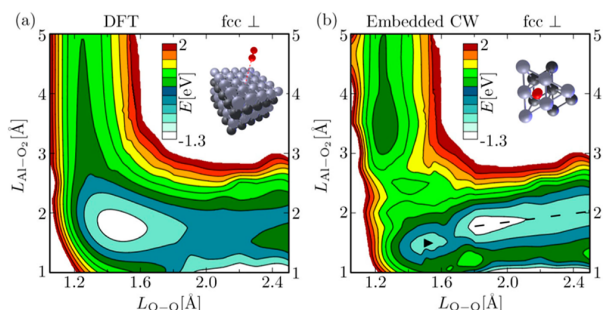


Figure 18. Elbow plots showing the potential energy as a function of the Al–O₂ distance and the O–O distance. (a) In the GGA-DFT case, there is no barrier, but (b) in the embedded wave function calculation there is a barrier of 0.36 eV. Reprinted with permission from ref 624. Copyright 2012 American Physical Society.

Overall, the literature suggests that the spin transition may not play a large role in O₂ dissociation on most metal surfaces. However, the results are far from conclusive, and careful studies are needed properly resolve this question.

On magnetic metal surfaces, the magnetic dipoles of O₂ may interact with the magnetic dipoles of the surface. Indeed, an experimental study showed that the sticking probability is higher if the O₂ spins are antiparallel to the surface spin (Figure 19).^{473,623} Similarly, a DFT study on O₂ dissociation on Ni(111) has shown that the transition state is lower in energy if the O₂ spins are aligned with the surface spins than if the spins are antialigned (Figure 19). The energy difference is 0.036 eV, which is roughly half of the total activation energy. This also raises the question of whether the spin rotations are slow enough that the system does not always stay in its ground-state spin configuration.

8.3. Hot Atoms

Several studies have examined the question: when O₂ dissociates, do the O atoms stay in adjacent sites or do they travel some distance due to the kinetic energy gained from the dissociation? This question about the existence of so-called hot atoms could affect surface chemistry, as hot atoms could cause other molecules to desorb or react.⁶

STM studies on Pt(111) have shown that, after O₂ dissociation at around 150 K, the O atoms do not lie in adjacent sites (Figure 20). Since these temperatures are below the temperature where O adatom diffusion occurs, this suggests that dissociation imparts enough energy to the O atoms for one or both to travel a short distance away from the dissociation event.⁶²⁷ The hot atom mechanism was supported by kinetic Monte Carlo simulations, where the diffusion barriers were

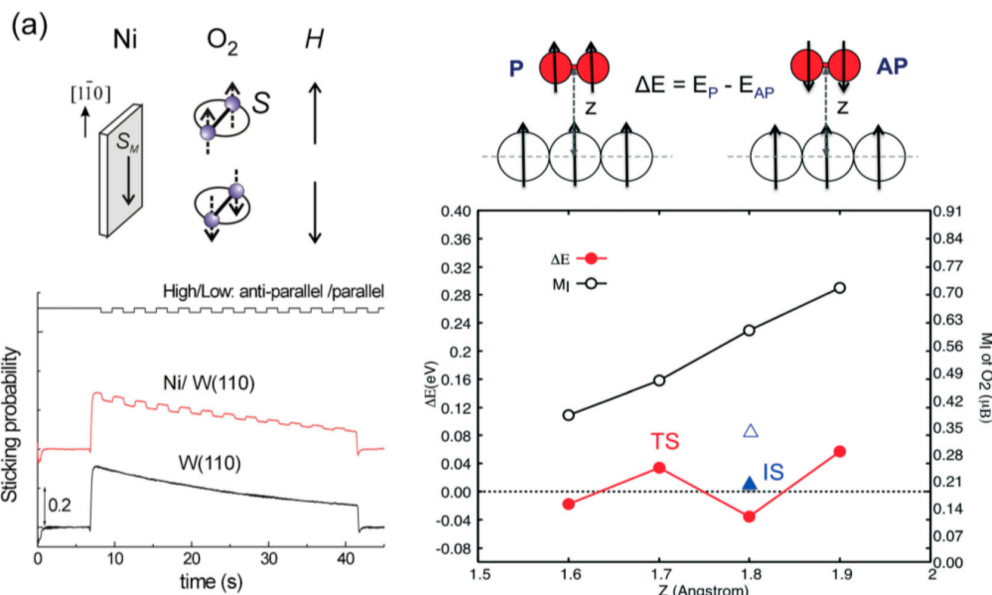


Figure 19. (Left) The highest line on the graph shows the control signal for a magnetic field. When this is high (low), the O_2 spins are antiparallel (parallel) to the spins of the surface, which increases (decreases) the sticking probability on a Ni-terminated surface but not a W-terminated surface, as shown by the other two lines. Reprinted with permission from ref 473. Copyright 2015 American Physical Society. (Right) Energy difference between O_2 having its spins parallel (P) or antiparallel (AP) to the spins of the Ni(111) surface, as well as the magnetic moment of O_2 , as a function of the O_2 -surface distance. Reproduced with permission from ref 626. Copyright 2017 The Royal Society of Chemistry.

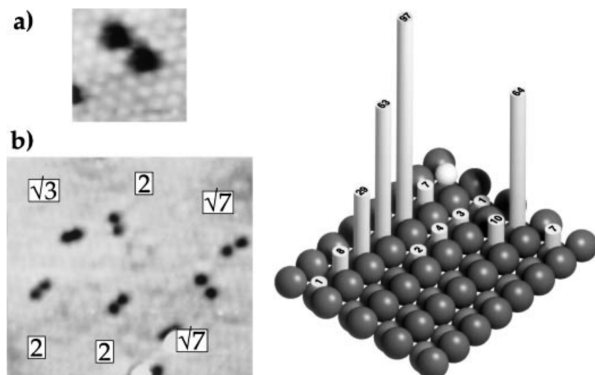


Figure 20. (Left) Dissociated O_2 - O_2 pairs on Pt(111) at 160 K, with the O_2 - O_2 distance in units of the lattice constant. (a) Close-up of a single pair and (b) several pairs. Reprinted with permission from ref 627. Copyright 1996 American Physical Society. (Right) Distribution of O_2 - O_2 pairs on Cu(110), with the location of the second O given relative to the first O, represented by the white sphere in the upper corner. Reprinted with permission from ref 283. Copyright 1997 American Physical Society.

chosen to reproduce the experimental distribution of distances.⁶²⁸ A similar effect has been observed on Ru(0001)³⁵⁶ and Cu(110)²⁸³ (Figure 20). Since strong O_2 - O_2 repulsion can occur for O atoms adsorbed in adjacent sites,²²⁵ it is possible that these repulsions play a role. More recent theoretical studies have examined O_2 on Pd(111) and Pd(100), showing that the hot atoms on Pd(100) have a shorter lifetime but travel a longer distance.^{629,630} On Ag(110), several studies have suggested that dissociating O_2 can produce hot O atoms that can displace other O_2 molecules, causing them to desorb.^{108,213,427,428}

9. EFFECT OF PRE-ADSORBED O ON O_2 DISSOCIATION

9.1. Repulsive Interaction with PreadSORBED O

The pathway for O_2 dissociation often involves both a molecularly adsorbed initial state and two separated O atoms for the final state; therefore, successful O_2 dissociation needs an ensemble of adsorption sites, which can be quite large.^{300,608} Due to the generally higher reactivity of O-free ensembles, the dissociation rate and sticking probability decreases with O coverage in most cases. Experimental studies have shown this, for example, for the (vicinal)^{525,526,631} Pt(111),^{452,632,633} Pt(100)-(1 \times 1),^{327,634} Pt(110)-(1 \times 2),^{453,635} Pd(111),^{636–638} Pd(100),^{335,469} Ir(110),³⁵² Ru(0001),^{639,640} Cu(111),⁶¹² Cu(100),⁶¹² Cu(110),^{435,612} Ag(111),³⁸¹ and Ag(110)⁶⁴¹ surfaces. However, under certain conditions, such as low surface temperature and incident kinetic energy, prolonged lifetime of the molecular precursor states mitigates this effect. At these conditions, diffusion enables the precursor to effectively explore the surface and to find an appropriate ensemble. As we discuss below, certain geometric configurations or reconstructions can also result in preadsorbed O facilitating O_2 dissociation.

PreadSORBED O usually destabilizes both the initial O_2 and final 2O state due to repulsive interactions, as shown by DFT calculations.³⁰⁰ The extent to which these interactions increase the barrier for O_2 dissociation and the O coverage at which this effect becomes significant varies between metals. In general, the repulsions have a larger effect on more inert metals. For example, on the Pd(100) surface the calculated barrier increases with coverage between 0 and 0.25 ML, while on the Rh(100) surface the dissociation of adsorbed O_2 remains barrierless in this range.³⁰⁰ For the Pt(111) surface, 1/16 ML preadsorbed O increases the calculated dissociation barrier by 0.04 eV, but the increases are much higher at higher coverage.³⁰³ Moreover, O

coadsorption also changes the dissociation pathway. Similar sharp increases have been calculated for the O₂ dissociation barrier on p(2 × 2)-O and the p(2 × 1)-O with a coverage of 0.25 and 0.5 ML, respectively (Figure 21).⁴⁴³ On the Nb(110)

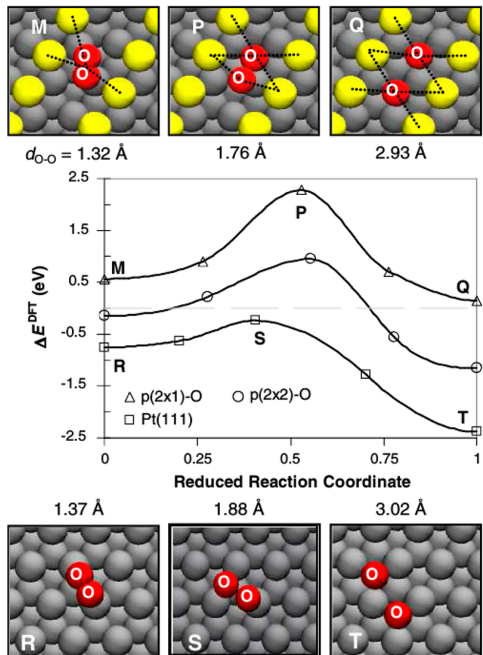


Figure 21. Initial, transition, and final states for O₂ dissociation on the p(2 × 1)-O/Pt(111) surface (top) and on the clean Pt(111) surface (bottom). (Middle) Energy profiles for O₂ dissociation. Reprinted with permission from ref 443. Copyright 2009 American Physical Society.

surface, adsorbed O₂ is not stable and dissociates directly for an O coverage of 0.25 ML.⁶⁴² At 0.50 ML, the calculated dissociation barrier is still just 0.02 eV; only a coverage of 1.0 ML inactivates this surface. For the Ir(110) surface, a very modest increase of 0.04 eV in dissociation barrier was measured for an O coverage of 0.3 ML.³⁵²

Another approach for probing the coverage effect in DFT is by comparing dissociation of a single O₂ molecule per unit cell with varying dimensions. However, this method is somewhat artificial because it assumes that all O₂ molecules dissociate simultaneously. For Pt(111), a decrease in reaction barrier was found for the unit cell dimensions that optimized the attractive interaction at a distance of twice the lattice spacing.¹⁰⁰ This coverage stabilized both the transition state and, related by a BEP relation, the final state of adsorbed O. On the other hand, a study using reactive force fields employing a unit cell with various dimension contradicts these findings and reports increasing barriers with increasing O coverage.⁶⁴³

9.2. Trapping of O₂ by Adsorbed O and O₂

If the lifetime of the molecular precursor state is long enough, adsorbed O can trap O₂ by changing the molecular orientation to allow O₂ to successfully chemisorb, or it can direct the molecule to a nearby adsorption site. These dynamic effects, steering and funneling, respectively, were observed using DFT-MD simulations on the Pd(100) surface.⁶⁴⁴ Experimentally, coadsorption of O₂ and O has been observed at low

temperature (typically, around 100 K) on the Pd(100) surface.^{299,335,336}

The presence of adsorbed O can possibly also stabilize O₂ adsorption and the transition state to dissociation, reducing the dissociation barrier with respect to desorption, particularly at step sites where attractive O–O interactions can occur. For AgAu alloys, such attractive interaction could originate in a stabilization of linear O–M–O motifs,^{53,93,645–647} whereas Pt seems to prefer a planar PtO₄ motif at higher coverages.^{2,457,535,536} This mechanism explains an observation made by STM on the Pt(111) surface by Ertl and co-workers.⁶⁴⁸ This surface was exposed to 1 L O₂ at 50–160 K. Above 95 K, O₂ dissociated and the resulting O atoms clustered into 1D lines. The extent of island formation and the total coverage decreased with increasing temperature. The resulting decrease in lifetime reduces the probability that the precursors encounter the adsorbed O.

Adsorbed O₂ can increase the sticking probability of impinging O₂. The enhanced adsorption probability onto and adjacent to islands of adsorbed O₂ is ascribed to more efficient energy dissipation between two O₂ molecules, leading to physisorption. This physisorbed state is labeled as an extrinsic precursor to differentiate from physisorption directly to the metallic surface, the so-called intrinsic precursor. Both these states lead to an enhanced chemisorption probability. In addition to this dynamical effect, the interaction of the gas-phase O₂ with the surface could be enhanced by preadsorbed O₂. However, as O₂ cannot molecularly chemisorb or dissociatively adsorb onto these islands, it needs to diffuse to the island perimeter. If islands are too large, the sticking probability decreases again, because physisorbed O₂ desorbs before reaching the edge of the island. This mechanism explains the increased sticking probability observed at low surface temperatures, for which adsorbed O₂ is (meta)stable. This has been observed, for example, for the (vicinal)^{525,526} Pt(111)⁶³² and the Pt(110)-(1 × 2)⁴⁵³ surfaces. For higher kinetic energy of the incoming O₂ molecule, the enhancement becomes negligible.^{525,526,632}

9.3. Oxygen-Induced Surface Reconstruction

Surface restructuring induced by adsorbed O can indirectly increase the O₂ dissociation rate by providing sites with lower coordinated atoms. On Pt(100), the coverage-dependent increase of the sticking probability is explained by the transition from the hex-R0.7° reconstruction to the (3 × 1) and with higher coverage to a complex, ordered reconstruction.³²⁷ Lifting of the hex-R0.7° reconstruction to the bulk (1 × 1) termination also enhanced the sticking probability.⁴⁵⁸ The latter surface termination has a higher activity for O₂ adsorption^{327,634} but is not stable without any adsorbates. For the kinked Au(321) surface, O-induced reconstructions are also predicted by DFT.⁶⁴⁹

On the Au(111) surface, O adsorption, formed by electron irradiation of adsorbed NO₂, changed the structure of the herringbone reconstruction.⁶⁵⁰ With increasing coverage, the periodicity of the elbow dislocations increased and completely disappeared at the highest coverage. This preadsorbed O increased the sticking probability of O₂ on the Au(111) surface by 3 orders of magnitude (Figure 22).⁶⁵¹ This was measured by the exchange of gas phase O₂¹⁸ with the preadsorbed O¹⁶. The mechanism could proceed either by the formation of a transient O₃ complex or by dissociation of O₂¹⁸ followed by recombination of O¹⁶O¹⁸.

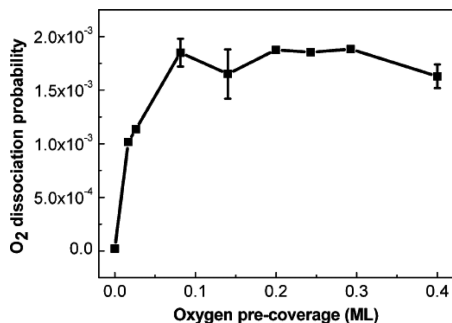


Figure 22. O₂ dissociation probability on the Au(111) surface as a function of preadsorbed O, generated by electron bombardment of adsorbed NO₂. Reprinted from ref 651. Copyright 2005 American Chemical Society.

10. CONCLUSIONS AND OUTLOOK

The studies reviewed here show the power of studying well-defined O₂/metal systems using a variety of experimental techniques as well as computational studies. Together, this allows a detailed, atomic-scale picture of O₂ adsorption states and O₂ dissociation processes. While computational studies give particular insight into the atomistic and electronic details, experimental studies provide crucial validation and guidance, and give insight into more complex, realistic conditions. Studying idealized surfaces with DFT has been remarkably successful in qualitatively reproducing experimental results in many cases, and it is clear that correspondences can often be drawn between theory and experiment.

We briefly reiterate a few trends. First, metals with a low O₂ dissociation barrier tend to adsorb O₂ and O strongly and oxidize easily. The lower-right section of the d block is the most inert with respect to O and O₂, and lower-left is the most reactive, at least with respect to O. In most cases of interest for catalysis, O₂ dissociation appears to proceed through a molecular precursor state. At higher incident beam energies or on more reactive surfaces direct dissociation becomes more important. In some cases, the molecular precursor states can be observed experimentally at low temperature and/or high O coverage. The distinction between superoxo and peroxy adsorbed O₂ states is useful but does not necessarily correlate cleanly with adsorption energies or dissociation barriers. More undercoordinated surfaces and sites are typically more reactive toward O₂.

Determining the energetics for O₂ adsorption and desorption with chemical accuracy (± 0.04 eV) is challenging both experimentally and theoretically. Even so, several types of experimental measurements, including molecular beam techniques, microcalorimetry, and temperature-programmed desorption methods, have been successfully used to provide accurate estimates of adsorption energies.^{28,453,652,653} The accuracy of theoretical calculations (DFT) depend on the details of the method and the model used (e.g., slab thickness, unit cell, etc.); however, state-of-the-art DFT calculations now provide absolute accuracy within roughly 0.2 eV and relative accuracy between similar systems that is somewhat better; for example, site preferences often match experiment even when energetic differences are modest. In many cases, theory and various experimental techniques give qualitatively similar values. For example, experimental and computational energetics for Ag(110) and Ni(111) agree within 0.05 to 0.1 eV (Table 7

and Table 8), while there is somewhat greater discrepancy for Pt(111) and Pd(111) of 0.15 to 0.25 eV (Table 8).

To get closer correspondence between theory and experiment, it will be necessary to ensure both theory and experiment are examining the surface in the same state. For example, DFT calculations should account for O and O₂ coverage effects and the formation of surface or bulk oxides, where applicable. Few DFT studies have explicitly tested the sensitivity of energetics and vibrational frequencies to these parameters, but the work that has been done suggests that these effects can be important. Experimental work should continue to reduce the effects of contaminants and defects, which can dominate measurements in some cases. Of course, improved functionals for DFT, and relaxation of numerical and computational assumptions (such as the harmonic approximation) may also improve the agreement between theory and experiment, but unless theory and experiment are considering O₂ in the same local environment, they cannot be expected to agree closely.

Experimental studies that carefully examine very low temperatures and coverages, as well as higher temperatures and coverages, especially those that quantitatively establish the coverage (both global and local) and structure of O, would allow connections to be made between changes in the surface state and changes in O₂ activation. This would improve connections between the understanding gained of the idealized surface and more realistic conditions. While the so-called “pressure gap” between UHV studies and ambient conditions has been much discussed, we suggest that it is often more useful to consider the coverage or chemical potential rather than the pressure. If the state of the surface is similar under UHV as it is under realistic conditions then its properties (such as activation barriers) should be similar, even if reaction rates are different at different temperatures. In addition to detailed studies of particular surfaces, additional studies that consider a range of surfaces with the same technique are useful for understanding trends. This is most straightforward with DFT but would be desirable for experimental studies as well.

ASSOCIATED CONTENT

Supporting Information

The Supporting Information is available free of charge on the ACS Publications website at DOI: 10.1021/acs.chemrev.7b00217.

Complete tables of molecularly absorbed O₂ states on particular metal surfaces and O₂ dissociation on various surfaces (ZIP)

AUTHOR INFORMATION

Corresponding Author

*E-mail: friend@fas.harvard.edu.

ORCID

Cynthia M. Friend: 0000-0002-8673-9046

Notes

The authors declare no competing financial interest.

Biographies

Matthew M. Montemore received his B.A. in physics from Grinnell College and his M.S./Ph.D. in Mechanical Engineering from the University of Colorado Boulder. He began a postdoc at Harvard University in 2014, joining the John A. Paulson School of Engineering and Applied Sciences and then the Department of Chemistry and

Chemical Biology. His research interests lie in understanding the behavior of metal surfaces and nanostructures and particularly their interactions with molecules and nonmetals.

Matthijs A. van Spronken received his Ph.D. in physics under the direction of Prof. Joost W. M. Frenken and Dr. Irene M.N. Groot at Leiden University in The Netherlands in 2016, after receiving both B.S. and M.S. degrees in chemistry at the same university. He is currently a postdoctoral researcher in the group of Prof. Friend at the Chemistry and Chemical Biology department at Harvard University. His research interests include behavior of model catalysts under realistic reaction conditions and the development of instruments to probe surfaces in these environments.

Robert J. Madix's pioneering fundamental research established the molecular foundation for elementary surface reactions on catalytic metals. Madix was the first surface scientist to undertake cutting-edge research on the surface chemistry of complex molecules on well-defined metallic surfaces. The first application of surface science studies to heterogeneous catalysis was achieved by Madix in the seminal studies of methanol oxidation to formaldehyde over Ag(110) surfaces. These seminal studies also significantly influenced the surface science community in subsequent years. These studies provided additional fundamental insight into the kinetics and mechanisms of surface reactions. Madix is the Charles Lee Powell Emeritus Professor of Chemical Engineering at Stanford University and Senior Research Fellow in the School of Applied Science & Engineering at Harvard University. He received a B.S. degree in chemical engineering from the University of Illinois and a Ph.D. degree in chemical engineering from the University of California, Berkeley. He is the recipient of an Alexander von Humboldt Senior Scientist Award, the Paul Emmett Award for Fundamental Studies in Heterogeneous Catalysis, the Alpha Chi Sigma Award for Fundamental Research from the AIChE, the Arthur Adamson Award of ACS, the Henry J. Albert Award of the International Institute of Precious Metals, and the Gabor Somorjai Award in Catalysis of the ACS.

Cynthia Friend, the T.W. Richards Professor of Chemistry and Professor of Materials Science, is the Director of the DOE-funded Energy Frontier Research Center, Integrated Mesoscale Architectures for Sustainable Catalysis (IMASC), and the Rowland Institute for Science at Harvard University. Friend's research is in surface chemistry and heterogeneous catalysis and is currently focused on developing energy-efficient catalytic processes. She was previously Associate Director at SLAC National Laboratory, Stanford. Friend is the recipient of the 2017 ACS Award in Surface Chemistry, the 2009 George Olah Award of the ACS, and the 1991 Garvan Medal from the American Chemical Society. She was an Alexander von Humboldt Senior Research Awardee (2007) and is a Fellow of the American Chemical Society and of the AAAS. Friend holds a Ph.D. from the University of California, Berkeley, and a B.S. in Chemistry from the University of California, Davis. She was a postdoctoral fellow at Stanford University prior to joining the Harvard faculty in 1982.

ACKNOWLEDGMENTS

This work was performed as part of Integrated Mesoscale Architectures for Sustainable Catalysis, an Energy Frontier Research Center funded by the U.S. Department of Energy, Office of Science, Basic Energy Sciences, under Award DE-SC0012573.

REFERENCES

- (1) Huang, W.; Sun, G.; Cao, T. Surface Chemistry of Group IB Metals and Related Oxides. *Chem. Soc. Rev.* **2017**, *46*, 1977–2000.
- (2) Stampfli, C.; Soon, A.; Piccinin, S.; Shi, H.; Zhang, H. Bridging the Temperature and Pressure Gaps: Close-Packed Transition Metal Surfaces in an Oxygen Environment. *J. Phys.: Condens. Matter* **2008**, *20*, 184021.
- (3) Lundgren, E.; Mikkelsen, A.; Andersen, J. N.; Kresse, G.; Schmid, M.; Varga, P. Surface Oxides on Close-Packed Surfaces of Late Transition Metals. *J. Phys.: Condens. Matter* **2006**, *18*, R481–R499.
- (4) Libuda, J.; Freund, H. J. Molecular Beam Experiments on Model Catalysts. *Surf. Sci. Rep.* **2005**, *57*, 157–298.
- (5) Jones, F. H. Teeth and Bones: Applications of Surface Science to Dental Materials and Related Biomaterials. *Surf. Sci. Rep.* **2001**, *42*, 75–205.
- (6) Roberts, M. W. Chemisorption and Reaction Pathways at Metal Surfaces: The Role of Surface Oxygen. *Chem. Soc. Rev.* **1989**, *18*, 451.
- (7) Serafin, J. G.; Liu, A. C.; Seyedmonir, S. R. Surface Science and the Silver-Catalyzed Epoxidation of Ethylene: An Industrial Perspective. *J. Mol. Catal. A: Chem.* **1998**, *131*, 157–168.
- (8) Chatterjee, D.; Deutschmann, O.; Warnatz, J. Detailed Surface Reaction Mechanism in a Three-Way Catalyst. *Faraday Discuss.* **2001**, *119*, 371–384.
- (9) Lefferts, L.; van Ommen, J. G.; Ross, J. R. H. The Oxidative Dehydrogenation of Methanol to Formaldehyde over Silver Catalysts in Relation to the Oxygen-Silver Interaction. *Appl. Catal.* **1986**, *23*, 385–402.
- (10) Pirie, B. J. M. The Manufacture of Hydrocyanic Acid by the Andrussov Process. *Platinum Met. Rev.* **1958**, *2*, 7–11.
- (11) Merchant Research and Consulting Ltd. *Formaldehyde: 2014 World Market Outlook and Forecast up to 2018*. <https://mcgroup.co.uk/researches/formaldehyde>, 2014.
- (12) Dutia, P. Ethylene Oxide: A Techno-Commercial Profile. *Chem. Wkly.* **2010**, *199*–203.
- (13) Rebsdat, S.; Mayer, D. Ethylene Oxide. In *Ullmann's Encyclopedia of Industrial Chemistry*; Wiley-VCH: Weinheim, Germany, 2001; pp 547–572.
- (14) U.S. Energy Information Administration. *Manufacturing Energy Consumption Survey*. <https://www.eia.gov/consumption/manufacturing/data/2010/>, 2010.
- (15) Song, J.; Wang, L.; Zibart, A.; Koch, C. Corrosion Protection of Electrically Conductive Surfaces. *Metals* **2012**, *2*, 450–477.
- (16) Saeki, I.; Konno, H.; Furuichi, R. The Initial Oxidation of Type 430 Stainless Steel in O₂-H₂O-N₂ Atmospheres at 1273 K. *Corros. Sci.* **1996**, *38*, 19–31.
- (17) Chattopadhyay, B.; Wood, G. C. The Transient Oxidation of Alloys. *Oxid. Met.* **1970**, *2*, 373–399.
- (18) Lausmaa, J.; Kasemo, B.; Mattsson, H. Surface Spectroscopic Characterization of Titanium Implant Materials. *Appl. Surf. Sci.* **1990**, *44*, 133–146.
- (19) Watson, D. T. P.; Harris, J. J. W.; King, D. A. Distinctive Roles of Chemisorbed Atomic Oxygen and Dioxygen in Methane Catalytic Oxidation on Pt{110}. *J. Phys. Chem. B* **2002**, *106*, 3416–3421.
- (20) Grabow, L. C.; Hvolbæk, B.; Nørskov, J. K. Understanding Trends in Catalytic Activity: The Effect of Adsorbate–Adsorbate Interactions for CO Oxidation Over Transition Metals. *Top. Catal.* **2010**, *53*, 298–310.
- (21) Abild-Pedersen, F.; Greeley, J.; Studt, F.; Rossmeisl, J.; Munter, T. R.; Moses, P. G.; Skúlason, E.; Bligaard, T.; Nørskov, J. K. Scaling Properties of Adsorption Energies for Hydrogen-Containing Molecules on Transition-Metal Surfaces. *Phys. Rev. Lett.* **2007**, *99*, 16105.
- (22) Guo, Z.; Liu, B.; Zhang, Q.; Deng, W.; Wang, Y.; Yang, Y. Recent Advances in Heterogeneous Selective Oxidation Catalysis for Sustainable Chemistry. *Chem. Soc. Rev.* **2014**, *43*, 3480.
- (23) Liu, X.; Madix, R. J.; Friend, C. M. Unraveling Molecular Transformations on Surfaces: A Critical Comparison of Oxidation Reactions on Coinage Metals. *Chem. Soc. Rev.* **2008**, *37*, 2243–2261.
- (24) Christian Enger, B.; Lødeng, R.; Holmen, A. A Review of Catalytic Partial Oxidation of Methane to Synthesis Gas with Emphasis on Reaction Mechanisms over Transition Metal Catalysts. *Appl. Catal., A* **2008**, *346*, 1–27.

- (25) Personick, M. L.; Montemore, M. M.; Kaxiras, E.; Madix, R. J.; Biener, J.; Friend, C. M. Catalyst Design for Enhanced Sustainability through Fundamental Surface Chemistry. *Philos. Trans. R. Soc., A* **2016**, *374*, 20150077.
- (26) Gattinoni, C.; Michaelides, A. Atomistic Details of Oxide Surfaces and Surface Oxidation: The Example of Copper and Its Oxides. *Surf. Sci. Rep.* **2015**, *70*, 424–447.
- (27) King, D. A.; Wells, M. G. Molecular Beam Investigation of Adsorption Kinetics on Bulk Metal Targets: Nitrogen on Tungsten. *Surf. Sci.* **1972**, *29*, 454–482.
- (28) Brown, W. A.; Kose, R.; King, D. A. Femtomole Adsorption Calorimetry on Single-Crystal Surfaces. *Chem. Rev.* **1998**, *98*, 797–832.
- (29) Rakić, V.; Damjanović, L. Temperature-Programmed Desorption (TPD) Methods. In *Calorimetry and Thermal Methods in Catalysis*; Springer: Berlin Heidelberg, 2013; pp 131–174.
- (30) Ibach, H. *Electron Energy Loss Spectrometers: The Technology of High Performance*; Springer Series in Optical Sciences; Springer: Berlin, 1991; Vol. 63.
- (31) Steininger, H.; Lehwald, S.; Ibach, H. Adsorption of Oxygen on Pt(111). *Surf. Sci.* **1982**, *123*, 1–17.
- (32) Van Hove, M. A.; Weinberg, W. H.; Chan, C.-M. *Low-Energy Electron Diffraction*; Springer Series in Surface Sciences; Springer: Berlin, 1986; Vol. 6.
- (33) Chen, C. J. *Introduction to Scanning Tunneling Microscopy*; Oxford University Press: New York, 2007.
- (34) Güntherodt, H.-J.; Wiesendanger, R. *Scanning Tunneling Microscopy I: General Principles and Applications to Clean and Adsorbate-Covered Surfaces*; Springer: Berlin, 1992.
- (35) Hohenberg, P.; Kohn, W. Inhomogeneous Electron Gas. *Phys. Rev.* **1964**, *136*, B864–B871.
- (36) Kohn, W.; Sham, L. J. Self-Consistent Equations Including Exchange and Correlation Effects. *Phys. Rev.* **1965**, *140*, A1133–A1138.
- (37) Perdew, J. P.; Wang, Y. Accurate and Simple Analytic Representation of the Electron-Gas Correlation Energy. *Phys. Rev. B: Condens. Matter Mater. Phys.* **1992**, *45*, 13244.
- (38) Perdew, J.; Burke, K.; Ernzerhof, M. Generalized Gradient Approximation Made Simple. *Phys. Rev. Lett.* **1996**, *77*, 3865–3868.
- (39) Hammer, B.; Hansen, L. B.; Nørskov, J. K. Improved Adsorption Energetics within Density-Functional Theory Using Revised Perdew-Burke-Ernzerhof Functionals. *Phys. Rev. B: Condens. Matter Mater. Phys.* **1999**, *59*, 7413–7421.
- (40) Wellendorff, J.; Silbaugh, T. L.; Garcia-Pintos, D.; Nørskov, J. K.; Bligaard, T.; Studt, F.; Campbell, C. T. A Benchmark Database for Adsorption Bond Energies to Transition Metal Surfaces and Comparison to Selected DFT Functionals. *Surf. Sci.* **2015**, *640*, 36–44.
- (41) Wellendorff, J.; Lundgaard, K. T.; Mogelhøj, A.; Petzold, V.; Landis, D. D.; Nørskov, J. K.; Bligaard, T.; Jacobsen, K. W. Density Functionals for Surface Science: Exchange-Correlation Model Development with Bayesian Error Estimation. *Phys. Rev. B: Condens. Matter Mater. Phys.* **2012**, *85*, 235149.
- (42) Tao, J.; Perdew, J. P.; Staroverov, V. N.; Scuseria, G. E. Climbing the Density Functional Ladder: Non-Empirical Meta-Generalized Gradient Approximation Designed for Molecules and Solids. *Phys. Rev. Lett.* **2003**, *91*, 146401.
- (43) Perdew, J. P.; Ruzsinszky, A.; Csonka, G. I.; Vydrov, O. A.; Scuseria, G. E.; Constantin, L. A.; Zhou, X.; Burke, K. Restoring the Density-Gradient Expansion for Exchange in Solids and Surfaces. *Phys. Rev. Lett.* **2008**, *100*, 136406.
- (44) Janthon, P.; Luo, S.; Kozlov, S. M.; Viñes, F.; Limtrakul, J.; Truhlar, D. G.; Illas, F. Bulk Properties of Transition Metals: A Challenge for the Design of Universal Density Functionals. *J. Chem. Theory Comput.* **2014**, *10*, 3832–3839.
- (45) Sun, J.; Remsing, R. C.; Zhang, Y.; Sun, Z.; Ruzsinszky, A.; Peng, H.; Yang, Z.; Paul, A.; Waghmare, U.; Wu, X.; et al. SCAN: An Efficient Density Functional Yielding Accurate Structures and Energies of Diversely-Bonded Materials. *arXiv:1511.01089*; 2015, 1–19.
- (46) Mardirossian, N.; Head-Gordon, M. ω B97M-V: A Combinatorially Optimized, Range-Separated Hybrid, Meta-GGA Density Functional with VV10 Nonlocal Correlation. *J. Chem. Phys.* **2016**, *144*, 214110.
- (47) Neese, F. Prediction of Molecular Properties and Molecular Spectroscopy with Density Functional Theory: From Fundamental Theory to Exchange-Coupling. *Coord. Chem. Rev.* **2009**, *293*, 526–563.
- (48) Paier, J.; Marsman, M.; Kresse, G. Why Does the B3LYP Hybrid Functional Fail for Metals? *J. Chem. Phys.* **2007**, *127*, 024103.
- (49) Stroppa, A.; Kresse, G. The Shortcomings of Semi-Local and Hybrid Functionals: What We Can Learn from Surface Science Studies. *New J. Phys.* **2008**, *10*, 063020.
- (50) Grimmel, S.; Hansen, A.; Brandenburg, J. G.; Bannwarth, C. Dispersion-Corrected Mean-Field Electronic Structure Methods. *Chem. Rev.* **2016**, *116*, 5105–5154.
- (51) Kulik, H. J. Perspective: Treating Electron over-Delocalization with the DFT+U Method. *J. Chem. Phys.* **2015**, *142*, 240901.
- (52) Sholl, D.; Steckel, J. A. *Density Functional Theory: A Practical Introduction*; John Wiley & Sons: Hoboken, 2011.
- (53) Moskaleva, L. V.; Weiss, T.; Klüner, T.; Bäumer, M. Chemisorbed Oxygen on the Au(321) Surface Alloyed with Silver: A First-Principles Investigation. *J. Phys. Chem. C* **2015**, *119*, 9215–9226.
- (54) Allouche, A. Quantum Modeling of Water and Oxygen Adsorption on Beryllium Surface. *J. Phys. Chem. C* **2012**, *116*, 4662–4670.
- (55) Cheng, J.; Libisch, F.; Carter, E. A. Dissociative Adsorption of O_2 on Al(111): The Role of Orientational Degrees of Freedom. *J. Phys. Chem. Lett.* **2015**, *6*, 1661–1665.
- (56) Herzberg, G.; Mrozowski, S. Molecular Spectra and Molecular Structure. I. Spectra of Diatomic Molecules. *Am. J. Phys.* **1951**, *19*, 390–391.
- (57) Ervin, K. M.; Anusiewicz, I.; Skurski, P.; Simons, J.; Lineberger, W. C. The Only Stable State of O_2^- Is the $X^2\Pi_g$ Ground State and It (Still!) Has an Adiabatic Electron Detachment Energy of 0.45 eV. *J. Phys. Chem. A* **2003**, *107*, 8521–8529.
- (58) Krupenie, P. H. The Spectrum of Molecular Oxygen. *J. Phys. Chem. Ref. Data* **1972**, *1*, 423–534.
- (59) Ruscic, B.; Pinzon, R. E.; Morton, M. L.; Srinivasan, N. K.; Su, M.-C.; Sutherland, J. W.; Michael, J. V. Active Thermochemical Tables: Accurate Enthalpy of Formation for Hydroperoxyl Radical, HO_2 . *J. Phys. Chem. A* **2006**, *110*, 6592.
- (60) Redington, R. L.; Olson, W. B.; Cross, P. C. Studies of Hydrogen Peroxide: The Infrared Spectrum and the Internal Rotation Problem. *J. Chem. Phys.* **1962**, *36*, 1311.
- (61) Shimanouchi, T. *Tables of Molecular Vibrational Frequencies, Consolidated Vol. I*. US. Department of Commerce, National Bureau of Standards: Washington, DC, 1972.
- (62) Alducin, M.; Sánchez-Portal, D.; Arnaud, A.; Lorente, N. Mixed-Valency Signature in Vibrational Inelastic Electron Tunneling Spectroscopy. *Phys. Rev. Lett.* **2010**, *104*, 136101.
- (63) Mkhonto, P.; Chauke, H.; Ngoepe, P. Ab Initio Studies of O_2 Adsorption on (110) Nickel-Rich Pentlandite ($Fe_4Ni_3S_8$) Mineral Surface. *Minerals* **2015**, *5*, 665–678.
- (64) Wasileski, S. A.; Janik, M. J. A First-Principles Study of Molecular Oxygen Dissociation at an Electrode Surface: A Comparison of Potential Variation and Coadsorption Effects. *Phys. Chem. Chem. Phys.* **2008**, *10*, 3613.
- (65) Eichler, A.; Mittendorfer, F.; Hafner, J. Precursor-Mediated Adsorption of Oxygen on the (111) Surfaces of Platinum-Group Metals. *Phys. Rev. B: Condens. Matter Mater. Phys.* **2000**, *62*, 4744.
- (66) van Spronsen, M. A.; Van Baarle, G. J. C.; Herbschleb, C. T.; Frenken, J. W. M.; Groot, I. M. N. High-Pressure Operando STM Studies Giving Insight in CO Oxidation and NO Reduction over Pt(110). *Catal. Today* **2015**, *244*, 85–95.
- (67) Heine, C.; Eren, B.; Lechner, B. A. J.; Salmeron, M. A Study of the O/Ag(111) System with Scanning Tunneling Microscopy and X-Ray Photoelectron Spectroscopy at Ambient Pressures. *Surf. Sci.* **2016**, *652*, 51–57.

- (68) Devarajan, S. P.; Hinojosa, J. A.; Weaver, J. F. STM Study of High-Coverage Structures of Atomic Oxygen on Pt(111): p(2 × 1) and Pt Oxide Chain Structures. *Surf. Sci.* **2008**, *602*, 3116–3124.
- (69) van Spronsen, M. A.; Frenken, J. W. M.; Groot, I. M. N. Surface Science under Reaction Conditions: CO Oxidation on Pt and Pd Model Catalysts. *Chem. Soc. Rev.* **2017**, *46*, 4347–4374.
- (70) Gland, J. L.; Korchak, V. N. The Adsorption of Oxygen on a Stepped Platinum Single Crystal Surface. *Surf. Sci.* **1978**, *75*, 733–750.
- (71) Hopster, H.; Ibach, H.; Comsa, G. Catalytic Oxidation of Carbon Monoxide on Stepped Platinum(111) Surfaces. *J. Catal.* **1977**, *46*, 37–48.
- (72) van Spronsen, M. A.; Frenken, J. W. M.; Groot, I. M. N. Observing the Oxidation of Platinum. *Nat. Commun.* **2017**, *8*, 429.
- (73) Gottfried, J.; Schmidt, K.; Schroeder, S. L.; Christmann, K. Spontaneous and Electron-Induced Adsorption of Oxygen on Au(110)-(1 × 2). *Surf. Sci.* **2002**, *511*, 65–82.
- (74) Lide, D. R. *CRC Handbook of Chemistry and Physics*, 83rd ed.; Taylor and Francis: Boca Raton, 2002.
- (75) Honkala, K.; Laasonen, K. Ab Initio Study of O₂ Precursor States on the Pd(111) Surface. *J. Chem. Phys.* **2001**, *115*, 2297–2302.
- (76) Li, R.; Li, H.; Liu, J. First Principles Study of O₂ Dissociation on Pt(111) Surface: Stepwise Mechanism. *Int. J. Quantum Chem.* **2016**, *116*, 908–914.
- (77) Xu, Y.; Mavrikakis, M. Adsorption and Dissociation of O₂ on Ir(111). *J. Chem. Phys.* **2002**, *116*, 10846–10853.
- (78) Vassilev, P.; Koper, M. T. M. Electrochemical Reduction of Oxygen on Gold Surfaces: A Density Functional Theory Study of Intermediates and Reaction Paths. *J. Phys. Chem. C* **2007**, *111*, 2607–2613.
- (79) Ma, X.; Xin, H. Orbitalwise Coordination Number for Predicting Adsorption Properties of Metal Nanocatalysts. *Phys. Rev. Lett.* **2017**, *118*, 36101.
- (80) Calle-Vallejo, F.; Loffreda, D.; Koper, M. T. M.; Sautet, P. Introducing Structural Sensitivity into Adsorption-Energy Scaling Relations by Means of Coordination Numbers. *Nat. Chem.* **2015**, *7*, 403–410.
- (81) Li, W.-X.; Stampfl, C.; Scheffler, M. Oxygen Adsorption on Ag(111): A Density-Functional Theory Investigation. *Phys. Rev. B: Condens. Matter Mater. Phys.* **2002**, *65*, 16–21.
- (82) Hammer, B.; Nørskov, J. K. Theoretical Surface Science and Catalysis: Calculations and Concepts. In *Advances in Catalysis*; Elsevier: Amsterdam, 2000; Vol. 45, pp 71–129.
- (83) Xu, Y.; Ruban, A. V.; Mavrikakis, M. Adsorption and Dissociation of O₂ on Pt-Co and Pt-Fe Alloys. *J. Am. Chem. Soc.* **2004**, *126*, 4717–4725.
- (84) Pettersson, L. G. M.; Nilsson, A. A Molecular Perspective on the d-Band Model: Synergy between Experiment and Theory. *Top. Catal.* **2014**, *57*, 2–13.
- (85) Montemore, M. M.; Medlin, J. W. Predicting and Comparing C–M and O–M Bond Strengths for Adsorption on Transition Metal Surfaces. *J. Phys. Chem. C* **2014**, *118*, 2666–2672.
- (86) Hyman, M. P.; Medlin, J. W. Effects of Electronic Structure Modifications on the Adsorption of Oxygen Reduction Reaction Intermediates on Model Pt(111)-Alloy Surfaces. *J. Phys. Chem. C* **2007**, *111*, 17052–17060.
- (87) Montemore, M. M.; Medlin, J. W. A Unified Picture of Adsorption on Transition Metals through Different Atoms. *J. Am. Chem. Soc.* **2014**, *136*, 9272–9275.
- (88) Hautier, G.; Ong, S. P.; Jain, A.; Moore, C. J.; Ceder, G. Accuracy of Density Functional Theory in Predicting Formation Energies of Ternary Oxides from Binary Oxides and Its Implication on Phase Stability. *Phys. Rev. B: Condens. Matter Mater. Phys.* **2012**, *85*, 155280.
- (89) Kubaschewski, O.; von Goldbeck, O. The Thermochemistry of Gold. *Gold Bull.* **1975**, *8*, 80–85.
- (90) Brennan, D.; Hayward, D. O.; Trapnell, B. M. W. The Calorimetric Determination of the Heats of Adsorption of Oxygen on Evaporated Metal Films. *Proc. R. Soc. London, Ser. A* **1960**, *256*, 81–105.
- (91) Rao, C. N. R.; Kamath, P. V.; Yashonath, S. Molecularly Adsorbed Oxygen on Metals: Electron Spectroscopic Studies. *Chem. Phys. Lett.* **1982**, *88*, 13–16.
- (92) Wu, C.; Schmidt, D. J.; Wolverton, C.; Schneider, W. F. Accurate Coverage-Dependence Incorporated into First-Principles Kinetic Models: Catalytic NO Oxidation on Pt (111). *J. Catal.* **2012**, *286*, 88–94.
- (93) Hiebel, F.; Montemore, M. M.; Kaxiras, E.; Friend, C. M. Direct Visualization of Quasi-Ordered Oxygen Chain Structures on Au(110)-(1 × 2). *Surf. Sci.* **2016**, *650*, 5–10.
- (94) Montemore, M. M.; Medlin, J. W. Scaling Relations between Adsorption Energies for Computational Screening and Design of Catalysts. *Catal. Sci. Technol.* **2014**, *4*, 3748–3761.
- (95) Okamoto, Y.; Sugino, O. Hyper-Volcano Surface for Oxygen Reduction Reactions over Noble Metals. *J. Phys. Chem. C* **2010**, *114*, 4473–4478.
- (96) Falsig, H.; Hvilsted, B.; Kristensen, I. S.; Jiang, T.; Bligaard, T.; Christensen, C. H.; Nørskov, J. K. Trends in the Catalytic CO Oxidation Activity of Nanoparticles. *Angew. Chem.* **2008**, *120*, 4913–4917.
- (97) Jiang, T.; Mowbray, D. J.; Dobrin, S.; Falsig, H.; Hvilsted, B.; Bligaard, T.; Nørskov, J. K. Trends in CO Oxidation Rates for Metal Nanoparticles and Close-Packed, Stepped, and Kinked Surfaces. *J. Phys. Chem. C* **2009**, *113*, 10548–10553.
- (98) Xin, H.; Linic, S. Communications: Exceptions to the d-Band Model of Chemisorption on Metal Surfaces: The Dominant Role of Repulsion between Adsorbate States and Metal d-States. *J. Chem. Phys.* **2010**, *132*, 221101.
- (99) Choudhary, T. V.; Banerjee, S.; Choudhary, V. R. Catalysts for Combustion of Methane and Lower Alkanes. *Appl. Catal., A* **2002**, *234*, 1–23.
- (100) Miller, D. J.; Öberg, H.; Näslund, L.-Å.; Anniyev, T.; Ogasawara, H.; Pettersson, L. G. M.; Nilsson, A. Low O₂ Dissociation Barrier on Pt(111) due to Adsorbate–adsorbate Interactions. *J. Chem. Phys.* **2010**, *133*, 224701.
- (101) Campbell, C. T.; Sun, Y.-K.; Weinberg, W. H. Trends in Preexponential Factors and Activation Energies in Dehydrogenation and Dissociation of Adsorbed Species. *Chem. Phys. Lett.* **1991**, *179*, 53–57.
- (102) Burnett, D. J.; Capitano, A. T.; Gabelnick, A. M.; Marsh, A. L.; Fischer, D. A.; Gland, J. L. In-Situ Soft X-Ray Studies of CO Oxidation on the Pt(111) Surface. *Surf. Sci.* **2004**, *564*, 29–37.
- (103) Bligaard, T.; Nørskov, J. K.; Dahl, S.; Matthiasen, J.; Christensen, C. H.; Sehested, J. The Brønsted-Evans-Polanyi Relation and the Volcano Curve in Heterogeneous Catalysis. *J. Catal.* **2004**, *224*, 206–217.
- (104) Falsig, H.; Hvilsted, B.; Kristensen, I. S.; Jiang, T.; Bligaard, T.; Christensen, C. H.; Nørskov, J. K. Trends in the Catalytic CO Oxidation Activity of Nanoparticles. *Angew. Chem., Int. Ed.* **2008**, *47*, 4835–4839.
- (105) Montemore, M. M.; Medlin, J. W. Site-Specific Scaling Relations for Hydrocarbon Adsorption on Transition Metal Surfaces. *J. Phys. Chem. C* **2013**, *117*, 20078–20088.
- (106) Zhang, T.; Driver, S. M.; Pratt, S. J.; King, D. A. Spillover of Oxygen Adatoms from Ir to Au on an Ir/Au{111} Bimetallic Surface. *Surf. Sci.* **2013**, *615*, 1–5.
- (107) Que, L., Jr.; Tolman, W. B. Biologically Inspired Oxidation Catalysis. *Nature* **2008**, *455*, 333–340.
- (108) Capote, A. J.; Roberts, J. T.; Madix, R. J. Reactions of Molecularly Adsorbed Oxygen on Metals: Carbon Monoxide and Sulfur Dioxide Reactions with Oxygen on Ag(110). *Surf. Sci.* **1989**, *209*, L151–L156.
- (109) Burghaus, U.; Conrad, H. Evidence for the Oxidation of CO by Molecular Oxygen Adsorbed on Ag(110). *Surf. Sci.* **1996**, *364*, 109–121.
- (110) Barth, J. V.; Zambelli, T. Oxidation of CO by Molecular Oxygen on a Ag(110) Surface Studied by Scanning Tunneling Microscopy. *Surf. Sci.* **2002**, *513*, 359–366.

- (111) Yu, W.-Y.; Zhang, L.; Mullen, G. M.; Henkelman, G.; Mullins, C. B. Oxygen Activation and Reaction on Pd–Au Bimetallic Surfaces. *J. Phys. Chem. C* **2015**, *119*, 11754–11762.
- (112) Kołasiński, K. W.; Čemič, F.; de Meijere, A.; Hasselbrink, E. Interactions in Co-Adsorbed CO + O₂/Pd(111) Layers. *Surf. Sci.* **1995**, *334*, 19–28.
- (113) Engel, T.; Ertl, G. Surface Residence Times and Reaction Mechanism in the Catalytic Oxidation of CO on Pd(111). *Chem. Phys. Lett.* **1978**, *54*, 95–98.
- (114) Engel, T.; Ertl, G. A Molecular Beam Investigation of the Catalytic Oxidation of CO on Pd(111). *J. Chem. Phys.* **1978**, *69*, 1267.
- (115) Engel, T.; Ertl, G. Elementary Steps in the Catalytic Oxidation of Carbon Monoxide on Platinum Metals. *Adv. Catal.* **1979**, *28*, 1–78.
- (116) Burghaus, U.; Conrad, H. Evidence for Two Kinetically Distinct Atomic Oxygen Species on Ag(110): A Molecular Beam Study of the CO Oxidation Reaction. *Surf. Sci.* **1995**, *338*, L869–L874.
- (117) Su, H.; Yang, M.; Bao, X.; Li, W. The Effect of Water on the CO Oxidation on Ag(111) and Au(111) Surfaces: A First-Principle Study. *J. Phys. Chem. C* **2008**, *112*, 17303–17310.
- (118) Matsushima, T. The Mechanism of the CO₂ Formation on Pt(111) and Polycrystalline Surfaces at Low Temperatures. *Surf. Sci.* **1983**, *127*, 403–423.
- (119) Matsushima, T. Angular Distribution of the Desorption of CO₂ Produced on Pt(111) Surface at Low Temperatures. *Surf. Sci. Lett.* **1982**, *123*, L663–L666.
- (120) Pacia, N.; Cassuto, A.; Pentenero, A.; Weber, B. Molecular Beam Study of the Mechanism of Carbon Monoxide Oxidation on Platinum and Isolation of Elementary Steps. *J. Catal.* **1976**, *41*, 455–465.
- (121) Shigeishi, R. A.; King, D. A. The Oxidation of Carbon Monoxide on Platinum {111}: Reflection-Absorption Infrared Spectroscopy. *Surf. Sci.* **1978**, *78*, L397–L400.
- (122) Krick Calderón, S.; Grabau, M.; Óvári, L.; Kress, B.; Steinrück, H. P.; Papp, C. CO Oxidation on Pt(111) at near Ambient Pressures. *J. Chem. Phys.* **2016**, *144*, 044706.
- (123) Stuve, E. M.; Madix, R. J.; Brundle, C. R. CO Oxidation on Pd(100): A Study of the Coadsorption of Oxygen and Carbon Monoxide. *Surf. Sci.* **1984**, *146*, 155–178.
- (124) Zheng, G.; Altman, E. I. The Reactivity of Surface Oxygen Phases on Pd(100) toward Reduction by CO. *J. Phys. Chem. B* **2002**, *106*, 1048–1057.
- (125) Duan, Z.; Henkelman, G. CO Oxidation on the Pd (111) Surface. *ACS Catal.* **2014**, *4*, 3435–3443.
- (126) Weaver, J. F.; Zhang, F.; Pan, L.; Li, T.; Asthagiri, A. Vacancy-Mediated Processes in the Oxidation of CO on PdO(101). *Acc. Chem. Res.* **2015**, *48*, 1515–1523.
- (127) Shipilin, M.; Gustafson, J.; Zhang, C.; Merte, L. R.; Stierle, A.; Hejral, U.; Ruett, U.; Gutowski, O.; Skoglundh, M.; Carlsson, P.-A.; et al. Transient Structures of PdO during CO Oxidation over Pd(100). *J. Phys. Chem. C* **2015**, *119*, 15469–15476.
- (128) Gao, F.; Wang, Y.; Goodman, D. W. Reaction Kinetics and Polarization-Modulation Infrared Reflection Absorption Spectroscopy (PM-IRAS) Investigation of CO Oxidation over Supported Pd–Au Alloy Catalysts. *J. Phys. Chem. C* **2010**, *114*, 4036–4043.
- (129) Min, B. K.; Alemozafar, A. R.; Pinnaduwage, D.; Deng, X.; Friend, C. M. Efficient CO Oxidation at Low Temperature on Au(111). *J. Phys. Chem. B* **2006**, *110*, 19833–19838.
- (130) Michael Gottfried, J.; Christmann, K. Oxidation of Carbon Monoxide over Au(110)-(1 × 2). *Surf. Sci.* **2004**, *566–568*, 1112–1117.
- (131) Fajín, J. L. C.; Cordeiro, M. N. D. S.; Gomes, J. R. B. DFT Study of the CO Oxidation on the Au(321) Surface. *J. Phys. Chem. C* **2008**, *112*, 17291–17302.
- (132) Wang, P.; Tang, X.; Tang, J.; Pei, Y. Density Functional Theory (DFT) Studies of CO Oxidation over Nanoporous Gold: Effects of Residual Ag and CO Self-Promoting Oxidation. *J. Phys. Chem. C* **2015**, *119*, 10345–10354.
- (133) Déronzier, T.; Morfin, F.; Lomello, M.; Rousset, J. L. Catalysis on Nanoporous Gold-Silver Systems: Synergistic Effects toward Oxidation Reactions and Influence of the Surface Composition. *J. Catal.* **2014**, *311*, 221–229.
- (134) Van Santen, R. A.; Kuipers, H. P. C. E. The Mechanism of Ethylene Epoxidation. *Adv. Catal.* **1987**, *35*, 265–321.
- (135) Roberts, J. T.; Madix, R. J. Epoxidation of Olefins on Silver: Conversion of Norbornene to Norbornene Oxide by Atomic Oxygen on Silver(110). *J. Am. Chem. Soc.* **1988**, *110*, 8540–8541.
- (136) Linic, S.; Bartea, M. A. Formation of a Stable Surface Oxametallacycle That Produces Ethylene Oxide. *J. Am. Chem. Soc.* **2002**, *124*, 310–317.
- (137) Özbek, M. O.; van Santen, R. A. The Mechanism of Ethylene Epoxidation Catalysis. *Catal. Lett.* **2013**, *143*, 131–141.
- (138) Grant, R. B.; Harbach, C. A. J.; Lambert, R. M.; Tan, S. A. Alkali Metal, Chlorine and Other Promoters in the Silver-Catalysed Selective Oxidation of Ethylene. *J. Chem. Soc., Faraday Trans. 1* **1987**, *83*, 2035–2046.
- (139) Grant, R. B.; Lambert, R. M. A Single Crystal Study of the Silver-Catalysed Selective Oxidation and Total Oxidation of Ethylene. *J. Catal.* **1985**, *92*, 364–375.
- (140) Lambert, R. M.; Williams, F. J.; Cropley, R. L.; Palermo, A. Heterogeneous Alkene Epoxidation: Past, Present and Future. *J. Mol. Catal. A: Chem.* **2005**, *228*, 27–33.
- (141) Gleaves, J. T.; Sault, A. G.; Madix, R. J.; Ebner, J. R. Ethylene Oxidation on Silver Powder: A Tap Reactor Study. *J. Catal.* **1990**, *121*, 202–218.
- (142) Hawker, S.; Mukoid, C.; Badyal, J. P. S.; Lambert, R. M. Molecular Mechanism of Heterogeneous Alkene Epoxidation: A Model Study with Styrene on Ag(111). *Surf. Sci. Lett.* **1989**, *219*, L615–L622.
- (143) Mukoid, C.; Hawker, S.; Badyal, J. P. S.; Lambert, R. M. Molecular Mechanism of Alkene Epoxidation: A Model Study with 3,3-Dimethyl-1-Butene on Ag(111). *Catal. Lett.* **1990**, *4*, 57–61.
- (144) Campbell, C. T. Chlorine Promoters in Selective Ethylene Epoxidation over Ag(111): A Comparison with Ag(110). *J. Catal.* **1986**, *99*, 28–38.
- (145) Lambert, R. M.; Cropley, R. L.; Husain, A.; Tikhov, M. S. Halogen-Induced Selectivity in Heterogeneous Epoxidation Is an Electronic Effect—fluorine, Chlorine, Bromine and Iodine in the Ag-Catalysed Selective Oxidation of Ethene. *Chem. Commun.* **2003**, 1184–1185.
- (146) Kokalj, A.; Gava, P.; de Gironcoli, S.; Baroni, S. What Determines the Catalyst's Selectivity in the Ethylene Epoxidation Reaction. *J. Catal.* **2008**, *254*, 304–309.
- (147) Ozbek, M. O.; Onal, I.; van Santen, R. A. Effect of Surface and Oxygen Coverage on Ethylene Epoxidation. *Top. Catal.* **2012**, *55*, 710–717.
- (148) Linic, S.; Jankowiak, J.; Bartea, M. A. Selectivity Driven Design of Bimetallic Ethylene Epoxidation Catalysts from First Principles. *J. Catal.* **2004**, *224*, 489–493.
- (149) Santra, A. K.; Cowell, J. J.; Lambert, R. M. Ultra-Selective Epoxidation of Styrene on Pure Cu{111} and the Effects of Cs Promotion. *Catal. Lett.* **2000**, *67*, 87–91.
- (150) Pinnaduwage, D. S.; Zhou, L.; Gao, W.; Friend, C. M. Chlorine Promotion of Styrene Epoxidation on Au(111). *J. Am. Chem. Soc.* **2007**, *129*, 1872–1873.
- (151) Deng, X.; Friend, C. M. Selective Oxidation of Styrene on an Oxygen-Covered Au(111). *J. Am. Chem. Soc.* **2005**, *127*, 17178–17179.
- (152) Torres, D.; Lopez, N.; Illas, F.; Lambert, R. M. Why Copper Is Intrinsically More Selective than Silver in Alkene Epoxidation: Ethylene Oxidation on Cu(111) versus Ag(111). *J. Am. Chem. Soc.* **2005**, *127*, 10774–10775.
- (153) Bukhtiyarov, V. I.; Nizovskii, A. I.; Bluhm, H.; Hävecker, M.; Kleimenov, E.; Knop-Gericke, A.; Schlögl, R. Combined In Situ XPS and PTRMS Study of Ethylene Epoxidation over Silver. *J. Catal.* **2006**, *238*, 260–269.
- (154) Williams, F. J.; Bird, D. P. C.; Palermo, A.; Santra, A. K.; Lambert, R. M. Mechanism, Selectivity Promotion, and New

- Ultraselective Pathways in Ag-Catalyzed Heterogeneous Epoxidation. *J. Am. Chem. Soc.* **2004**, *126*, 8509–8514.
- (155) Tan, S.; Grant, R. B.; Lambert, R. M. Secondary Chemistry in the Selective Oxidation of Ethylene: Effect of Cl and Cs Promoters on the Adsorption, Isomerisation, and Combustion of Ethylene Oxide on Ag(111). *J. Catal.* **1987**, *106*, 54–64.
- (156) Klust, A.; Madix, R. J. Partial Oxidation of Higher Olefins on Ag(111): Conversion of Styrene to Styrene Oxide, Benzene, and Benzoic Acid. *Surf. Sci.* **2006**, *600*, 5025–5040.
- (157) Pulido, A.; Concepción, P.; Boronat, M.; Corma, A. Aerobic Epoxidation of Propene over Silver (111) and (100) Facet Catalysts. *J. Catal.* **2012**, *292*, 138–147.
- (158) Williams, F. J.; Cropley, R. L.; Vaughan, O. P. H.; Urquhart, A. J.; Tikhov, M. S.; Kolczewski, C.; Hermann, K.; Lambert, R. M. Critical Influence of Adsorption Geometry in the Heterogeneous Epoxidation Of “allylic” alkenes: Structure and Reactivity of Three Phenylpropene Isomers on Cu(111). *J. Am. Chem. Soc.* **2005**, *127*, 17007–17011.
- (159) Cropley, R. L.; Williams, F. J.; Urquhart, A. J.; Vaughan, O. P. H.; Tikhov, M. S.; Lambert, R. M. Efficient Epoxidation of a Terminal Alkene Containing Allylic Hydrogen Atoms: Trans -Methylstyrene on Cu{111}. *J. Am. Chem. Soc.* **2005**, *127*, 6069–6076.
- (160) Torres, D.; Lopez, N.; Illas, F.; Lambert, R. M. Low-Basicity Oxygen Atoms: A Key in the Search for Propylene Epoxidation Catalysts. *Angew. Chem., Int. Ed.* **2007**, *46*, 2055–2058.
- (161) Cropley, R. L.; Williams, F. J.; Vaughan, O. P. H.; Urquhart, A. J.; Tikhov, M. S.; Lambert, R. M. Copper Is Highly Effective for the Epoxidation of a “difficult” Alkene, Whereas Silver Is Not. *Surf. Sci.* **2005**, *578*, L85–L88.
- (162) Cowell, J. J.; Santra, A. K.; Lambert, R. M. Ultraselective Epoxidation of Butadiene on Cu{111} and the Effects of Cs Promotion. *J. Am. Chem. Soc.* **2000**, *122*, 2381–2382.
- (163) Roberts, J. The Rate-Limiting Step for Olefin Combustion on Silver: Experiment Compared to Theory. *J. Catal.* **1993**, *141*, 300–307.
- (164) Deng, X.; Min, B. K.; Liu, X.; Friend, C. M. Partial Oxidation of Propene on Oxygen-Covered Au(111). *J. Phys. Chem. B* **2006**, *110*, 15982–15987.
- (165) Davis, K. A.; Goodman, D. W. Propene Adsorption on Clean and Oxygen-Covered Au(111) and Au(100) Surfaces. *J. Phys. Chem. B* **2000**, *104*, 8557–8562.
- (166) Hayashi, T.; Tanaka, K.; Haruta, M. Selective Vapor-Phase Epoxidation of Propylene over Au/TiO₂ Catalysts in the Presence of Oxygen and Hydrogen. *J. Catal.* **1998**, *178*, 566–575.
- (167) Roberts, J. T.; Capote, A. J.; Madix, R. J. Surface-Mediated Cycloaddition: 1,4-Addition of Atomically Adsorbed Oxygen to 1,3-Butadiene on Silver(110). *J. Am. Chem. Soc.* **1991**, *113*, 9848–9851.
- (168) Roberts, J. T.; Capote, A. J.; Madix, R. J. Partial Oxidation of Hydrocarbons on Silver: Conversion of 1-Butene to Maleic Anhydride by Atomically Adsorbed Oxygen on Ag(110). *Surf. Sci.* **1991**, *253*, 13–23.
- (169) Roberts, J. T.; Madix, R. J. Reactions of Weak Organic Acids with Oxygen Atoms on Ag(100): Facile and Selective Conversion of Cyclohexene to Benzene. *Surf. Sci.* **1990**, *226*, L71–L78.
- (170) Gabelnick, A. M.; Capitano, A. T.; Kane, S. M.; Gland, J. L.; Fischer, D. A. Propylene Oxidation Mechanisms and Intermediates Using In Situ Soft X-Ray Fluorescence Methods on the Pt(111) Surface. *J. Am. Chem. Soc.* **2000**, *122*, 143–149.
- (171) Berlowitz, P.; Megiris, C.; Butt, J. B.; Kung, H. H. Temperature-Programmed Desorption Study of Ethylene on a Clean, a Hydrogen-Covered, and an Oxygen-Covered Platinum(111) Surface. *Langmuir* **1985**, *1*, 206–212.
- (172) Dannetun, H.; Lundström, I.; Petersson, L. G. Reactions between Hydrocarbons and an Oxygen Covered Palladium Surface. *Surf. Sci.* **1988**, *193*, 109–131.
- (173) Zhong, W.; Liang, J.; Hu, W.; Cao, X.; Jia, C.; Jiang, J. The O, OH and OOH-Assisted Selective Coupling of Methanol on Au–Ag(111). *Phys. Chem. Chem. Phys.* **2016**, *18*, 9969–9978.
- (174) Wu, K.; Wang, D.; Wei, X.; Cao, Y.; Guo, X. The Role of Dioxygen in Methanol Oxidation on Ag. *Surf. Sci.* **1994**, *304*, L475–L480.
- (175) Endo, M.; Matsumoto, T.; Kubota, J.; Domen, K.; Hirose, C. Oxidation of Methanol by Molecularly Adsorbed Oxygen on Pt(111) under Vacuum and Ambient Pressure Conditions Studied by Infrared Reflection Absorption Spectroscopy: Identification of Formate Intermediate. *Surf. Sci.* **1999**, *441*, L931–L937.
- (176) Sawada, T.; Liu, Z.; Takagi, N.; Watanabe, K.; Matsumoto, Y. Reactivity of Molecular Oxygen: Conversion of Methanol to Formate at Low Temperatures on Pt(111). *Chem. Phys. Lett.* **2004**, *392*, 334–339.
- (177) Endo, M.; Matsumoto, T.; Kubota, J.; Domen, K.; Hirose, C. Formation of Formate in the Deep Oxidation of Methanol on Pt(111) under UHV Condition Studied by IRAS. *J. Phys. Chem. B* **2000**, *104*, 4916–4922.
- (178) Personick, M. L.; Madix, R. J.; Friend, C. M. Selective Oxygen-Assisted Reactions of Alcohols and Amines Catalyzed by Metallic Gold: Paradigms for the Design of Catalytic Processes. *ACS Catal.* **2017**, *7*, 965–985.
- (179) Medlin, J. W. Understanding and Controlling Reactivity of Unsaturated Oxygenates and Polyols on Metal Catalysts. *ACS Catal.* **2011**, *1*, 1284–1297.
- (180) Xu, B.; Haubrich, J.; Freyschlag, C. G.; Madix, R. J.; Friend, C. M. Oxygen-Assisted Cross-Coupling of Methanol with Alkyl Alcohols on Metallic Gold. *Chem. Sci.* **2010**, *1*, 310.
- (181) Yan, T.; Gong, J.; Mullins, C. B. Oxygen Exchange in the Selective Oxidation of 2-Butanol on Oxygen Precovered Au(111). *J. Am. Chem. Soc.* **2009**, *131*, 16189–16194.
- (182) Xu, B.; Liu, X.; Haubrich, J.; Madix, R. J.; Friend, C. M. Selectivity Control in Gold-Mediated Esterification of Methanol. *Angew. Chem., Int. Ed.* **2009**, *48*, 4206–4209.
- (183) Gong, J.; Flaherty, D. W.; Ojifinni, R. A.; White, J. M.; Mullins, C. B. Surface Chemistry of Methanol on Clean and Atomic Oxygen Pre-Covered Au(111). *J. Phys. Chem. C* **2008**, *112*, 5501–5509.
- (184) Gong, J.; Flaherty, D. W.; Yan, T.; Mullins, C. B. Selective Oxidation of Propanol on Au(111): Mechanistic Insights into Aerobic Oxidation of Alcohols. *ChemPhysChem* **2008**, *9*, 2461–2466.
- (185) Madix, R. J. Molecular Transformations on Single Crystal Metal Surfaces. *Science* **1986**, *233*, 1159–1166.
- (186) Meng, Q.; Shen, Y.; Xu, J.; Gong, J. Mechanistic Insights into Selective Oxidation of Ethanol on Au(111): A DFT Study. *Chin. J. Catal.* **2012**, *33*, 407–415.
- (187) Xu, B.; Haubrich, J.; Baker, T. A.; Kaxiras, E.; Friend, C. M. Theoretical Study of O-Assisted Selective Coupling of Methanol on Au(111). *J. Phys. Chem. C* **2011**, *115*, 3703–3708.
- (188) Zope, B. N.; Hibbitts, D. D.; Neurock, M.; Davis, R. J. Reactivity of the Gold/Water Interface During Selective Oxidation Catalysis. *Science* **2010**, *330*, 74–78.
- (189) Griffin, M. B.; Rodriguez, A. A.; Montemore, M. M.; Monnier, J. R.; Williams, C. T.; Medlin, J. W. The Selective Oxidation of Ethylene Glycol and 1,2-Propanediol on Au, Pd, and Au–Pd Bimetallic Catalysts. *J. Catal.* **2013**, *307*, 111–120.
- (190) Ayre, C. R.; Madix, R. J. The Adsorption and Reaction of 1,2-Propanediol on Ag(110) under Oxygen Lean Conditions. *Surf. Sci.* **1994**, *303*, 279–296.
- (191) Barnes, C.; Pudney, P.; Guo, Q.; Bowker, M. Molecular-Beam Studies of Methanol Partial Oxidation on Cu(110). *J. Chem. Soc., Faraday Trans.* **1990**, *86*, 2693.
- (192) Wachs, I. E.; Madix, R. J. The Selective Oxidation of CH₃OH to H₂CO on a copper(110) Catalyst. *J. Catal.* **1978**, *53*, 208–227.
- (193) Wachs, I. E.; Madix, R. J. The Oxidation of Ethanol on Cu(110) and Ag(110) Catalysts. *Appl. Surf. Sci.* **1978**, *1*, 303–328.
- (194) Xu, B.; Siler, C.; Madix, R. J.; Friend, C. M. Ag/Au Mixed Sites Promote Oxidative Coupling of Methanol on the Alloy Surface. *Chem. - Eur. J.* **2014**, *20*, 4646–4652.
- (195) Wachs, I. E.; Madix, R. J. The Oxidation of Methanol on a Silver (110) Catalyst. *Surf. Sci.* **1978**, *76*, 531–558.

- (196) Francis, S. M.; Leibsle, F. M.; Haq, S.; Xiang, N.; Bowker, M. Methanol Oxidation on Cu(110). *Surf. Sci.* **1994**, *315*, 284–292.
- (197) Bao, X.; Muhler, M.; Pettinger, B.; Schlögl, R.; Ertl, G. On the Nature of the Active State of Silver During Catalytic-Oxidation of Methanol. *Catal. Lett.* **1993**, *22*, 215–225.
- (198) Barreau, M. A.; Madix, R. J. A Study of the Relative Brönsted Acidities of Surface Complexes on Ag(110). *Surf. Sci.* **1982**, *120*, 262–272.
- (199) Williams, R. M.; Medlin, J. W. The Influence of Oxygen on the Surface Chemistry of 1,2-Propanediol on Pd(111). *Surf. Sci.* **2014**, *619*, 30–38.
- (200) Davis, J. L.; Barreau, M. A. The Influence of Oxygen on the Selectivity of Alcohol Conversion on the Pd(111) Surface. *Surf. Sci.* **1988**, *197*, 123–152.
- (201) Miller, A. V.; Kachev, V. V.; Prosvirin, I. P.; Bukhtiyarov, V. I. Mechanistic Study of Methanol Decomposition and Oxidation on Pt(111). *J. Phys. Chem. C* **2013**, *117*, 8189–8197.
- (202) Sexton, B. A. Methanol Decomposition on Platinum (111). *Surf. Sci.* **1981**, *102*, 271–281.
- (203) Xu, X.; Friend, C. M. Enhanced Kinetic Stability of γ -C-H Bonds in Surface Alkoxides: The Reactions of Tert-Butyl Alcohol on Clean and Oxygen-Covered Rh(111). *Langmuir* **1992**, *8*, 1103–1110.
- (204) Chen, D. A.; Friend, C. M. Controlling Deoxygenation Selectivity by Surface Modification: Reactions of Ethanol on Oxygen- and Sulfur-Covered Mo(110). *J. Am. Chem. Soc.* **1998**, *120*, 5017–5023.
- (205) Solymosi, F.; Tarnóczti, T. I.; Berkó, A. Methanol Absorption and Decomposition on Oxygen-Precovered Rhodium(111). *J. Phys. Chem.* **1984**, *88*, 6170–6174.
- (206) Carley, A. F.; Davies, P. R.; Roberts, M. W.; Thomas, K. K. Transient Oxygen States in Catalysis: Ammonia Oxidation at Ag(111). *Langmuir* **2010**, *26*, 16221–16225.
- (207) Madix, R. J.; Roberts, J. T. *Surface Reactions*; Madix, R. J., Ed.; Springer Series in Surface Sciences; Springer: Berlin, 1994; Vol. 34.
- (208) Capote, A. J.; Hamza, A. V.; Canning, N. D. S.; Madix, R. J. The Adsorption and Reaction of Acetonitrile on Clean and Oxygen-Covered Ag(110) Surfaces. *Surf. Sci.* **1986**, *175*, 445–464.
- (209) Solomon, J. L.; Madix, R. J. Kinetics and Mechanism of the Oxidation of Allyl Alcohol on Ag(110). *J. Phys. Chem.* **1987**, *91*, 6241–6244.
- (210) Carter, R. N.; Anton, A. B.; Apai, G. Reactions of π -Allyl with Atomic Oxygen and Hydroxyl on Ag(110). *Surf. Sci.* **1993**, *290*, 319–334.
- (211) Barreau, M. A.; Madix, R. J. Lateral Interaction Effects on the Reaction of CO₂ and Oxygen Adsorbed on Ag(110). *J. Chem. Phys.* **1981**, *74*, 4144.
- (212) Carley, A. F.; Davies, P. R.; Roberts, M. W.; Thomas, K. K. Hydroxylation of Molecularly Adsorbed Water at Ag(111) and Cu(100) Surfaces by Dioxygen: Photoelectron and Vibrational Spectroscopic Studies. *Surf. Sci.* **1990**, *238*, L467–L472.
- (213) Madix, R. J.; Roberts, J. T. The Coadsorption of Water and Molecular Oxygen on Ag(110): Absence of O-O Bond Activation by Water. *Surf. Sci.* **1992**, *273*, 121–128.
- (214) Ford, D. C.; Nilekar, A. U.; Xu, Y.; Mavrikakis, M. Partial and Complete Reduction of O₂ by Hydrogen on Transition Metal Surfaces. *Surf. Sci.* **2010**, *604*, 1565–1575.
- (215) Carley, A. F.; Hawkins, G.; Read, S.; Roberts, M. W. Reactions of Co-Adsorbed Carbon Dioxide and Dioxygen at the Mg(0001) Surface at Low Temperatures. *Top. Catal.* **1999**, *8*, 243–248.
- (216) Sen, P.; Rao, C. N. R. An EELS Study of Water, Methanol, Formaldehyde and Formic Acid Adsorbed on Clean and Oxygen-Covered Zinc(0001) Surfaces. *Surf. Sci.* **1986**, *172*, 269–280.
- (217) Carley, A. F.; Roberts, M. W.; Yan, S. Intermolecular Charge-Transfer and the Cleavage of the Dioxygen Bond at Metal Surfaces: Oxygen at Zn(0001). *Catal. Lett.* **1988**, *1*, 265–269.
- (218) Carley, A. F.; Davies, P. R.; Roberts, M. W. The Development of a New Concept: The Role of Oxygen Transients, Defect and Precursor States in Surface Reactions. *Catal. Lett.* **2002**, *80*, 25–34.
- (219) Afsin, B.; Davies, P. R.; Pashusky, A.; Roberts, M. W.; Vincent, D. Reaction Pathways in the Oxydehydrogenation of Ammonia at Cu(110) Surfaces. *Surf. Sci.* **1993**, *284*, 109–120.
- (220) Boronin, A.; Pashusky, A.; Roberts, M. W. A New Approach to the Mechanism of Heterogeneously Catalysed Reactions: The Oxydehydrogenation of Ammonia at a Cu(111) Surface. *Catal. Lett.* **1992**, *16*, 345–350.
- (221) Au, C. T.; Roberts, M. W. Specific Role of Transient O-(s) at Mg(0001) Surfaces in Activation of Ammonia by Dioxygen and Nitrous Oxide. *Nature* **1986**, *319*, 206–208.
- (222) Wong, K.; Kang, S. J.; Bielawski, C. W.; Ruoff, R. S.; Kwak, S. K. First-Principles Study of the Role of O₂ and H₂O in the Decoupling of Graphene on Cu(111). *J. Am. Chem. Soc.* **2016**, *138*, 10986–10994.
- (223) López-Moreno, S.; Romero, A. H. Atomic and Molecular Oxygen Adsorbed on (111) Transition Metal Surfaces: Cu and Ni. *J. Chem. Phys.* **2015**, *142*, 154702.
- (224) Sueyoshi, T.; Sasaki, T.; Iwasawa, Y. Molecular and Atomic Adsorption States of Oxygen on Cu(111) at 100–300 K. *Surf. Sci.* **1996**, *365*, 310–318.
- (225) Xu, Y.; Mavrikakis, M. Adsorption and Dissociation of O₂ on Cu(111): Thermochemistry, Reaction Barrier and the Effect of Strain. *Surf. Sci.* **2001**, *494*, 131–144.
- (226) Xu, Y.; Mavrikakis, M. The Adsorption and Dissociation of O₂ Molecular Precursors on Cu: The Effect of Steps. *Surf. Sci.* **2003**, *538*, 219–232.
- (227) Nai, C. T.; Xu, H.; Tan, S. J. R.; Loh, K. P. Analyzing Dirac Cone and Phonon Dispersion in Highly Oriented Nanocrystalline Graphene. *ACS Nano* **2016**, *10*, 1681–1689.
- (228) Liem, S. Y.; Clarke, J. H. R.; Kresse, G. Pathways to Dissociation of O₂ on Cu(110) Surface: First Principles Simulations. *Surf. Sci.* **2000**, *459*, 104–114.
- (229) Katayama, T.; Sekiba, D.; Mukai, K.; Yamashita, Y.; Komori, F.; Yoshinobu, J. Adsorption States and Dissociation Processes of Oxygen Molecules on Cu(100) at Low Temperature. *J. Phys. Chem. C* **2007**, *111*, 15059–15063.
- (230) Yokoyama, T.; Arvanitis, D.; Lederer, T.; Tischer, M.; Tröger, L.; Baberschke, K.; Comelli, G. Adsorption of Oxygen on Cu(100). II. Molecular Adsorption and Dissociation by Means of O K-Edge X-Ray-Absorption Fine Structure. *Phys. Rev. B: Condens. Matter Mater. Phys.* **1993**, *48*, 15405–15416.
- (231) Fajin, J. L. C.; Cordeiro, M. N. D. S.; Gomes, J. R. B. On the Theoretical Understanding of the Unexpected O₂ Activation by Nanoporous Gold. *Chem. Commun.* **2011**, *47*, 8403–8405.
- (232) Xu, Y.; Greeley, J.; Mavrikakis, M. Effect of Subsurface Oxygen on the Reactivity of the Ag(111) Surface. *J. Am. Chem. Soc.* **2005**, *127*, 12823–12827.
- (233) Yan, M.; Huang, Z.; Zhang, Y.; Chang, C. Trends in Water-Promoted Oxygen Dissociation on the Transition Metal Surfaces from First Principles. *Phys. Chem. Chem. Phys.* **2017**, *19*, 2364–2371.
- (234) Monturet, S.; Alducin, M.; Lorente, N. Role of Molecular Electronic Structure in Inelastic Electron Tunneling Spectroscopy: O₂ on Ag(110). *Phys. Rev. B: Condens. Matter Mater. Phys.* **2010**, *82*, 85447.
- (235) Gravil, P.; Bird, D.; White, J. Adsorption and Dissociation of O₂ on Ag(110). *Phys. Rev. Lett.* **1996**, *77*, 3933–3936.
- (236) Rawal, T. B.; Hong, S.; Pulkkinen, A.; Alatalo, M.; Rahman, T. S. Adsorption, Diffusion, and Vibration of Oxygen on Ag(110). *Phys. Rev. B: Condens. Matter Mater. Phys.* **2015**, *92*, 35444.
- (237) Montemore, M. M.; Cubuk, E. D.; Klobas, J. E.; Schmid, M.; Madix, R. J.; Friend, C. M.; Kaxiras, E. Controlling O Coverage and Stability by Alloying Au and Ag. *Phys. Chem. Chem. Phys.* **2016**, *18*, 26844–26853.
- (238) Lončarić, I.; Alducin, M.; Juaristi, I. Dissociative Dynamics of O₂ on Ag(110). *Phys. Chem. Chem. Phys.* **2015**, *17*, 9436–9445.
- (239) Roy, S.; Mujica, V.; Ratner, M. A. Chemistry at Molecular Junctions: Rotation and Dissociation of O₂ on the Ag(110) Surface Induced by a Scanning Tunneling Microscope. *J. Chem. Phys.* **2013**, *139*, 074702.

- (240) Bartolucci, F.; Franchy, R.; Barnard, J.; Palmer, R. Two Chemisorbed Species of O₂ on Ag(110). *Phys. Rev. Lett.* **1998**, *80*, S224–S227.
- (241) Smerieri, M.; Savio, L.; Vattuone, L.; Rocca, M. O₂ Dissociation before the Onset of Added Row Nucleation on Ag(110): An Atomistic Scanning Tunnelling Microscopy View. *J. Phys.: Condens. Matter* **2010**, *22*, 304015.
- (242) Outka, D. A.; Stöhr, J.; Jark, W.; Stevens, P.; Solomon, J.; Madix, R. J. Orientation and Bond Length of Molecular Oxygen on Ag(110) and Pt(111): A near-Edge X-Ray-Absorption Fine-Structure Study. *Phys. Rev. B: Condens. Matter Mater. Phys.* **1987**, *35*, 4119.
- (243) Backx, C.; De Groot, C. P. M.; Biloen, P. Adsorption of Oxygen on Ag(110) Studied by High Resolution ELS and TPD. *Surf. Sci.* **1981**, *104*, 300–317.
- (244) Sexton, B. A.; Madix, R. J. Vibrational Spectra of Molecular and Atomic Oxygen on Ag(110). *Chem. Phys. Lett.* **1980**, *76*, 294–297.
- (245) Gajdoš, M.; Eichler, A.; Hafner, J. Ab Initio Density Functional Study of O on the Ag(001) Surface. *Surf. Sci.* **2003**, *531*, 272–286.
- (246) Vattuone, L.; Gambardella, P.; Valbusa, U.; Rocca, M. HREELS Study of O₂ Molecular Chemisorption on Ag(001). *Surf. Sci.* **1997**, *377*–379, 671–675.
- (247) Buatier de Mongeot, F.; Cupolillo, A.; Valbusa, U.; Rocca, M. Anharmonicity of the O₂-Ag(001) Chemisorption Potential. *J. Chem. Phys.* **1997**, *106*, 9297.
- (248) Boronat, M.; Corma, A. Oxygen Activation on Gold Nanoparticles: Separating the Influence of Particle Size, Particle Shape and Support Interaction. *Dalt. Trans.* **2010**, *39*, 8538.
- (249) Barrio, L.; Liu, P.; Rodriguez, J. A.; Campos-Martin, J. M.; Fierro, J. L. G. Effects of Hydrogen on the Reactivity of O₂ toward Gold Nanoparticles and Surfaces. *J. Phys. Chem. C* **2007**, *111*, 19001–19008.
- (250) Stiehl, J. D.; Kim, T. S.; McClure, S. M.; Mullins, C. B. Evidence for Molecularly Chemisorbed Oxygen on TiO₂ Supported Gold Nanoclusters and Au(111). *J. Am. Chem. Soc.* **2004**, *126*, 1606–1607.
- (251) Stiehl, J. D.; Kim, T. S.; McClure, S. M.; Mullins, C. B. Formation of Molecularly Chemisorbed Oxygen on TiO₂-Supported Gold Nanoclusters and Au(111) from Exposure to an Oxygen Plasma Jet. *J. Phys. Chem. B* **2005**, *109*, 6316–6322.
- (252) Kleyn, A. W. The Interaction of O₂ with Ag(111) Probed by Beam Experiments. In *Elementary Processes in Excitations and Reactions on Solid Surfaces*; Okiji, A., Kasai, H., Makoshi, K., Eds.; Springer-Verlag: Berlin, 1996; Vol. 121, pp 89–98.
- (253) Franchy, R.; Bartolucci, F.; Mongeot, F. B.; Cemic, F.; Rocca, M.; Valbusa, U.; Vattuone, L.; Lacombe, S.; Jacobi, K.; Tang, K. B. K.; et al. Negative Ion Resonances of O₂ Adsorbed on Ag Surfaces. *J. Phys.: Condens. Matter* **2000**, *12*, R53–R82.
- (254) Raukema, A.; Butler, D. A.; Kleyn, A. W. O₂ Transient Trapping-Desorption at the Ag(111) Surface. *J. Chem. Phys.* **1997**, *106*, 2477–2491.
- (255) Kleyn, A. W.; Butler, D. A.; Raukema, A. Dynamics of the Interaction of O₂ with Silver Surfaces. *Surf. Sci.* **1996**, *363*, 29–41.
- (256) Rocca, M. Anisotropy of the Oxygen Interaction with Ag Surfaces. *Phys. Scr.* **1996**, *T66*, 262–267.
- (257) de Mongeot, F. B.; Valbusa, U.; Rocca, M. Oxygen Adsorption on Ag(111). *Surf. Sci.* **1995**, *339*, 291–296.
- (258) Raukema, A.; Kleyn, A. W. Transient Trapping Desorption of Molecules at Surfaces. *Phys. Rev. Lett.* **1995**, *74*, 4333–4336.
- (259) Reijnen, P. H. F.; van Slooten, U.; Kleyn, A. W. Negative Ion Formation and Dissociation in Scattering of Fast O₂ and NO from Ag(111) and Pt(111). *J. Chem. Phys.* **1991**, *94*, 695–703.
- (260) Benndorf, C.; Franck, M.; Thieme, F. Oxygen Adsorption on Ag(111) in the Temperature Range from 100–500 K: UPS, XPS and EELS Investigations. *Surf. Sci.* **1983**, *128*, 417–423.
- (261) Campbell, C. T. Atomic and Molecular Oxygen Adsorption on Ag(111). *Surf. Sci.* **1985**, *157*, 43–60.
- (262) Raukema, A.; Dirksen, R. J.; Kleyn, A. W. Probing the (Dual) Repulsive Wall in the Interaction of O₂, N₂, and Ar with the Ag(111) Surface. *J. Chem. Phys.* **1995**, *103*, 6217–6231.
- (263) Schmeisser, D.; Jacobi, K. The Interaction of Oxygen with Silver Clusters and Surfaces. *Surf. Sci.* **1985**, *156*, 911–919.
- (264) Grant, R. B.; Lambert, R. M. Basic Studies of the Oxygen Surface Chemistry of Silver: Chemisorbed Atomic and Molecular Species on Pure Ag(111). *Surf. Sci.* **1984**, *146*, 256–268.
- (265) Rajumon, M. K.; Prabhakaran, K.; Rao, C. N. R. Adsorption of Oxygen on (100), (110) and (111) Surfaces of Ag, Cu and Ni: An Electron Spectroscopic Study. *Surf. Sci.* **1990**, *233*, L237–L242.
- (266) Campbell, C. T. An XPS Study of Molecularly Chemisorbed Oxygen on Ag(111). *Surf. Sci.* **1986**, *173*, L641–L646.
- (267) Goikoetxea, I.; Beltrán, J.; Meyer, J.; Juaristi, J. I.; Alducin, M.; Reuter, K. Non-Adiabatic Effects during the Dissociative Adsorption of O₂ at Ag(111): A First-Principles Divide and Conquer Study. *New J. Phys.* **2012**, *14*, 013050.
- (268) Raukema, A.; Butler, D. A.; Kleyn, A. W. Reply to “Comment on ‘Dissociative and Non-Dissociative Sticking of O₂ at the Ag(111) Surface’” by M. Rocca et Al. *Surf. Sci.* **1997**, *373*, 127–128.
- (269) Rocca, M.; Cemcić, F.; de Mongeot, F. B.; Valbusa, U.; Lacombe, S.; Jacobi, K. Comment on “Dissociative and Non-Dissociative Sticking of O₂ at the Ag(111) Surface” by A. Raukema, D.A. Butler, F.M.A. Box and A.W. Kleyn. *Surf. Sci.* **1997**, *373*, 125–126.
- (270) Engelhardt, H. A.; Menzel, D. Adsorption of Oxygen on Silver Single Crystal Surfaces. *Surf. Sci.* **1976**, *57*, 591–618.
- (271) Hahn, J. R.; Ho, W. Orbital Specific Chemistry: Controlling the Pathway in Single-Molecule Dissociation. *J. Chem. Phys.* **2005**, *122*, 244704.
- (272) Hahn, J. R.; Ho, W. Chemisorption and Dissociation of Single Oxygen Molecules on Ag(110). *J. Chem. Phys.* **2005**, *123*, 214702.
- (273) Barth, J. V.; Zambelli, T.; Winterlin, J.; Schuster, R.; Ertl, G. Direct Observation of Mobility and Interactions of Oxygen Molecules Chemisorbed on the Ag(110) Surface. *Phys. Rev. B: Condens. Matter Mater. Phys.* **1997**, *55*, 12902–12905.
- (274) Vattuone, L.; Rocca, M.; Boragno, C.; Valbusa, U. Initial Sticking Coefficient of O₂ on Ag(110). *J. Chem. Phys.* **1994**, *101*, 713–725.
- (275) Guest, R. J.; Hernnäs, B.; Bennich, P.; Björneholm, O.; Nilsson, A.; Palmer, R. E.; Mårtensson, N. Orientation of a Molecular Precursor: A NEXAFS Study of O₂/Ag(110). *Surf. Sci.* **1992**, *278*, 239–245.
- (276) Prince, K. C.; Paolucci, G.; Bradshaw, A. M. Oxygen Adsorption on Silver (110): Dispersion, Bonding and Precursor State. *Surf. Sci.* **1986**, *175*, 101–122.
- (277) Messerli, S.; Schintke, S.; Morgenstern, K.; Nieminen, J.; Schneider, W.-D. Oxygen Molecules on Ag(001): Superstructure, Binding Site and Molecular Orientation. *Chem. Phys. Lett.* **2000**, *328*, 330–336.
- (278) Garfunkel, E. L.; Ding, X.; Dong, G.; Yang, S.; Hou, X.; Wang, X. The Coadsorption of Sodium and Oxygen on Ag(100): An XPS, UPS and HREELS Study. *Surf. Sci.* **1985**, *164*, 511–525.
- (279) de Mongeot, F. B.; Cupolillo, A.; Valbusa, U.; Rocca, M. O₂ Dissociation on Ag(001): The Role of Kink Sites. *Chem. Phys. Lett.* **1997**, *270*, 345–350.
- (280) Spitzer, A.; Lüth, H. The Adsorption of Oxygen on Copper Surfaces. *Surf. Sci.* **1982**, *118*, 136–144.
- (281) Ma, L.; Zeng, X. C.; Wang, J. Oxygen Intercalation of Graphene on Transition Metal Substrate: An Edge-Limited Mechanism. *J. Phys. Chem. Lett.* **2015**, *6*, 4099–4105.
- (282) Wendelken, J. F. The Chemisorption of Oxygen on Cu(110) Studied by EELS and LEED. *Surf. Sci.* **1981**, *108*, 605–616.
- (283) Briner, B. G.; Doering, M.; Rust, H.-P.; Bradshaw, A. M. Mobility and Trapping of Molecules During Oxygen Adsorption on Cu(110). *Phys. Rev. Lett.* **1997**, *78*, 1516–1519.
- (284) Prabhakaran, K.; Sen, P.; Rao, C. N. R. Studies of Molecular Oxygen Adsorbed on Cu Surfaces. *Surf. Sci.* **1986**, *177*, L971–L977.
- (285) Spitzer, A.; Lüth, H. The Adsorption of Oxygen on Copper Surfaces. I. Cu(100) and Cu(110). *Surf. Sci.* **1982**, *118*, 121–135.
- (286) Prabhakaran, K.; Rao, C. N. R. Comment on “Oxygen Chemisorption on Cu(110)” by J.M. Mundener, A.P. Baddorf, E.W.

- Plummer, L.G. Sneddon, R.A. Didio and D.M. Zehner. *Surf. Sci.* **1988**, *198*, L307–L308.
- (287) Balkenende, A. R.; den Daas, H.; Huisman, M.; Gijzeman, O. L. J.; Geus, J. W. The Interaction of NO, O₂ and CO with Cu(100) and Cu(110). *Appl. Surf. Sci.* **1991**, *47*, 341–353.
- (288) Gruzalski, G. R.; Zehner, D. M.; Wendelken, J. F. An XPS Study of Oxygen Adsorption on Cu(110). *Surf. Sci.* **1985**, *159*, 353–368.
- (289) García-Mota, M.; López, N. The Role of Long-Lived Oxygen Precursors on AuM Alloys (M = Ni, Pd, Pt) in CO Oxidation. *Phys. Chem. Chem. Phys.* **2011**, *13*, 5790.
- (290) Kim, C. M.; Jeong, H. S.; Kim, E. H. NEXAFS and XPS Characterization of Molecular Oxygen Adsorbed on Ni(100) at 80 K. *Surf. Sci.* **2000**, *459*, L457–L461.
- (291) Ham, H. C.; Stephens, J. A.; Hwang, G. S.; Han, J.; Nam, S. W.; Lim, T. H. Pd Ensemble Effects on Oxygen Hydrogenation in AuPd Alloys: A Combined Density Functional Theory and Monte Carlo Study. *Catal. Today* **2011**, *165*, 138–144.
- (292) Li, J.; Staykov, A.; Ishihara, T.; Yoshizawa, K. Theoretical Study of the Decomposition and Hydrogenation of H₂O₂ on Pd and Au@Pd Surfaces: Understanding toward High Selectivity of H₂O₂ Synthesis. *J. Phys. Chem. C* **2011**, *115*, 7392–7398.
- (293) Imbihl, R.; Demuth, J. E. Adsorption of Oxygen on a Pd(111) Surface Studied by High Resolution Electron Energy Loss Spectroscopy (EELS). *Surf. Sci.* **1986**, *173*, 395–410.
- (294) Nolan, P. D.; Lutz, B. R.; Tanaka, P. L.; Mullins, C. B. Direct Verification of a High-Translational-Energy Molecular Precursor to Oxygen Dissociation on Pd(111). *Surf. Sci.* **1998**, *419*, L107–L113.
- (295) Cemcić, F.; Dippel, O.; Kolasinski, K. W.; Hasselbrink, E. Negative Ion Resonances in Electron Scattering from Chemisorbed O₂. *Surf. Sci.* **1995**, *331*–333, 267–271.
- (296) Kolasinski, K. W.; Cemic, F.; Hasselbrink, E. O₂/Pd(111). Clarification of the Correspondence between Thermal Desorption Features and Chemisorption States. *Chem. Phys. Lett.* **1994**, *219*, 113–117.
- (297) Wolf, M.; Hasselbrink, E.; Ertl, G.; Zhu, X. Y.; White, J. M. Excitation Mechanism in the Photodissociation of Dioxygen Adsorbed on Pd(111). *Surf. Sci.* **1991**, *248*, L235–L239.
- (298) Fernández, J. L.; White, J. M.; Sun, Y.; Tang, W.; Henkelman, G.; Bard, A. J. Characterization and Theory of Electrocatalysts Based on Scanning Electrochemical Microscopy Screening Methods. *Langmuir* **2006**, *22*, 10426–10431.
- (299) Nyberg, C.; Tengstål, C. G. Vibrational Excitations of Hydrogen and Oxygen on Pd(100). *Surf. Sci.* **1983**, *126*, 163–169.
- (300) Liu, D. J.; Evans, J. W. Dissociative Adsorption of O₂ on Unreconstructed Metal (100) Surfaces: Pathways, Energetics, and Sticking Kinetics. *Phys. Rev. B: Condens. Matter Mater. Phys.* **2014**, *89*, 205406.
- (301) Shao, M. H.; Liu, P.; Adzic, R. R. Superoxide Anion Is the Intermediate in the Oxygen Reduction Reaction on Platinum Electrodes. *J. Am. Chem. Soc.* **2006**, *128*, 7408–7409.
- (302) Lischka, M.; Mosch, C.; Groß, A. Tuning Catalytic Properties of Bimetallic Surfaces: Oxygen Adsorption on Pseudomorphic Pt/Ru Overlays. *Electrochim. Acta* **2007**, *52*, 2219–2228.
- (303) McEwen, J. S.; Bray, J. M.; Wu, C.; Schneider, W. F. How Low Can You Go? Minimum Energy Pathways for O₂ Dissociation on Pt(111). *Phys. Chem. Chem. Phys.* **2012**, *14*, 16677–16685.
- (304) Nolan, P. D.; Lutz, B. R.; Tanaka, P. L.; Davis, J. E.; Mullins, C. B. Translational Energy Selection of Molecular Precursors to Oxygen Adsorption on Pt(111). *Phys. Rev. Lett.* **1998**, *81*, 3179–3182.
- (305) Nolan, P. D.; Lutz, B. R.; Tanaka, P. L.; Davis, J. E.; Mullins, C. B. Molecularly Chemisorbed Intermediates to Oxygen Adsorption on Pt(111): A Molecular Beam and Electron Energy-Loss Spectroscopy Study. *J. Chem. Phys.* **1999**, *111*, 3696–3704.
- (306) Gland, J. L.; Sexton, B. A.; Fisher, G. B. Oxygen Interactions with the Pt(111) Surface. *Surf. Sci.* **1980**, *95*, 587–602.
- (307) Puglia, C.; Nilsson, A.; Hernnäs, B.; Karis, O.; Bennich, P.; Mårtensson, N. Physisorbed, Chemisorbed and Dissociated O₂ on Pt(111) Studied by Different Core Level Spectroscopy Methods. *Surf. Sci.* **1995**, *342*, 119–133.
- (308) Wurth, W.; Stöhr, J.; Feulner, P.; Pan, X.; Bauchspies, K. R.; Baba, Y.; Hudel, E.; Rocker, G.; Menzel, D. Bonding, Structure, and Magnetism of Physisorbed and Chemisorbed O₂ on Pt(111). *Phys. Rev. Lett.* **1990**, *65*, 2426–2429.
- (309) Petersen, M.; Jenkins, S.; King, D. Ridge-Bridge Adsorption of Molecular Oxygen on Pt{110}(1 × 2) from First Principles. *J. Phys. Chem. B* **2006**, *110*, 11962–11970.
- (310) Schmidt, J.; Stuhlmann, C.; Ibach, H. Oxygen Adsorption on the Pt(110)(1 × 2) Surface Studied with EELS. *Surf. Sci.* **1993**, *284*, 121–128.
- (311) Sobyanin, V. A.; Zamaraev, K. I. Study of Oxygen Adsorption on Pt(110) Surface with EELS. *React. Kinet. Catal. Lett.* **1986**, *31*, 273–277.
- (312) Panchenko, A.; Koper, M. T. M.; Shubina, T. E.; Mitchell, S. J.; Roduner, E. Ab Initio Calculations of Intermediates of Oxygen Reduction on Low-Index Platinum Surfaces. *J. Electrochem. Soc.* **2004**, *151*, A2016.
- (313) Vasic, D.; Pasti, I.; Gavrilov, N.; Mentus, S. DFT Study of Interaction of O, O₂, and OH with Unreconstructed Pt(hkl) (h, k, l = 0, 1) Surfaces—Similarities, Differences, and Universalities. *Russ. J. Phys. Chem. A* **2013**, *87*, 2214–2218.
- (314) Qi, L.; Yu, J.; Li, J. Coverage Dependence and Hydroperoxyl-Mediated Pathway of Catalytic Water Formation on Pt (111) Surface. *J. Chem. Phys.* **2006**, *125*, 054701.
- (315) Luntz, A. C.; Grimalt, J.; Fowler, D. E. Sequential Precursors in Dissociative Chemisorption: O₂ on Pt(111). *Phys. Rev. B: Condens. Matter Mater. Phys.* **1989**, *39*, 12903–12906.
- (316) Elg, A.-P.; Eisert, F.; Rosén, A. The Temperature Dependence of the Initial Sticking Probability of Oxygen on Pt(111) Probed with Second Harmonic Generation. *Surf. Sci.* **1997**, *382*, 57–66.
- (317) Artsyukhovich, A. N.; Ukrainstsev, V. A.; Harrison, I. Low Temperature Sticking and Desorption Dynamics of Oxygen on Pt(111). *Surf. Sci.* **1996**, *347*, 303–318.
- (318) Ou, L.; Yang, F.; Liu, Y.; Chen, S. First-Principle Study of the Adsorption and Dissociation of O₂ on Pt(111) in Acidic Media. *J. Phys. Chem. C* **2009**, *113*, 20657–20665.
- (319) Ohno, Y.; Matsushima, T.; Tanaka, S. I.; Kamada, M. Desorption, Dissociation and Orientation of Oxygen Admolecules on a Reconstructed Platinum(110)(1 × 2) Surface Studied by Thermal Desorption and near-Edge X-Ray-Absorption Fine-Structure. *Jpn. J. Appl. Phys.* **1993**, *32*, 383–385.
- (320) Ducros, R.; Fusy, J. Oxygen Adsorption on Pt(110)(1 × 2): Surface Characterization by Photoemission of Adsorbed Xenon (PAX). *Appl. Surf. Sci.* **1990**, *44*, 59–64.
- (321) Fusy, J.; Ducros, R. Oxygen Adsorption on Pt(110)(1 × 2) at 100 K. *Surf. Sci.* **1989**, *214*, 337–346.
- (322) Prince, K. C.; Dücker, K.; Horn, K.; Cháb, V. Orientation of Molecular Oxygen on Pt(110). *Surf. Sci.* **1988**, *200*, L451–L459.
- (323) Freyer, N.; Kisikova, M.; Bonzel, H. P.; Pirug, G. Oxygen Adsorption on Pt(110)-(1 × 2) and Pt(110)-(1 × 1). *Surf. Sci.* **1986**, *166*, 206–220.
- (324) Ferrer, S.; Bonzel, H. P. The Preparation, Thermal Stability and Adsorption Characteristics of the Non-Reconstructed Pt(110)-1 × 1 Surface. *Surf. Sci.* **1982**, *119*, 234–250.
- (325) Li, K.; Li, Y.; Wang, Y.; He, F.; Jiao, M.; Tang, H.; Wu, Z. The Oxygen Reduction Reaction on Pt(111) and Pt(100) Surfaces Substituted by Subsurface Cu: A Theoretical Perspective. *J. Mater. Chem. A* **2015**, *3*, 11444–11452.
- (326) Duan, Z.; Wang, G. Comparison of Reaction Energetics for Oxygen Reduction Reactions on Pt(100), Pt(111), Pt/Ni(100), and Pt/Ni(111) Surfaces: A First-Principles Study. *J. Phys. Chem. C* **2013**, *117*, 6284–6292.
- (327) Norton, P. R.; Griffiths, K.; Bindner, P. E. Interaction of O₂ with Pt(100). II. Kinetics and Energetics. *Surf. Sci.* **1984**, *138*, 125–147.

- (328) Rose, M. K.; Borg, A.; Dunphy, J. C.; Mitsui, T.; Ogletree, D. F.; Salmeron, M. Chemisorption of Atomic Oxygen on Pd(111) Studied by STM. *Surf. Sci.* **2004**, *561*, 69–78.
- (329) Rose, M. K.; Borg, A.; Dunphy, J. C.; Mitsui, T.; Ogletree, D. F.; Salmeron, M. Chemisorption and Dissociation of O₂ on Pd(111) Studied by STM. *Surf. Sci.* **2003**, *547*, 162–170.
- (330) Goschnick, J.; Wolf, M.; Grunze, M.; Unertl, W. N.; Block, J. H.; Loboda-Cackovic, J. Adsorption of O₂ on Pd(110). *Surf. Sci.* **1986**, *178*, 831–841.
- (331) Sjövall, P.; Uvdal, P. Oxygen Sticking on Pd(111): Double Precursors, Corrugation and Substrate Temperature Effects. *Chem. Phys. Lett.* **1998**, *282*, 355–360.
- (332) Sjövall, P.; Uvdal, P. Adsorption of Oxygen on Pd(111): Precursor Kinetics and Coverage-Dependent Sticking. *J. Vac. Sci. Technol., A* **1998**, *16*, 943.
- (333) Milun, M.; Pervan, P.; Vajić, M.; Wandelt, K. Thermal Desorption Spectroscopy of the O₂/Pd(110) System. *Surf. Sci.* **1989**, *211–212*, 887–895.
- (334) He, J.-W.; Memmert, U.; Norton, P. R. Interaction of Oxygen with a Pd(110) Surface. II. Kinetics and Energetics. *J. Chem. Phys.* **1989**, *90*, 5088.
- (335) den Dunnen, A.; Jacobse, L.; Wiegman, S.; Berg, O. T.; Juurlink, L. B. F. Coverage-Dependent Adsorption and Desorption of Oxygen on Pd(100). *J. Chem. Phys.* **2016**, *144*, 244706.
- (336) Nyberg, C.; Tengstål, C. G. Vibrational Excitations of p(2 × 2) Oxygen and c(2 × 2) Hydrogen on Pd(100). *Solid State Commun.* **1982**, *44*, 251–254.
- (337) Beutl, M.; Rendulic, K. D.; Castro, G. R. Does the Rotational State of a Molecule Influence Trapping in a Precursor? An Investigation of N₂/W(100), CO/FeSi(100) and O₂/Ni(111). *Surf. Sci.* **1997**, *385*, 97–106.
- (338) Rettew, R. E.; Meyer, A.; Senanayake, S. D.; Chen, T.-L.; Petersburg, C.; Ingo Flege, J.; Falta, J.; Alamgir, F. M. Interactions of Oxygen and Ethylene with Submonolayer Ag Films Supported on Ni(111). *Phys. Chem. Chem. Phys.* **2011**, *13*, 11034–11044.
- (339) Shayegan, M.; Cavallo, J. M.; Glover, R. E.; Park, R. L. Precursor Adsorption of Oxygen on Ni(111) and the Activation Energy for Chemisorption. *Phys. Rev. Lett.* **1984**, *53*, 1578–1581.
- (340) Beckerle, J. D.; Yang, Q. Y.; Johnson, A. D.; Ceyer, S. T. The Adsorption of CO and O₂ on Ni(111) at 8 K. *Surf. Sci.* **1988**, *195*, 77–93.
- (341) Komeda, T.; Sakisaka, Y.; Onchi, M.; Kato, H.; Masuda, S.; Yagi, K. Angle-Resolved Photoemission Study of the Interaction of Oxygen with a Ni(110) Surface. *Surf. Sci.* **1987**, *188*, 45–62.
- (342) Hsu, Y.; Jacobi, K.; Rotermund, H. H. Adsorption of N₂, CO and O₂ on Ni(110) at 20 K. *Surf. Sci.* **1982**, *117*, 581–589.
- (343) Holloway, P. H.; Hudson, J. B. Kinetics of the Reaction of Oxygen with Clean Nickel Single Crystal Surfaces. II. Ni(111) Surface. *Surf. Sci.* **1974**, *43*, 141–149.
- (344) Walter, E. J.; Lewis, S. P.; Rappe, A. M. Investigation of Chemisorbed Molecular States for Oxygen on Rhodium (111). *J. Chem. Phys.* **2000**, *113*, 4388–4391.
- (345) Davis, J. E.; Nolan, P. D.; Karseboom, S. G.; Mullins, C. B. Kinetics and Dynamics of the Dissociative Chemisorption of Oxygen on Ir(111). *J. Chem. Phys.* **1997**, *107*, 943–952.
- (346) Erikat, I. A.; Hamad, B. A.; Khalifeh, J. M. A Density Functional Study on Adsorption and Dissociation of O₂ on Ir(100) Surface. *Chem. Phys.* **2011**, *385*, 35–40.
- (347) Marinova, T. S.; Kostov, K. L. Interaction of Oxygen with a Clean Ir(111) Surface. *Surf. Sci.* **1987**, *185*, 203–212.
- (348) Taylor, J. L.; Ibbotson, D. E.; Weinberg, W. H. The Chemisorption of Oxygen on the (110) Surface of Iridium. *Surf. Sci.* **1979**, *79*, 349–384.
- (349) Mullins, C. B.; Wang, Y.; Weinberg, W. H. A Molecular-beam Study of the Dissociative Chemisorption of O₂ on Ir(110)-(1 × 2). *J. Vac. Sci. Technol., A* **1989**, *7*, 2125–2126.
- (350) Kelly, D.; Verhoef, R. W.; Weinberg, W. H. Effect of Internal Energy on the Dissociative Chemisorption of Oxygen on Ir(110). *Surf. Sci.* **1994**, *321*, L157–L163.
- (351) Kelly, D.; Verhoef, R. W.; Weinberg, W. H. Initial Probability of Dissociative Chemisorption of Oxygen on Iridium(110). *J. Chem. Phys.* **1995**, *102*, 3440–3447.
- (352) Verhoef, R. W.; Kelly, D.; Weinberg, W. H. Dissociative Chemisorption of Oxygen on Ir(110) as a Function of Surface Coverage. *Surf. Sci.* **1995**, *328*, 1–20.
- (353) Ladas, S.; Kennou, S.; Hartmann, N.; Imbihl, R. Characterisation of the Oxygen Adsorption States on Clean and Oxidized Ir(110) Surfaces. *Surf. Sci.* **1997**, *382*, 49–56.
- (354) Brault, P.; Range, H.; Toennies, J. P.; Wöll, C. The Low Temperature Adsorption of Oxygen on Rh(111). *Z. Phys. Chem.* **1997**, *198*, 1–17.
- (355) Mitchell, W. J.; Xie, J.; Lyons, K. J.; Weinberg, W. H. Dissociative Chemisorption of Oxygen on the Ru(001) Surface: Spectroscopic Identification of Precursor Intermediates at Low Surface Temperatures. *J. Vac. Sci. Technol., A* **1994**, *12*, 2250–2254.
- (356) Nilius, N.; Mitte, M.; Neddermeyer, H. Low-Temperature Scanning Tunnelling Microscopy Study of O₂ Adsorption on Ru(0001). *Appl. Phys. A: Mater. Sci. Process.* **1998**, *66*, S519–S523.
- (357) Osovskii, V. D.; Ptushinskii, Y. G.; Sukretnyi, V. G.; Chuikov, B. A.; Medvedev, V. K.; Suchorski, Y. Molecular Adsorption States of O₂ on W(111) at Low Temperatures (Down to 5 K). *Surf. Sci.* **1997**, *377–379*, 664–670.
- (358) Wendelken, J. F. Atomic and Molecular States of Oxygen Chemisorbed on Tungsten(112). *J. Vac. Sci. Technol., A* **1988**, *6*, 662–664.
- (359) Opila, R.; Gomer, R. Adsorption of Oxygen on the Tungsten (110) Plane at Low Temperatures; Spectroscopic Measurements. *Surf. Sci.* **1981**, *105*, 41–47.
- (360) Tatarenko, S.; Dolle, P.; Morancho, R.; Alnot, M.; Ehrhardt, J. J.; Ducros, R. XPS and UPS Study of Oxygen Adsorption on Re(0001) at Low Temperatures. *Surf. Sci.* **1983**, *134*, L505–L512.
- (361) Takano, A.; Ueda, K. A Study of the Oxygen Adsorption Process on a Titanium Single Crystal Surface by Electron Stimulated Desorption. *Surf. Sci.* **1991**, *242*, 450–453.
- (362) Shinn, N. D.; Madey, T. E. Oxygen Chemisorption on Cr(110) I. Dissociative Adsorption. *Surf. Sci.* **1986**, *173*, 379–394.
- (363) Shinn, N. D.; Madey, T. E. Oxygen Chemisorption on Cr(110) II. Evidence for Molecular O₂ (ads). *Surf. Sci.* **1986**, *176*, 635–652.
- (364) Shinn, N. D.; Madey, T. E. Chemisorption and Dissociation of O₂ on Cr(110): An EELS/ESDIAD Study. *Nucl. Instrum. Methods Phys. Res., Sect. B* **1986**, *13*, 537–540.
- (365) Zhang, P.; Sun, B.; Yang, Y. Adsorption and Dissociation of O₂ at Be(0001): First-Principles Prediction of an Energy Barrier on the Adiabatic Potential Energy Surface. *Phys. Rev. B: Condens. Matter Mater. Phys.* **2009**, *79*, 165416.
- (366) Li, S. F.; Xue, X.; Li, P.; Li, X.; Jia, Y. First-Principles Studies on the Adsorption of Molecular Oxygen on Ba(110) Surface. *Phys. Lett. A* **2006**, *352*, 526–530.
- (367) Yang, Y.; Zhou, G.; Wu, J.; Duan, W.; Xue, Q. K.; Gu, B. L.; Jiang, P.; Ma, X.; Zhang, S. B. The Adsorption of O₂ on Pb Films and the Effect of Quantum Modulation: A First-Principles Prediction. *J. Chem. Phys.* **2008**, *128*, 164705.
- (368) Yang, Y.; Zhang, P. Dissociation of O₂ Molecules on Strained Pb (111) Surfaces. *J. Phys. Chem. C* **2011**, *115*, 17378–17383.
- (369) Ma, X.; Jiang, P.; Qi, Y.; Jia, J.; Yang, Y. Y.; Duan, W.; Li, W.-X. W.-X.; Bao, X.; Zhang, S. B.; Xue, Q.-K. Experimental Observation of Quantum Oscillation of Surface Chemical Reactivities. *Proc. Natl. Acad. Sci. U. S. A.* **2007**, *104*, 9204–9208.
- (370) Hu, Z. Y.; Yang, Y.; Sun, B.; Zhang, P.; Wang, W. C.; Shao, X. H. Dissociations of O₂ Molecules on Ultrathin Pb(111) Films: First-Principles Plane Wave Calculations. *Chin. Phys. B* **2012**, *21*, 016801.
- (371) Sen, P.; Rao, C. N. R. Interaction of Oxygen with Zn(0001) Surface. *Solid State Commun.* **1985**, *54*, 309–312.
- (372) Habraken, F. H. P. M.; Kieffer, E. P.; Bootsma, G. A. A Study of the Kinetics of the Interactions of O₂ and N₂O with a Cu(111) Surface and of the Reaction of CO with Adsorbed Oxygen Using AES, LEED and Ellipsometry. *Surf. Sci.* **1979**, *83*, 45–59.

- (373) Lian, X.; Xiao, P.; Yang, S.-C.; Liu, R.; Henkelman, G. Calculations of Oxide Formation on Low-Index Cu Surfaces. *J. Chem. Phys.* **2016**, *145*, 044711.
- (374) Pudney, P.; Bowker, M. Activated Dissociation of Oxygen on Cu(110). *Chem. Phys. Lett.* **1990**, *171*, 373–376.
- (375) Habraken, F. H. P. M.; Bootsma, G. A. The Kinetics of the Interactions of O₂ and N₂O with a Cu(110) Surface and of the Reaction of CO with Adsorbed Oxygen Studied by Means of Ellipsometry, AES and LEED. *Surf. Sci.* **1979**, *87*, 333–347.
- (376) Ahonen, M.; Hirsimäki, M.; Puusto, A.; Auvinen, S.; Valden, M.; Alatalo, M. Adsorption Dynamics of O₂ on Cu(100): The Role of Vacancies, Steps and Adatoms in Dissociative Chemisorption of O₂. *Chem. Phys. Lett.* **2008**, *456*, 211–214.
- (377) Habraken, F. H. P. M.; Mesters, C. M. A. M.; Bootsma, G. A. The Adsorption and Incorporation of Oxygen on Cu(100) and Its Reaction with Carbon Monoxide; Comparison with Cu(111) and Cu(110). *Surf. Sci.* **1980**, *97*, 264–282.
- (378) Benndorf, C.; Egert, B.; Keller, G.; Seidel, H.; Thieme, F. Oxygen Interaction with Cu(100) Studied by AES, ELS, LEED and Work Function Changes. *J. Phys. Chem. Solids* **1979**, *40*, 877–886.
- (379) Hofmann, P.; Unwin, R.; Wyrobisch, W.; Bradshaw, A. M. The Adsorption and Incorporation of Oxygen on Cu(100) at T ≥ 300 K. *Surf. Sci.* **1978**, *72*, 635–644.
- (380) Xin, H.; Linic, S. Analyzing Relationships between Surface Perturbations and Local Chemical Reactivity of Metal Sites: Alkali Promotion of O₂ Dissociation on Ag(111). *J. Chem. Phys.* **2016**, *144*, 234704.
- (381) Raukema, A.; Butler, D. A.; Box, F. M. A.; Kleyn, A. W. Dissociative and Non-Dissociative Sticking of O₂ at the Ag(111) Surface. *Surf. Sci.* **1996**, *347*, 151–168.
- (382) Kim, J.; Samano, E.; Koel, B. E. Oxygen Adsorption and Oxidation Reactions on Au(211) Surfaces: Exposures Using O₂ at High Pressures and Ozone (O₃) in UHV. *Surf. Sci.* **2006**, *600*, 4622–4632.
- (383) Huang, L.; Chevrier, J.; Zeppenfeld, P.; Cosma, G. Observation by Scanning Tunneling Microscopy of a Hexagonal Au(111) Surface Reconstruction Induced by Oxygen. *Appl. Phys. Lett.* **1995**, *66*, 935.
- (384) Huang, L.; Zeppenfeld, P.; Chevrier, J.; Comsa, G. Surface Morphology of Au(111) after Exposure to Oxygen at High Temperature and Pressure. *Surf. Sci.* **1996**, *352*–354, 285–289.
- (385) Fajín, J. L. C.; Cordeiro, M. N. D. S.; Gomes, J. R. B. Adsorption of Atomic and Molecular Oxygen on the Au(321) Surface: DFT Study. *J. Phys. Chem. C* **2007**, *111*, 17311–17321.
- (386) Pireaux, J. J.; Chtaib, M.; Delrue, J. P.; Thiry, P. A.; Liehr, M.; Caudano, R. Electron Spectroscopic Characterization of Oxygen Adsorption on Gold Surfaces. *Surf. Sci.* **1984**, *141*, 211–220.
- (387) Gong, J. Structure and Surface Chemistry of Gold-Based Model Catalysts. *Chem. Rev.* **2012**, *112*, 2987–3054.
- (388) Chesters, M. A.; Somorjai, G. A. The Chemisorption of Oxygen, Water and Selected Hydrocarbons on the (111) and Stepped Gold Surfaces. *Surf. Sci.* **1975**, *52*, 21–28.
- (389) Schrader, M. E. Auger Electron Spectroscopic Study of Chemisorption of Oxygen to (111)-Oriented Gold Surfaces. *J. Colloid Interface Sci.* **1977**, *59*, 456–460.
- (390) Légaré, P.; Hilaire, L.; Sotto, M.; Maire, G. Interaction of Oxygen with Au Surfaces: A LEED, AES and ELS Study. *Surf. Sci.* **1980**, *91*, 175–186.
- (391) Meyer, R.; Lemire, C.; Shaikhutdinov, S. K.; Freund, H.-J. Surface Chemistry of Catalysis by Gold. *Gold Bull.* **2004**, *37*, 72–124.
- (392) Abad, A.; Concepción, P.; Corma, A.; García, H. A Collaborative Effect between Gold and a Support Induces the Selective Oxidation of Alcohols. *Angew. Chem., Int. Ed.* **2005**, *44*, 4066–4069.
- (393) Green, I. X.; Tang, W.; Neurock, M.; Yates, J. T. Spectroscopic Observation of Dual Catalytic Sites During Oxidation of CO on a Au/TiO₂ Catalyst. *Science* **2011**, *333*, 736–739.
- (394) Saavedra, J.; Doan, H. A.; Pursell, C. J.; Grabow, L. C.; Chandler, B. D. The Critical Role of Water at the Gold-Titania Interface in Catalytic CO Oxidation. *Science* **2014**, *345*, 1599–1602.
- (395) Chowdhury, B.; Bravo-Suárez, J. J.; Mimura, N.; Lu, J.; Bando, K. K.; Tsubota, S.; Haruta, M. In Situ UV-vis and EPR Study on the Formation of Hydroperoxide Species during Direct Gas Phase Propylene Epoxidation over Au/Ti-SiO₂ Catalyst. *J. Phys. Chem. B* **2006**, *110*, 22995–22999.
- (396) Saavedra, J.; Whittaker, T.; Chen, Z.; Pursell, C. J.; Rioux, R. M.; Chandler, B. D. Controlling Activity and Selectivity Using Water in the Au-Catalyzed Preferential Oxidation of CO in H₂. *Nat. Chem.* **2016**, *8*, 584–589.
- (397) Tran, H. V.; Doan, H. A.; Chandler, B. D.; Grabow, L. C. Water-Assisted Oxygen Activation during Selective Oxidation Reactions. *Curr. Opin. Chem. Eng.* **2016**, *13*, 100–108.
- (398) Roldán, A.; González, S.; Ricart, J. M.; Illas, F. Critical Size for O₂ Dissociation by Au Nanoparticles. *ChemPhysChem* **2009**, *10*, 348–351.
- (399) Roldán, A.; Ricart, J.; Illas, F. Origin of the Size Dependence of Au Nanoparticles toward Molecular Oxygen Dissociation. *Theor. Chem. Acc.* **2011**, *128*, 675–681.
- (400) Socaciú, L. D.; Hagen, J.; Bernhardt, T. M.; Wöste, L.; Heiz, U.; Häkkinen, H.; Landman, U. Catalytic CO Oxidation by Free Au²⁺: Experiment and Theory. *J. Am. Chem. Soc.* **2003**, *125*, 10437–10445.
- (401) Bär, T.; Visart De Bocarme, T.; Nieuwenhuys, B. E.; Kruse, N. CO Oxidation on Gold Surfaces Studied on the Atomic Scale. *Catal. Lett.* **2001**, *74*, 127–131.
- (402) Klyushin, A. Y.; Arrigo, R.; Youngmi, Y.; Xie, Z.; Hävecker, M.; Bukhtiyarov, A. V.; Prosvirin, I. P.; Bukhtiyarov, V. I.; Knop-Gericke, A.; Schlögl, R. Are Au Nanoparticles on Oxygen-Free Supports Catalytically Active? *Top. Catal.* **2016**, *59*, 469–477.
- (403) Klyushin, A. Y.; Greiner, M. T.; Huang, X.; Lunkenbein, T.; Li, X.; Timpe, O.; Friedrich, M.; Hävecker, M.; Knop-Gericke, A.; Schlögl, R. Is Nanostructuring Sufficient To Get Catalytically Active Au? *ACS Catal.* **2016**, *6*, 3372–3380.
- (404) Visart de Bocarme, T.; Chau, T.-D.; Kruse, N. The Interaction of CO-O₂ Gas Mixtures with Au Tips: in Situ Imaging and Local Chemical Probing. *Surf. Interface Anal.* **2007**, *39*, 166–171.
- (405) Krajić, M.; Kameoka, S.; Tsai, A.-P. Understanding the Catalytic Activity of Nanoporous Gold: Role of Twinning in Fcc Lattice. *J. Chem. Phys.* **2017**, *147*, 044713.
- (406) Rebelli, J.; Ma, S.; Williams, C. T.; Monnier, J. R.; Rodriguez, A. A. Preparation and Characterization of Silica-Supported, Group IB-Pd Bimetallic Catalysts Prepared by Electroless Deposition Methods. *Catal. Today* **2011**, *160*, 170–178.
- (407) Fajín, J. L. C. C.; Cordeiro, M. N. D. S. S.; Gomes, J. R. B. B. DFT Study on the Reaction of O₂ Dissociation Catalyzed by Gold Surfaces Doped with Transition Metal Atoms. *Appl. Catal., A* **2013**, *458*, 90–102.
- (408) Li, Z.; Gao, F.; Tysoe, W. T. Carbon Monoxide Oxidation over Au/Pd (100) Model Alloy Catalysts. *J. Phys. Chem. C* **2010**, *114*, 16909–16916.
- (409) Gao, F.; Wang, Y.; Goodman, D. W. CO Oxidation over AuPd(100) from Ultrahigh Vacuum to Near-Atmospheric Pressures: The Critical Role of Contiguous Pd Atoms. *J. Am. Chem. Soc.* **2009**, *131*, 5734–5735.
- (410) Kim, H. Y.; Henkelman, G. CO Adsorption-Driven Surface Segregation of Pd on Au/Pd Bimetallic Surfaces: Role of Defects and Effect on CO Oxidation. *ACS Catal.* **2013**, *3*, 2541–2546.
- (411) Wang, T.; Li, B.; Yang, J.; Chen, H.; Chen, L. First Principles Study of Oxygen Adsorption and Dissociation on the Pd/Au Surface Alloys. *Phys. Chem. Chem. Phys.* **2011**, *13*, 7112–7120.
- (412) Ham, H. C.; Stephens, J. A.; Hwang, G. S.; Han, J.; Nam, S. W.; Lim, T. H. Role of Small Pd Ensembles in Boosting CO Oxidation in AuPd Alloys. *J. Phys. Chem. Lett.* **2012**, *3*, 566–570.
- (413) Yuan, D. W.; Liu, Z. R.; Chen, J. H. Catalytic Activity of Pd Ensembles over Au(111) Surface for CO Oxidation: A First-Principles Study. *J. Chem. Phys.* **2011**, *134*, 054704.
- (414) Yuan, D. W.; Liu, Z. R. Catalytic Activity of Pd Ensembles Incorporated into Au Nanocluster for CO Oxidation: A First-Principles Study. *Phys. Lett. A* **2011**, *375*, 2405–2410.

- (415) Yuan, Y.; Yam, C. M.; Shmakova, O. E.; Colorado, R.; Graupe, M.; Fukushima, H.; Moore, H. J.; Lee, T. R. Solution-Phase Desorption of Self-Assembled Monolayers on Gold Derived From Terminally Perfluorinated Alkanethiols. *J. Phys. Chem. C* **2011**, *115*, 19749–19760.
- (416) Wittstock, A.; Zielasek, V.; Biener, J.; Friend, C. M.; Bäumer, M. Nanoporous Gold Catalysts for Selective Methanol at Low Temperature. *Science* **2010**, *327*, 319–322.
- (417) Xu, C.; Su, J.; Xu, X.; Liu, P.; Zhao, H.; Tian, F.; Ding, Y. Low Temperature CO Oxidation over Unsupported Nanoporous Gold. *J. Am. Chem. Soc.* **2007**, *129*, 42–43.
- (418) Zielasek, V.; Jürgens, B.; Schulz, C.; Biener, J.; Biener, M. M.; Hamza, A. V.; Bäumer, M. Gold Catalysts: Nanoporous Gold Foams. *Angew. Chem., Int. Ed.* **2006**, *45*, 8241–8244.
- (419) Wang, A. Q.; Liu, J. H.; Lin, S. D.; Lin, T. S.; Mou, C. Y. A Novel Efficient Au-Ag Alloy Catalyst System: Preparation, Activity, and Characterization. *J. Catal.* **2005**, *233*, 186–197.
- (420) Moskaleva, L. V.; Röhe, S.; Wittstock, A.; Zielasek, V.; Klüner, T.; Neyman, K. M.; Bäumer, M. Silver Residues as a Possible Key to a Remarkable Oxidative Catalytic Activity of Nanoporous Gold. *Phys. Chem. Chem. Phys.* **2011**, *13*, 4529.
- (421) Wang, L.-C.; Personick, M. L.; Karakatos, S.; Fushimi, R.; Friend, C. M.; Madix, R. J. Active Sites for Methanol Partial Oxidation on Nanoporous Gold Catalysts. *J. Catal.* **2016**, *344*, 778–783.
- (422) Montemore, M. M.; Madix, R. J.; Kaxiras, E. How Does Nanoporous Gold Dissociate Molecular Oxygen? *J. Phys. Chem. C* **2016**, *120*, 16636–16640.
- (423) Schrader, M. E. Chemisorption of Oxygen to Gold: AES Study of Catalytic Effect of Calcium. *Surf. Sci.* **1978**, *78*, L227–L232.
- (424) Spruit, M. E. M.; Kleyn, A. W. Dissociative Adsorption of O₂ on Ag(111). *Chem. Phys. Lett.* **1989**, *159*, 342–348.
- (425) Albers, H.; Van Der Wal, W. J. J.; Bootsma, G. Ellipsometric Study of Oxygen Adsorption and the Carbon Monoxide-Oxygen Interaction on Ordered and Damaged Ag(111). *Surf. Sci.* **1977**, *68*, 47–56.
- (426) Zambelli, T.; Barth, J. V.; Wintterlin, J. Thermal Dissociation of Chemisorbed Oxygen Molecules on Ag(110): An Investigation by Scanning Tunnelling Microscopy. *J. Phys.: Condens. Matter* **2002**, *14*, 4241–4250.
- (427) Klobas, J. E.; Schmid, M.; Friend, C. M.; Madix, R. J. The Dissociation-Induced Displacement of Chemisorbed O₂ by Mobile O Atoms and the Autocatalytic Recombination of O due to Chain Fragmentation on Ag(110). *Surf. Sci.* **2014**, *630*, 187–194.
- (428) Xin, Q. S.; Zhu, X. Y. Is Localized Collision Responsible for O₂ Photodesorption from Ag(110)? *Surf. Sci.* **1996**, *347*, 346–354.
- (429) Pascal, M.; Lamont, C. L.; Baumgärtel, P.; Terborg, R.; Hoeft, J.; Schaff, O.; Polcik, M.; Bradshaw, A.; Toomes, R.; Woodruff, D. Photoelectron Diffraction Study of the Ag(110)-(2 × 1)-O Reconstruction. *Surf. Sci.* **2000**, *464*, 83–90.
- (430) Alducin, M.; Busnengo, H. F.; Muiño, R. D. Dissociative Dynamics of Spin-Triplet and Spin-Singlet O₂ on Ag(100). *J. Chem. Phys.* **2008**, *129*, 224702.
- (431) Buatier de Mongeot, F.; Rocca, M.; Cupolillo, A.; Valbusa, U.; Kreuzer, H. J.; Payne, S. H. Sticking and Thermal Desorption of O₂ on Ag(001). *J. Chem. Phys.* **1997**, *106*, 711–718.
- (432) Rocca, M.; Savio, L.; Vattuone, L.; Burghaus, U.; Palomba, V.; Novelli, N.; Buatier de Mongeot, F.; Valbusa, U.; Gunnella, R.; Comelli, G.; et al. Phase Transition of Dissociatively Adsorbed Oxygen on Ag(001). *Phys. Rev. B: Condens. Matter Mater. Phys.* **2000**, *61*, 213–227.
- (433) Wiame, F.; Maurice, V.; Marcus, P. Initial Stages of Oxidation of Cu(111). *Surf. Sci.* **2007**, *601*, 1193–1204.
- (434) Hodgson, A.; Lewin, A.; Nesbitt, A. Dissociative Chemisorption of O₂ on Cu (110). *Surf. Sci.* **1993**, *293*, 211–226.
- (435) Moritani, K.; Okada, M.; Teraoka, Y.; Yoshigoe, A.; Kasai, T. Kinetics of Oxygen Adsorption and Initial Oxidation on Cu(110) by Hyperthermal Oxygen Molecular Beams. *J. Phys. Chem. A* **2009**, *113*, 15217–15222.
- (436) Sun, L.; Hohage, M.; Denk, R.; Zeppenfeld, P. Oxygen Adsorption on Cu(110) at Low Temperature. *Phys. Rev. B: Condens. Matter Mater. Phys.* **2007**, *76*, 245412.
- (437) Ohno, S. Y.; Yagyu, K.; Nakatsuji, K.; Komori, F. Dissociation Preference of Oxygen Molecules on an Inhomogeneously Strained Cu(0 0 1) Surface. *Surf. Sci.* **2004**, *554*, 183–192.
- (438) Yata, M.; Rouch, H. Control of the Initial Oxidation on Cu(001) Surface by Selection of Translational Energy of O₂ Molecules. *Appl. Phys. Lett.* **1999**, *75*, 1021.
- (439) Hirsimäki, M.; Chorkendorff, I. Effects of Steps and Defects on O₂ Dissociation on Clean and Modified Cu(100). *Surf. Sci.* **2003**, *538*, 233–239.
- (440) Junell, P.; Ahonen, M.; Hirsimäki, M.; Valden, M. Influence of Surface Modification on the Adsorption Dynamics of O₂ on Cu {100}. *Surf. Rev. Lett.* **2004**, *11*, 457–461.
- (441) Alatalo, M.; Puisto, A.; Pitkänen, H.; Foster, a. S.; Laasonen, K. Adsorption Dynamics of O₂ on Cu(100). *Surf. Sci.* **2006**, *600*, 1574–1578.
- (442) Junell, P.; Honkala, K.; Hirsimäki, M.; Valden, M.; Laasonen, K. Molecularly Chemisorbed Intermediate State to Oxygen Adsorption on Pd{110}. *Surf. Sci.* **2003**, *546*, L797–L802.
- (443) Getman, R. B.; Schneider, W. F.; Smeltz, A. D.; Delgass, W. N.; Ribeiro, F. H. Oxygen-Coverage Effects on Molecular Dissociations at a Pt Metal Surface. *Phys. Rev. Lett.* **2009**, *102*, 76101.
- (444) Šljivančanin, Z.; Hammer, B. Oxygen Dissociation at Close-Packed Pt Terraces, Pt Steps, and Ag-Covered Pt Steps Studied with Density Functional Theory. *Surf. Sci.* **2002**, *515*, 235–244.
- (445) Hyman, M. P.; Medlin, J. Mechanistic Study of the Electrochemical Oxygen Reduction Reaction on Pt (111) Using Density Functional Theory. *J. Phys. Chem. B* **2006**, *110*, 15338–15344.
- (446) Sha, Y.; Yu, T. H.; Liu, Y.; Merinov, B. V.; Goddard, W. A. Theoretical Study of Solvent Effects on the Platinum-Catalyzed Oxygen Reduction Reaction. *J. Phys. Chem. Lett.* **2010**, *1*, 856–861.
- (447) Matsushima, T. Dissociation of Oxygen Admolecules on Rh(111), Pt(111) and Pd(111) Surfaces at Low Temperatures. *Surf. Sci.* **1985**, *157*, 297–318.
- (448) Gland, J. L. Molecular and Atomic Adsorption of Oxygen on the Pt(111) and Pt(S)-12(111) × (111) Surfaces. *Surf. Sci.* **1980**, *93*, 487–514.
- (449) Groß, A. Ab Initio Molecular Dynamics Simulations of the O₂/Pt(111) Interaction. *Catal. Today* **2016**, *260*, 60–65.
- (450) Derry, G. N.; Ross, P. N. A Work Function Change Study of Oxygen Adsorption on Pt(111) and Pt(100). *J. Chem. Phys.* **1985**, *82*, 2772.
- (451) Bonzel, H. P.; Ku, R. On the Kinetics of Oxygen Adsorption on a Pt(111) Surface. *Surf. Sci.* **1973**, *40*, 85–101.
- (452) Campbell, C. T.; Ertl, G.; Kuipers, H.; Segner, J. A Molecular Beam Study of the Adsorption and Desorption of Oxygen from a Pt(111) Surface. *Surf. Sci.* **1981**, *107*, 220–236.
- (453) Walker, A. V.; Klötzer, B.; King, D. A. Dynamics and Kinetics of Oxygen Dissociative Adsorption on Pt{110}(1 × 2). *J. Chem. Phys.* **1998**, *109*, 6879–6888.
- (454) Wilf, M.; Dawson, P. T. The Adsorption and Desorption of Oxygen on the Pt(110) Surface; A Thermal Desorption and LEED/AES Study. *Surf. Sci.* **1977**, *65*, 399–418.
- (455) Walker, A. V.; King, D. A. Reaction of Gaseous Oxygen with Adsorbed Carbon on Pt{110}(1 × 2). *J. Chem. Phys.* **2000**, *112*, 1937–1945.
- (456) Ducros, R.; Merrill, R. P. The Interaction of Oxygen with Pt(110). *Surf. Sci.* **1976**, *55*, 227–245.
- (457) Li, W. X.; Österlund, L.; Vestergaard, E. K.; Vang, R. T.; Matthiesen, J.; Pedersen, T. M.; Lægsgaard, E.; Hammer, B.; Besenbacher, F. Oxidation of Pt(110). *Phys. Rev. Lett.* **2004**, *93*, 146104.
- (458) Guo, X. C.; Bradley, J. M.; Hopkinson, A.; King, D. A. O₂ Interaction with Pt{100}-Hex-R0.7°: Scattering, Sticking and Saturating. *Surf. Sci.* **1994**, *310*, 163–182.
- (459) Guo, X. C.; Bradley, J. M.; Hopkinson, A.; King, D. A. Dynamics of O₂ on Pt{100}-Hex-R0.7°: Activated Adsorption with a

- Strong Surface Temperature Enhancement. *Surf. Sci. Lett.* **1993**, *292*, L791–L790.
- (460) Voogt, E. H.; Mens, A. J. M.; Gijzeman, O. L. J.; Geus, J. W. Adsorption of Oxygen and Surface Oxide Formation on Pd(111) and Pd Foil Studied with Ellipsometry, LEED, AES and XPS. *Surf. Sci.* **1997**, *373*, 210–220.
- (461) Farías, D.; Minniti, M.; Miranda, R. Reactivity of O₂ on Pd/Ru(0001) and PdRu/Ru(0001) Surface Alloys. *J. Chem. Phys.* **2017**, *146*, 204701.
- (462) Inoğlu, N.; Kitchin, J. R. Identification of Sulfur-Tolerant Bimetallic Surfaces Using DFT Parametrized Models and Atomistic Thermodynamics. *ACS Catal.* **2011**, *1*, 399–407.
- (463) Schweitzer, N.; Nikolla, E.; Miller, J. T.; Linic, S.; Xin, H. Establishing Relationships between the Geometric Structure and Chemical Reactivity of Alloy Catalysts Based on Their Measured Electronic Structure. *Top. Catal.* **2010**, *53*, 348.
- (464) Yagi, K.; Sekiba, D.; Fukutani, H. Adsorption and Desorption Kinetics of Oxygen on the Pd(110) Surface. *Surf. Sci.* **1999**, *442*, 307–317.
- (465) den Dunnen, A.; Wiegman, S.; Jacobse, L.; Juurlink, L. B. F. Reaction Dynamics of Initial O₂ Sticking on Pd(100). *J. Chem. Phys.* **2015**, *142*, 214708.
- (466) Bukas, V. J.; Mitra, S.; Meyer, J.; Reuter, K. Fingerprints of Energy Dissipation for Exothermic Surface Chemical Reactions: O₂ on Pd(100). *J. Chem. Phys.* **2015**, *143*, 034705.
- (467) Lahti, M.; Puisto, A.; Alatalo, M.; Rahman, T. S. The Role of PreadSORBED Sulphur and Oxygen in O₂ Dissociation on Pd(100). *Surf. Sci.* **2008**, *602*, 3660–3666.
- (468) Todorova, M.; Lundgren, E.; Blum, V.; Mikkelsen, A.; Gray, S.; Gustafson, J.; Borg, M.; Rogal, J.; Reuter, K.; Andersen, J. N.; et al. The Pd(100)–($\sqrt{5} \times \sqrt{5}$)R27°-O Surface Oxide Revisited. *Surf. Sci.* **2003**, *541*, 101–112.
- (469) Chang, S. L.; Thiel, P. A. Formation of a Metastable Ordered Surface Phase due to Competitive Diffusion and Adsorption Kinetics: Oxygen on Pd(100). *Phys. Rev. Lett.* **1987**, *59*, 296–299.
- (470) Winkler, A.; Rendulic, K. D.; Wendl, K. Quantitative Measurement of the Sticking Coefficient for Oxygen on Nickel. *Appl. Surf. Sci.* **1983**, *14*, 209–220.
- (471) Inoue, K.; Teraoka, Y. Time-Evolution of Oxidation States at the Ni(111) Surface: O₂ Incident Translational Energy Dependence. *J. Phys.: Conf. Ser.* **2013**, *417*, 012034.
- (472) Inoue, K.; Teraoka, Y. Initial Sticking Rate of O₂ Molecular Beams on Ni(111) Surface Depending on Kinetic Energy. *Astrophysics and Space Science Proceedings*; Kleiman, J., Tagawa, M., Kimoto, Y., Eds.; Springer: Berlin, 2013; Vol. 32, pp 521–529.
- (473) Kurahashi, M.; Yamauchi, Y. Spin Correlation in O₂ Chemisorption on Ni(111). *Phys. Rev. Lett.* **2015**, *114*, 16101.
- (474) Brundle, C. R.; Behm, J.; Barker, J. A. How Many Metal Atoms Are Involved in Dissociative Chemisorption? *J. Vac. Sci. Technol., A* **1984**, *2*, 1038–1039.
- (475) Karmazyn, A. D.; Fiorin, V.; King, D. A. Direct Sticking and Differential Adsorption Heats as Probes of Structural Transitions: O₂ on the Stepped Ni{211} Surface. *J. Am. Chem. Soc.* **2004**, *126*, 14273–14277.
- (476) Domnick, R.; Held, G.; Steinrück, H. P. Temperature Dependent Oxidation of Thin Ni Layers on Cu(111). *Surf. Sci.* **2002**, *516*, 95–102.
- (477) Norton, P. R.; Tapping, R. L.; Goodale, J. W. A Photoemission Study of the Interaction of Ni(100), (110) and (111) Surfaces with Oxygen. *Surf. Sci.* **1977**, *65*, 13–36.
- (478) Zion, B. D.; Hanbicki, A. T.; Sibener, S. J. Kinetic Energy Effects on the Oxidation of Ni(111) Using O₂ Molecular Beams. *Surf. Sci.* **1998**, *417*, L154–L159.
- (479) Mitchell, D. F.; Sewell, P. B.; Cohen, M. A Kinetic Study of the Initial Oxidation of the Ni(110) Surface by RHEED and X-Ray Emission. *Surf. Sci.* **1977**, *69*, 310–324.
- (480) Holloway, P. H.; Hudson, J. B. Kinetics of the Reaction of Oxygen with Clean Nickel Single Crystal Surfaces. I. Ni(100) Surface. *Surf. Sci.* **1974**, *43*, 123–140.
- (481) Knudsen, J.; Merte, L. R.; Peng, G.; Vang, R. T.; Resta, A.; Lægsgaard, E.; Andersen, J. N.; Mavrikakis, M.; Besenbacher, F. Low-Temperature CO Oxidation on Ni(111) and on a Au/Ni(111) Surface Alloy. *ACS Nano* **2010**, *4*, 4380–4387.
- (482) Ivanov, V. P.; Boreskov, G. K.; Savchenko, V. I.; Egelhoff, W. F.; Weinberg, W. H. The Chemisorption of Oxygen on the Iridium (111) Surface. *Surf. Sci.* **1976**, *61*, 207–220.
- (483) Ali, T.; Klötzer, B.; Walker, A. V.; Ge, Q.; King, D. A. Surface Kinetics of a Nonlinear Oxygen-Induced (1 × 5)–(1 × 1) Phase Transition on Ir{100}. *J. Chem. Phys.* **1998**, *109*, 9967–9976.
- (484) Küppers, J.; Michel, H. Preparation of Ir(100)-1 × 1 Surface Structures by Surface Reactions and Its Reconstruction Kinetics as Determined with LEED, UPS and Work Function Measurements. *Appl. Surf. Sci.* **1979**, *3*, 179–195.
- (485) He, Y. B.; Stierle, A.; Li, W. X.; Farkas, A.; Kasper, N.; Over, H. Oxidation of Ir(111): From O-Ir-O Trilayer to Bulk Oxide Formation. *J. Phys. Chem. C* **2008**, *112*, 11946–11953.
- (486) Inderwildi, O. R.; Lebiedz, D.; Deutschmann, O.; Warnatz, J. Coverage Dependence of Oxygen Decomposition and Surface Diffusion on Rhodium (111): A DFT Study. *J. Chem. Phys.* **2005**, *122*, 034710.
- (487) Bridge, M. E.; Lambert, R. M. Oxygen Chemisorption, Surface Oxidation, and the Oxidation of Carbon Monoxide on Cobalt (0001). *Surf. Sci.* **1979**, *82*, 413–424.
- (488) Kizilkaya, A. C.; Niemantsverdriet, J. W.; Weststrate, C. J. Oxygen Adsorption and Water Formation on Co(0001). *J. Phys. Chem. C* **2016**, *120*, 4833–4842.
- (489) Klingenberg, B.; Grellner, F.; Borgmann, D.; Wedler, G. Oxygen Adsorption and Oxide Formation on Co(1120). *Surf. Sci.* **1993**, *296*, 374–382.
- (490) Görts, P. C.; Dorren, B. H. P.; Habraken, F. H. P. M. Oxidation of the Co(1010) Surface. *Surf. Sci.* **1993**, *287–288*, 255–259.
- (491) Lahtinen, J.; Vaari, J.; Taio, A.; Vehanen, A.; Hautojärvi, P. Adsorption and Desorption Measurements of CO and O₂ on Cobalt. *Vacuum* **1990**, *41*, 112–114.
- (492) Liu, J.; Fan, X.; Sun, C.; Zhu, W. Oxidation of the Titanium(0001) Surface: Diffusion Processes of Oxygen from DFT. *RSC Adv.* **2016**, *6*, 71311–71318.
- (493) Franchy, R.; Bartke, T. U.; Gassmann, P. The Interaction of Oxygen with Nb(110) at 300, 80 and 20 K. *Surf. Sci.* **1996**, *366*, 60–70.
- (494) Zaera, F.; Somorjai, G. A. The Chemisorption of O₂, CO, D₂ and C₂H₄ over Epitaxially Grown Rhodium Crystalline Films. *Surf. Sci.* **1985**, *154*, 303–314.
- (495) Wang, C.; Gomer, R. Sticking Coefficients of CO, O₂ and Xe on the (110) and (100) Planes of Tungsten. *Surf. Sci.* **1979**, *84*, 329–354.
- (496) Rettner, C. T.; DeLouise, L. A.; Auerbach, D. J. Effect of Incidence Kinetic Energy and Surface Coverage on the Dissociative Chemisorption of Oxygen on W(110). *J. Chem. Phys.* **1986**, *85*, 1131–1149.
- (497) Linsmeier, C.; Wanner, J. Reactions of Oxygen Atoms and Molecules with Au, Be, and W Surfaces. *Surf. Sci.* **2000**, *454*–456, 305–309.
- (498) Azoulay, A.; Shamir, N.; Fromm, E.; Mintz, M. H. The Initial Interactions of Oxygen with Polycrystalline Titanium Surfaces. *Surf. Sci.* **1997**, *370*, 1–16.
- (499) Zhang, C.; van Hove, M. A.; Somorjai, G. A. The Interaction of Oxygen with the Mo(100) and Mo(111) Single-Crystal Surfaces: Chemisorption and Oxidation at High Temperatures. *Surf. Sci.* **1985**, *149*, 326–340.
- (500) Sakisaka, Y.; Miyano, T.; Onchi, M. Electron-Energy-Loss-Spectroscopy Study of Oxygen Chemisorption and Initial Oxidation of Fe(100). *Phys. Rev. B: Condens. Matter Mater. Phys.* **1984**, *30*, 6849–6855.
- (501) Hanson, D. M.; Stockbauer, R.; Maday, T. E. Photon-Stimulated Desorption and Other Spectroscopic Studies of the Interaction of Oxygen with a Titanium (001) Surface. *Phys. Rev. B: Condens. Matter Mater. Phys.* **1981**, *24*, 5513–5521.

- (S02) Ducros, R.; Alnot, M.; Ehrhardt, J. J.; Housley, M.; Piquard, G.; Cassuto, A. A Study of the Adsorption of Several Oxygen-Containing Molecules (O_2 , CO, NO, H_2O) on Re(0001) by XPS, UPS and Temperature Programmed Desorption. *Surf. Sci.* **1980**, *94*, 154–168.
- (S03) Davies, R.; Edwards, D.; Gräfe, J.; Gilbert, L.; Davies, P.; Hutchings, G.; Bowker, M. The Oxidation of Fe(111). *Surf. Sci.* **2011**, *605*, 1754–1762.
- (S04) Roosendaal, S. J.; Vredenberg, A. M.; Habraken, F. H. P. M. Oxidation of Iron: The Relation between Oxidation Kinetics and Oxide Electronic Structure. *Phys. Rev. Lett.* **2000**, *84*, 3366–3369.
- (S05) Bertel, E.; Stockbauer, R.; Madey, T. E. Electron Emission and Ion Desorption Spectroscopy of Clean and Oxidized Ti(0001). *Surf. Sci.* **1984**, *141*, 355–387.
- (S06) Hofmann, P.; Horn, K.; Bradshaw, A. M.; Jacobi, K. The Adsorption and Condensation of Oxygen on Aluminium at Low Temperature. *Surf. Sci.* **1979**, *82*, L610–L614.
- (S07) Brune, H.; Winterlin, J.; Behm, R. J.; Ertl, G. Surface Migration of Hot Adatoms in the Course of Dissociative Chemisorption of Oxygen on Al(111). *Phys. Rev. Lett.* **1992**, *68*, 624–626.
- (S08) Zalkind, S.; Polak, M.; Shamir, N. The Initial Interactions of Beryllium with O_2 and H_2O Vapor at Elevated Temperatures. *Surf. Sci.* **2007**, *601*, 1326–1332.
- (S09) Zalkind, S.; Polak, M.; Shamir, N. Effects of Preadsorbed Hydrogen on the Adsorption of O_2 , CO and H_2O on Beryllium. *Surf. Sci.* **2003**, *539*, 81–90.
- (S10) Krozer, A.; Kasemo, B. Kinetics of Initial Oxidation of UHV Prepared Zn Films. *Surf. Sci.* **1980**, *97*, L339–L344.
- (S11) Unertl, W. N.; Blakely, J. M. The Oxidation of Zn(0001): The First Stage. *J. Colloid Interface Sci.* **1976**, *55*, 320–328.
- (S12) Gainey, T. C.; Hopkins, B. J. Oxidation of the Zn(0001) Surface. *J. Phys. C: Solid State Phys.* **1981**, *14*, 5763–5768.
- (S13) Huda, M. N.; Ray, A. K. Ab Initio Study of Molecular Oxygen Adsorption on Pu (111) Surface. *Int. J. Quantum Chem.* **2005**, *105*, 280–291.
- (S14) Nie, J. L.; Ao, L.; Zu, X. T.; Gao, H. First-Principles Study of O_2 Adsorption on the α -U(001) Surface. *J. Phys. Chem. Solids* **2014**, *75*, 130–135.
- (S15) Almeida, T.; Cox, L. E.; Ward, J. W.; Naegele, J. R. Gas Adsorption Studies on Pu Metal by Photoemission Spectroscopy. *Surf. Sci.* **1993**, *287*–288, 141–145.
- (S16) Haschke, J. M. Corrosion of Uranium in Air and Water Vapor: Consequences for Environmental Dispersal. *J. Alloys Compd.* **1998**, *278*, 149–160.
- (S17) McLean, W.; Colmenares, C. A.; Smith, R. L.; Somorjai, G. A. Electron-Spectroscopy Studies of Clean Thorium and Uranium Surfaces. Chemisorption and Initial Stages of Reaction with O_2 , CO, and CO_2 . *Phys. Rev. B: Condens. Matter Mater. Phys.* **1982**, *25*, 8–24.
- (S18) Ritchie, A. G. A Review of the Rates of Reaction of Uranium with Oxygen and Water Vapour at Temperatures up to 300° C. *J. Nucl. Mater.* **1981**, *102*, 170–182.
- (S19) Cohen, S.; Shamir, N.; Mintz, M. H.; Jacob, I.; Zalkind, S. The Interaction of O_2 with the Surface of Polycrystalline Gadolinium at the Temperature Range 300–670 K. *Surf. Sci.* **2011**, *605*, 1589–1594.
- (S20) Huda, M. N.; Ray, A. K. Density Functional Study of O_2 Adsorption on (100) Surface of γ -Uranium. *Int. J. Quantum Chem.* **2005**, *102*, 98–105.
- (S21) Getzlaff, M.; Bode, M.; Pascal, R.; Wiesendanger, R. Adsorbates on Gd(0001): A Combined Scanning Tunneling Microscopy and Photoemission Study. *Phys. Rev. B: Condens. Matter Mater. Phys.* **1999**, *59*, 8195–8208.
- (S22) Vattuone, L.; Savio, L.; Rocca, M. Bridging the Structure Gap: Chemistry of Nanostructured Surfaces at Well-Defined Defects. *Surf. Sci. Rep.* **2008**, *63*, 101–168.
- (S23) Wu, J.; Yang, H. Platinum-Based Oxygen Reduction Electro-catalysts. *Acc. Chem. Res.* **2013**, *46*, 1848–1857.
- (S24) Haruta, M.; Yamada, N.; Kobayashi, T.; Iijima, S. Gold Catalysts Prepared by Coprecipitation for Low-Temperature Oxida-
- tion of Hydrogen and of Carbon Monoxide. *J. Catal.* **1989**, *115*, 301–309.
- (S25) Gee, A. T.; Hayden, B. E. Dynamics of O_2 Adsorption on Pt(533): Step Mediated Molecular Chemisorption and Dissociation. *J. Chem. Phys.* **2000**, *113*, 10333–10343.
- (S26) Jacobse, L.; Den Dunnen, A.; Juurlink, L. B. F. The Molecular Dynamics of Adsorption and Dissociation of O_2 on Pt(553). *J. Chem. Phys.* **2015**, *143*, 014703.
- (S27) Luntz, A. C.; Williams, M. D.; Bethune, D. S. The Sticking of O_2 on a Pt(111) Surface. *J. Chem. Phys.* **1988**, *89*, 4381.
- (S28) Fiorin, V.; Borthwick, D.; King, D. A. Microcalorimetry of O_2 and NO on Flat and Stepped Platinum Surfaces. *Surf. Sci.* **2009**, *603*, 1360–1364.
- (S29) Karp, E. M.; Campbell, C. T.; Studt, F.; Abild-Pedersen, F.; Nørskov, J. K. Energetics of Oxygen Adatoms, Hydroxyl Species and Water Dissociation on Pt(111). *J. Phys. Chem. C* **2012**, *116*, 25772–25776.
- (S30) Bray, J. M.; Schneider, W. F. Potential Energy Surfaces for Oxygen Adsorption, Dissociation, and Diffusion at the Pt(321) Surface. *Langmuir* **2011**, *27*, 8177–8186.
- (S31) Yue, J.; Du, Z.; Shao, M. Mechanisms of Enhanced Electrocatalytic Activity for Oxygen Reduction Reaction on High-Index Platinum n(111)-(111) Surfaces. *J. Phys. Chem. Lett.* **2015**, *6*, 3346–3351.
- (S32) Gambardella, P.; Šljivančanin, Ž.; Hammer, B.; Blanc, M.; Kuhnke, K.; Kern, K. Oxygen Dissociation at Pt Steps. *Phys. Rev. Lett.* **2001**, *87*, 56103.
- (S33) Badan, C.; Koper, M. T. M.; Juurlink, L. B. F. How Well Does Pt(211) Represent Pt[n (111) × (100)] Surfaces in Adsorption/desorption? *J. Phys. Chem. C* **2015**, *119*, 13551.
- (S34) Van Der Nieuw, M. J. T. C.; Den Dunnen, A.; Juurlink, L. B. F.; Koper, M. T. M. A Detailed TPD Study of H_2O and Pre-Adsorbed O on the Stepped Pt(553) Surface. *Phys. Chem. Chem. Phys.* **2011**, *13*, 1629–1638.
- (S35) Bandlow, J.; Kaghazchi, P.; Jacob, T.; Papp, C.; Tränkenschuh, B.; Streber, R.; Lorenz, M.; Fuhrmann, T.; Denecke, R.; Steinrück, H.-P. Oxidation of Stepped Pt(111) Studied by X-Ray Photoelectron Spectroscopy and Density Functional Theory. *Phys. Rev. B: Condens. Matter Mater. Phys.* **2011**, *83*, 174107.
- (S36) Wang, J. G.; Li, W. X.; Borg, M.; Gustafson, J.; Mikkelsen, A.; Pedersen, T. M.; Lundgren, E.; Weissenrieder, J.; Klikovits, J.; Schmid, M.; et al. One-Dimensional PtO_2 at Pt Steps: Formation and Reaction with CO. *Phys. Rev. Lett.* **2005**, *95*, 256102.
- (S37) Zhu, Z.; Tao, F.; Zheng, F.; Chang, R.; Li, Y.; Heinke, L.; Liu, Z.; Salmeron, M. B.; Somorjai, G. A. Formation of Nanometer-Sized Surface Platinum Oxide Clusters on a Stepped Pt(557) Single Crystal Surface Induced by Oxygen: A High-Pressure STM and Ambient-Pressure XPS Study. *Nano Lett.* **2012**, *12*, 1491–1497.
- (S38) van der Nieuw, M. J. T. C.; den Dunnen, A.; Juurlink, L. B. F.; Koper, M. T. M. The Influence of Step Geometry on the Desorption Characteristics of O_2 , D_2 , and H_2O from Stepped Pt Surfaces. *J. Chem. Phys.* **2010**, *132*, 174705.
- (S39) Kolb, M. J.; Calle-Vallejo, F.; Juurlink, L. B. F.; Koper, M. T. M. Density Functional Theory Study of Adsorption of H_2O , H, O, and OH on Stepped Platinum Surfaces. *J. Chem. Phys.* **2014**, *140*, 134708.
- (S40) Jinnouchi, R.; Kodama, K.; Morimoto, Y. DFT Calculations on H, OH and O Adsorbate Formations on Pt(111) and Pt(332) Electrodes. *J. Electroanal. Chem.* **2014**, *716*, 31–44.
- (S41) Ogawa, T.; Kuwabara, A.; Fisher, C. A. J.; Moriwake, H.; Miwa, T. Adsorption and Diffusion of Oxygen Atoms on a Pt(211) Stepped Surface. *J. Phys. Chem. C* **2013**, *117*, 9772–9778.
- (S42) Nagoya, A.; Jinnouchi, R.; Kodama, K.; Morimoto, Y. DFT Calculations on H, OH and O Adsorbate Formations on Pt(322) Electrode. *J. Electroanal. Chem.* **2015**, *757*, 116–127.
- (S43) Ogawa, T.; Kuwabara, A.; Fisher, C. A. J.; Moriwake, H. A Density Functional Study of Oxygen Adatoms on a Step-Doubled Platinum Surface. *J. Phys. Chem. C* **2014**, *118*, 23675–23681.

- (544) Gambu, T. A. Ph.D. Thesis. DFT Study of the Interaction of O_x with Pt Nanorod Edge Sites: A Model for the ORR Activity on Pt Nanoparticle Edges, 2015.
- (545) Blomberg, S.; Zetterberg, J.; Zhou, J.; Merte, L. R.; Gustafson, J.; Shipilin, M.; Trinchero, A.; Miccio, L. A.; Magaña, A.; Ilyn, M.; et al. Strain Dependent Light-off Temperature in Catalysis Revealed by Planar Laser-Induced Fluorescence. *ACS Catal.* **2017**, *7*, 110–114.
- (546) Trinchero, A.; Klacar, S.; Paz-Borbón, L. O.; Hellman, A.; Grönbeck, H. Oxidation at the Subnanometer Scale. *J. Phys. Chem. C* **2015**, *119*, 10797–10803.
- (547) Oemry, F.; Padama, A. A. B.; Kishi, H.; Kunikata, S.; Nakanishi, H.; Kasai, H.; Maekawa, H.; Osumi, K.; Sato, K. Effects of Cluster Size on Platinum–Oxygen Bonds Formation in Small Platinum Clusters. *Jpn. J. Appl. Phys.* **2012**, *51*, 035002.
- (548) Lv, P.; Lu, Z.; Li, S.; Ma, D.; Zhang, W.; Zhang, Y.; Yang, Z. Tuning Metal Cluster Catalytic Activity with Morphology and Composition: A DFT Study of O₂ Dissociation at the Global Minimum of Pt_mPd_n ($m + n = 5$) Clusters. *RSC Adv.* **2016**, *6*, 104388–104397.
- (549) Xu, Y.; Shelton, W. A.; Schneider, W. F. Effect of Particle Size on the Oxidizability of Platinum Clusters. *J. Phys. Chem. A* **2006**, *110*, 5839–5846.
- (550) Kerpel, C.; Harding, D. J.; Hermes, A. C.; Meijer, G.; Mackenzie, S. R.; Fielicke, A. Structures of Platinum Oxide Clusters in the Gas Phase. *J. Phys. Chem. A* **2013**, *117*, 1233–1239.
- (551) Jennings, P. C.; Aleksandrov, H. A.; Neyman, K. M.; Johnston, R. L. A DFT Study of Oxygen Dissociation on Platinum Based Nanoparticles. *Nanoscale* **2014**, *6*, 1153–1165.
- (552) Jennings, P. C.; Aleksandrov, H. A.; Neyman, K. M.; Johnston, R. L. DFT Studies of Oxygen Dissociation on the 116-Atom Platinum Truncated Octahedron Particle. *Phys. Chem. Chem. Phys.* **2014**, *16*, 26539–26545.
- (553) Han, B. C.; Miranda, C. R.; Ceder, G. Effect of Particle Size and Surface Structure on Adsorption of O and OH on Platinum Nanoparticles: A First - Principles Study. *Phys. Rev. B: Condens. Matter Mater. Phys.* **2008**, *77*, 075410.
- (554) Gai, L.; Shin, Y. K.; Raju, M.; van Duin, A. C. T.; Raman, S. Atomistic Adsorption of Oxygen and Hydrogen on Platinum Catalysts by Hybrid Grand Canonical Monte Carlo/Reactive Molecular Dynamics. *J. Phys. Chem. C* **2016**, *120*, 9780–9793.
- (555) Matanović, I.; Kent, P. R. C.; Garzon, F. H.; Henson, N. J. Density Functional Theory Study of Oxygen Reduction Activity on Ultrathin Platinum Nanotubes. *J. Phys. Chem. C* **2012**, *116*, 16499–16510.
- (556) Matanovic, I.; Kent, P. R. C.; Garzon, F. H.; Henson, N. J. Density Functional Study of the Structure, Stability and Oxygen Reduction Activity of Ultrathin Platinum Nanowires. *J. Electrochem. Soc.* **2013**, *160*, F548–F553.
- (557) Visart de Bocarmé, T.; Chau, T. D.; Tielens, F.; Andrés, J.; Gaspard, P.; Wang, R. L. C.; Kreuzer, H. J.; Kruse, N. Oxygen Adsorption on Gold Nanofacets and Model Clusters. *J. Chem. Phys.* **2006**, *125*, 054703.
- (558) Mavrikakis, M.; Stoltze, P.; Nørskov, J. K. Making Gold Less Noble. *Catal. Lett.* **2000**, *64*, 101–106.
- (559) Xu, Y.; Mavrikakis, M. Adsorption and Dissociation of O₂ on Gold Surfaces: Effect of Steps and Strain. *J. Phys. Chem. B* **2003**, *107*, 9298–9307.
- (560) Hussain, A.; Muller, A. J.; Nieuwenhuys, B. E.; Gracia, J. M.; Niemantsverdriet, J. W. Two Gold Surfaces and a Cluster with Remarkable Reactivity for CO Oxidation, a Density Functional Theory Study. *Top. Catal.* **2011**, *54*, 415–423.
- (561) Mills, G.; Gordon, M. S.; Metiu, H. Oxygen Adsorption on Au Clusters and a Rough Au(111) Surface: The Role of Surface Flatness, Electron Confinement, Excess Electrons, and Band Gap. *J. Chem. Phys.* **2003**, *118*, 4198–4205.
- (562) Liu, Z. P.; Hu, P.; Alavi, A. Catalytic Role of Gold in Gold-Based Catalysts: A Density Functional Theory Study on the CO Oxidation on Gold. *J. Am. Chem. Soc.* **2002**, *124*, 14770–14779.
- (563) Ouyang, G.; Zhu, K. J.; Zhang, L.; Cui, P. F.; Teng, B. T.; Wen, X. D. Effects of Coordination Number of Au Catalyst on Oxygen Species and Their Catalytic Roles. *Appl. Surf. Sci.* **2016**, *387*, 875–881.
- (564) Vinod, C. P.; Niemantsverdriet, J. W.; Nieuwenhuys, B. E. Interaction of Small Molecules with Au(310): Decomposition of NO. *Appl. Catal., A* **2005**, *291*, 93–97.
- (565) Eley, D. D.; Moore, P. B. Adsorption of Oxygen on Gold. *Surf. Sci.* **1978**, *76*, L599–L602.
- (566) Canning, N. D. S.; Outka, D.; Madix, R. J. The Adsorption of Oxygen on Gold. *Surf. Sci.* **1984**, *141*, 240–254.
- (567) Wang, J.; Voss, M. R.; Busse, H.; Koel, B. E. Chemisorbed Oxygen on Au(111) Produced by a Novel Route: Reaction in Condensed Films of NO₂ + H₂O. *J. Phys. Chem. B* **1998**, *102*, 4693–4696.
- (568) Nakamura, I.; Takahashi, A.; Fujitani, T. Selective Dissociation of O₃ and Adsorption of CO on Various Au Single Crystal Surfaces. *Catal. Lett.* **2009**, *129*, 400–403.
- (569) van Spronsen, M. A.; Weststrate, K.-J.; Juurlink, L. B. F. A Comparison of CO Oxidation by Hydroxyl and Atomic Oxygen from Water on Low-Coordinated Au Atoms. *ACS Catal.* **2016**, *6*, 7051–7058.
- (570) Saliba, N. A.; Tsai, Y.-L.; Panja, C.; Koel, B. E. Oxidation of Pt(111) by Ozone (O₃) under UHV Conditions. *Surf. Sci.* **1999**, *419*, 79–88.
- (571) Wu, Z.; Jin, Y.; Xu, L.; Yuan, Q.; Xiong, F.; Jiang, Z.; Huang, W. Reactivity of Oxygen Adatoms on Stepped Au(997) Surface toward NO and NO₂. *J. Phys. Chem. C* **2014**, *118*, 8397–8405.
- (572) Liao, M.-S.; Watts, J. D.; Huang, M.-J. Theoretical Comparative Study of Oxygen Adsorption on Neutral and Anionic Ag_n and Au_n Clusters (N = 2–25). *J. Phys. Chem. C* **2014**, *118*, 21911–21927.
- (573) An, H.; Kwon, S.; Ha, H.; Kim, H. Y.; Lee, H. M. Reactive Structural Motifs of Au Nanoclusters for Oxygen Activation and Subsequent CO Oxidation. *J. Phys. Chem. C* **2016**, *120*, 9292–9298.
- (574) Gao, M.; Horita, D.; Ono, Y.; Lyalin, A.; Maeda, S.; Taketsugu, T. Isomerization in Gold Clusters upon O₂ Adsorption. *J. Phys. Chem. C* **2017**, *121*, 2661–2668.
- (575) Zhang, W.; Zhu, J.; Cheng, D. Theoretical Study of CO Catalytic Oxidation on Free and Defective Graphene-Supported Au – Pd Bimetallic Clusters. *RSC Adv.* **2014**, *4*, 42554–42561.
- (576) Ma, W.; Chen, F. CO Oxidation on the Ag-Doped Au Nanoparticles. *Catal. Lett.* **2013**, *143*, 84–92.
- (577) Morishita, T.; Ueno, T.; Panomsuwan, G.; Hieda, J.; Bratescu, M. A.; Saito, N. Differences in Intermediate Structures and Electronic States Associated with Oxygen Adsorption onto Pt, Cu, and Au Clusters as Oxygen Reduction Catalysts. *J. Phys. D: Appl. Phys.* **2016**, *49*, 415305.
- (578) Baishya, S.; Deka, R. C. Catalytic Activities of Au₆, Au₆₋, and Au₆₊ Clusters for CO Oxidation: A Density Functional Study. *Int. J. Quantum Chem.* **2014**, *114*, 1559–1566.
- (579) Gao, Y.; Shao, N.; Pei, Y.; Chen, Z.; Zeng, X. C. Catalytic Activities of Subnanometer Gold Clusters (Au₁₆–Au₁₈, Au₂₀, and Au₂₇–Au₃₅) for CO Oxidation. *ACS Nano* **2011**, *5*, 7818–7829.
- (580) Manzoor, D.; Krishnamurty, S.; Pal, S. Endohedrally Doped Gold Nanocages: Efficient Catalysts for O₂ Activation and CO Oxidation. *Phys. Chem. Chem. Phys.* **2016**, *18*, 7068–7074.
- (581) Li, L.; Gao, Y.; Li, H.; Zhao, Y.; Pei, Y.; Chen, Z.; Zeng, X. C. CO Oxidation on TiO₂ (110) Supported Subnanometer Gold Clusters: Size and Shape Effects. *J. Am. Chem. Soc.* **2013**, *135*, 19336–19346.
- (582) Polynskaya, Y. G.; Pichugina, D. A.; Kuz'menko, N. E. Correlation between Electronic Properties and Reactivity toward Oxygen of Tetrahedral Gold–silver Clusters. *Comput. Theor. Chem.* **2015**, *1055*, 61–67.
- (583) Teng, B. T.; Lang, J. J.; Wen, X. D.; Zhang, C.; Fan, M.; Harris, H. G. O₂ Adsorption and Oxidative Activity on Gold-Based Catalysts with and without a Ceria Support. *J. Phys. Chem. C* **2013**, *117*, 18986–18993.

- (584) Lee, C.-C.; Chen, H.-T. Adsorption and Reaction of C_2H_4 and O_2 on a Nanosized Gold Cluster: A Computational Study. *J. Phys. Chem. A* **2015**, *119*, 8547–8555.
- (585) Staykov, A.; Derekar, D.; Yamamura, K. Oxygen Dissociation on Palladium and Gold Core/shell Nanoparticles. *Int. J. Quantum Chem.* **2016**, *116*, 1486–1492.
- (586) Ohkawa, T.; Kuramoto, K. Theoretical Study of CO and O_2 Adsorption and CO Oxidation on Linear-Shape Gold. *AIP Adv.* **2016**, *6*, 095206.
- (587) Liu, X. J.; Hamilton, I. Adsorption of Small Molecules on Helical Gold Nanorods: A Relativistic Density Functional Study. *J. Comput. Chem.* **2014**, *35*, 1967–1976.
- (588) Gao, Y.; Zeng, X. C. Water-Promoted O_2 Dissociation on Small-Sized Anionic Gold Clusters. *ACS Catal.* **2012**, *2*, 2614–2621.
- (589) Cheng, D.; Xu, H.; Fortunelli, A. Tuning the Catalytic Activity of Au-Pd Nanoalloys in CO Oxidation via Composition. *J. Catal.* **2014**, *314*, 47–55.
- (590) Lee, H. M.; Lee, K. H.; Lee, G.; Kim, K. S. Geometrical and Electronic Characteristics of Au_nO_{2-} ($n = 2–7$). *J. Phys. Chem. C* **2015**, *119*, 14383–14391.
- (591) Staykov, A.; Nishimi, T.; Yoshizawa, K.; Ishihara, T. Oxygen Activation on Nanometer-Size Gold Nanoparticles. *J. Phys. Chem. C* **2012**, *116*, 15992–16000.
- (592) Okumura, M.; Kitagawa, Y.; Haruta, M.; Yamaguchi, K. DFT Studies of Interaction between O_2 and Au Clusters. The Role of Anionic Surface Au Atoms on Au Clusters for Catalyzed Oxygenation. *Chem. Phys. Lett.* **2001**, *346*, 163–168.
- (593) Mills, G.; Gordon, M. S.; Metiu, H. The Adsorption of Molecular Oxygen on Neutral and Negative Au_n Clusters ($n = 2–5$). *Chem. Phys. Lett.* **2002**, *359*, 493–499.
- (594) Amft, M.; Johansson, B.; Skorodumova, N. Influence of the Cluster Dimensionality on the Binding Behavior of CO and O_2 on Au_{13} . *J. Chem. Phys.* **2012**, *136*, 024312.
- (595) Chen, H.-T.; Chang, J.-G.; Ju, S.-P.; Chen, H.-L. First-Principle Calculations on CO Oxidation Catalyzed by a Gold Nanoparticle. *J. Comput. Chem.* **2009**, *31*, 258–265.
- (596) Li, H. J.; Ho, J. J. Theoretical Calculations on the Oxidation of CO on $Au_{55}Ag_{13}Au_{42}$, $Au_{13}Ag_{42}$, and Ag_{55} Clusters of Nanometer Size. *J. Phys. Chem. C* **2012**, *116*, 13196–13201.
- (597) Davran-Candan, T.; Aksoylu, A. E.; Yildirim, R. Reaction Pathway Analysis for CO Oxidation over Anionic Gold Hexamers Using DFT. *J. Mol. Catal. A: Chem.* **2009**, *306*, 118–122.
- (598) Wells, B. A.; Chaffee, A. L. Gas Binding to Au_{13} , $Au_{12}Pd$, and $Au_{11}Pd_2$ Nanoclusters in the Context of Catalytic Oxidation and Reduction Reactions. *J. Chem. Phys.* **2008**, *129*, 164712.
- (599) Roldán, A.; Ricart, J. M.; Illas, F.; Pachioni, G. O_2 Adsorption and Dissociation on Neutral, Positively and Negatively Charged Au_n ($n = 5–79$) Clusters. *Phys. Chem. Chem. Phys.* **2010**, *12*, 10723–10729.
- (600) Lyalin, A.; Taketsugu, T. Reactant-Promoted Oxygen Dissociation on Gold Clusters. *J. Phys. Chem. Lett.* **2010**, *1*, 1752–1757.
- (601) Howard, K. L.; Willock, D. J. A Periodic DFT Study of the Activation of O_2 by Au Nanoparticles on $\alpha\text{-Fe}_2\text{O}_3$. *Faraday Discuss.* **2011**, *152*, 135–151.
- (602) Roldán, A.; Ricart, J. M.; Illas, F.; Pachioni, G. O_2 Activation by Au_n Clusters Stabilized on Clean and Electron-Rich MgO Stepped Surfaces. *J. Phys. Chem. C* **2010**, *114*, 16973–16978.
- (603) Ding, X.-L.; Liao, H.-L.; Zhang, Y.; Chen, Y.-M.; Wang, D.; Wang, Y.-Y.; Zhang, H.-Y. Geometric and Electronic Properties of Gold Clusters Doped with a Single Oxygen Atom. *Phys. Chem. Chem. Phys.* **2016**, *18*, 28960–28972.
- (604) Golibrzuch, K.; Bartels, N.; Auerbach, D. J.; Wodtke, A. M. The Dynamics of Molecular Interactions and Chemical Reactions at Metal Surfaces: Testing the Foundations of Theory. *Annu. Rev. Phys. Chem.* **2015**, *66*, 399–425.
- (605) Díaz, C.; Martín, F. Using Molecular Reflectivity to Explore Reaction Dynamics at Metal Surfaces. In *Dynamics of Gas-Surface Interactions: Atomic-level Understanding of Scattering Processes at Surfaces*; Díez Muñoz, R., Busnengo, H. F., Eds.; Springer: Berlin, 2013; pp 75–100.
- (606) Gross, A.; Wilke, S.; Scheffler, M. Six-Dimensional Quantum Dynamics of Adsorption and Desorption of H_2 at Pd(100): Steering and Steric Effects. *Phys. Rev. Lett.* **1995**, *75*, 2718–2721.
- (607) Valentini, P.; Schwartzenbauer, T. E.; Cozmuta, I. Molecular Dynamics Simulation of O_2 Sticking on Pt(111) Using the Ab Initio Based ReaxFF Reactive Force Field. *J. Chem. Phys.* **2010**, *133*, 084703.
- (608) Evans, J. W.; Liu, D. J. Statistical Mechanical Models for Dissociative Adsorption of O_2 on metal(100) Surfaces with Blocking, Steering, and Funneling. *J. Chem. Phys.* **2014**, *140*, 205406.
- (609) Jaatinen, S.; Blomqvist, J.; Salo, P.; Puisto, A.; Alatalo, M.; Hirsimäki, M.; Ahonen, M.; Valden, M. Adsorption and Diffusion Dynamics of Atomic and Molecular Oxygen on Reconstructed Cu(100). *Phys. Rev. B: Condens. Matter Mater. Phys.* **2007**, *75*, 075402.
- (610) Shimizu, K.; Agerico Diño, W.; Kasai, H. Rotational Effects on the Dissociative Adsorption and Abstraction Dynamics of O_2 /Al(111). *J. Phys. Soc. Jpn.* **2013**, *82*, 113602.
- (611) Groß, A.; Eichler, A.; Hafner, J.; Mehl, M. J.; Papaconstantopoulos, D. A Unified Picture of the Molecular Adsorption Process: $O_2/Pt(111)$. *Surf. Sci.* **2003**, *539*, L542–L548.
- (612) Moritani, K.; Tsuda, M.; Teraoka, Y.; Okada, M.; Yoshigoe, A.; Fukuyama, T.; Kasai, T.; Kasai, H. Effects of Vibrational and Rotational Excitations on the Dissociative Adsorption of O_2 on Cu Surfaces. *J. Phys. Chem. C* **2007**, *111*, 9961–9967.
- (613) Hall, J.; Saksager, O.; Chorkendorff, I. Dissociative Chemisorption of O_2 on Cu(100). Effects of Mechanical Energy Transfer and Recoil. *Chem. Phys. Lett.* **1993**, *216*, 413–417.
- (614) Harvey, J. N. Understanding the Kinetics of Spin-Forbidden Chemical Reactions. *Phys. Chem. Chem. Phys.* **2007**, *9*, 331–343.
- (615) Goodrow, A.; Bell, A. T.; Head-Gordon, M. Are Spin-Forbidden Crossings Bottleneck in Methanol Oxidation? *J. Phys. Chem. C* **2009**, *113*, 19361–19364.
- (616) Österlund, L.; Zoric-acute, I.; Kasemo, B. Dissociative Sticking of O_2 on Al(111). *Phys. Rev. B: Condens. Matter Mater. Phys.* **1997**, *55*, 15452–15455.
- (617) Behler, J.; Delley, B.; Lorenz, S.; Reuter, K.; Scheffler, M. Dissociation of O_2 at Al(111): The Role of Spin Selection Rules. *Phys. Rev. Lett.* **2005**, *94*, 036104.
- (618) Behler, J.; Reuter, K.; Scheffler, M. Nonadiabatic Effects in the Dissociation of Oxygen Molecules at the Al(111) Surface. *Phys. Rev. B: Condens. Matter Mater. Phys.* **2008**, *77*, 115421.
- (619) Hellman, A. Nonadiabaticity in the Initial Oxidation of Mg(0001): First-Principles Density-Functional Calculations. *Phys. Rev. B: Condens. Matter Mater. Phys.* **2005**, *72*, 201403.
- (620) Carbogno, C.; Behler, J.; Reuter, K.; Groß, A. Signatures of Nonadiabatic O_2 Dissociation at Al(111): First-Principles Fewest-Switches Study. *Phys. Rev. B: Condens. Matter Mater. Phys.* **2010**, *81*, 35410.
- (621) Katz, G.; Kosloff, R.; Zeiri, Y. Abstractive Dissociation of Oxygen over Al(111): A Nonadiabatic Quantum Model. *J. Chem. Phys.* **2004**, *120*, 3931–3948.
- (622) Kurahashi, M.; Yamauchi, Y. Steric Effect in O_2 Sticking on Al(111): Preference for Parallel Geometry. *Phys. Rev. Lett.* **2013**, *110*, 246102.
- (623) Kurahashi, M. Oxygen Adsorption on Surfaces Studied by a Spin- and Alignment-Controlled O_2 Beam. *Prog. Surf. Sci.* **2016**, *91*, 29–55.
- (624) Libisch, F.; Huang, C.; Liao, P.; Pavone, M.; Carter, E. A. Origin of the Energy Barrier to Chemical Reactions of O_2 on Al(111): Evidence for Charge Transfer, Not Spin Selection. *Phys. Rev. Lett.* **2012**, *109*, 198303.
- (625) Carbogno, C.; Behler, J.; Groß, A.; Reuter, K. Fingerprints for Spin-Selection Rules in the Interaction Dynamics of O_2 at Al(111). *Phys. Rev. Lett.* **2008**, *101*, 096104.
- (626) Escaño, M. C. S.; Kasai, H. A Novel Mechanism of Spin-Orientation Dependence of O_2 Reactivity from First Principles Methods. *Catal. Sci. Technol.* **2017**, *7*, 1040–1044.

- (627) Wintterlin, J.; Schuster, R.; Ertl, G. Existence of a “Hot” Atom Mechanism for the Dissociation of O₂ on Pt(111). *Phys. Rev. Lett.* **1996**, *77*, 123–126.
- (628) Sendner, C.; Gross, A. Kinetic Monte Carlo Simulations of the Interaction of Oxygen with Pt(111). *J. Chem. Phys.* **2007**, *127*, 014704.
- (629) Meyer, J.; Reuter, K. Modeling Heat Dissipation at the Nanoscale: An Embedding Approach for Chemical Reaction Dynamics on Metal Surfaces. *Angew. Chem., Int. Ed.* **2014**, *53*, 4721–4724.
- (630) Lukas, V. J.; Reuter, K. Hot Adatom Diffusion Following Oxygen Dissociation on Pd(100) and Pd(111): A First-Principles Study of the Equilibration Dynamics of Exothermic Surface Reactions. *Phys. Rev. Lett.* **2016**, *117*, 146101.
- (631) Farber, R. G.; Turano, M. E.; Oskorep, E. C. N.; Wands, N. T.; Juurlink, L. B. F.; Killelea, D. R. Exposure of Pt(5 5 3) and Rh(1 1 1) to Atomic and Molecular Oxygen: Do Defects Enhance Subsurface Oxygen Formation? *J. Phys.: Condens. Matter* **2017**, *29*, 164002.
- (632) Rettner, C. T.; Mullins, C. B. Dynamics of the Chemisorption of O₂ on Pt(111): Dissociation via Direct Population of a Molecularly Chemisorbed Precursor at High Incidence Kinetic Energy. *J. Chem. Phys.* **1991**, *94*, 1626–1635.
- (633) Yeo, Y. Y.; Vattuone, L.; King, D. A. Calorimetric Heats for CO and Oxygen Adsorption and for the Catalytic CO Oxidation Reaction on Pt{111}. *J. Chem. Phys.* **1997**, *106*, 392–401.
- (634) Bradley, J. M.; Guo, X.-C.; Hopkinson, A.; King, D. A. A Molecular Beam Investigation into the Dynamics and Kinetics of Dissociative O₂ Adsorption on Pt{100}-(1 × 1). *J. Chem. Phys.* **1996**, *104*, 4283.
- (635) Wartnaby, C. E.; Stuck, A.; Yeo, Y. Y.; King, D. A. Microcalorimetric Heats of Adsorption for CO, NO, and Oxygen on Pt{110}. *J. Phys. Chem.* **1996**, *100*, 12483–12488.
- (636) Klötzer, B.; Hayek, K.; Konvicka, C.; Lundgren, E.; Varga, P. Oxygen-Induced Surface Phase Transformation of Pd(111): Sticking, Adsorption and Desorption Kinetics. *Surf. Sci.* **2001**, *482–485*, 237–242.
- (637) Leisenberger, F. P.; Koller, G.; Sock, M.; Surnev, S.; Ramsey, M. G.; Netzer, F. P.; Klötzer, B.; Hayek, K. Surface and Subsurface Oxygen on Pd(111). *Surf. Sci.* **2000**, *445*, 380–393.
- (638) Zheng, G.; Altman, E. I. The Oxidation of Pd(111). *Surf. Sci.* **2000**, *462*, 151–168.
- (639) Takahashi, S.; Fujimoto, Y.; Teraoka, Y.; Yoshigoe, A.; Aruga, T. vibrationally Assisted Dissociative Adsorption of Oxygen on Ru(0001). *Chem. Phys. Lett.* **2006**, *433*, 58–61.
- (640) Takahashi, S.; Fujimoto, Y.; Teraoka, Y.; Yoshigoe, A.; Okuyama, H.; Aruga, T. vibrationally-Assisted Dissociative Adsorption of Oxygen on Ru(0001)-p(2 × 1)-O. *Surf. Sci.* **2007**, *601*, 3809–3812.
- (641) Vattuone, L.; Rocca, M.; Boragno, C.; Valbusa, U. Coverage Dependence of Sticking Coefficient of O₂ on Ag(110). *J. Chem. Phys.* **1994**, *101*, 726.
- (642) Wang, Q.-G.; Shang, J.-X. Effects of O Atom Coverage on the Dissociation of O₂ Molecules on the Nb (110) Surface. *Acta Phys. Chim. Sin.* **2013**, *29*, 365–370.
- (643) Valentini, P.; Schwartzenruber, T. E.; Cozmuta, I. ReaxFF Grand Canonical Monte Carlo Simulation of Adsorption and Dissociation of Oxygen on Platinum (111). *Surf. Sci.* **2011**, *605*, 1941–1950.
- (644) Liu, D. J.; Evans, J. W. Interactions between Oxygen Atoms on Pt(100): Implications for Ordering during Chemisorption and Catalysis. *ChemPhysChem* **2010**, *11*, 2174–2181.
- (645) Liu, K.; Chen, T.; He, S.; Robbins, J. P.; Podkolzin, S. G.; Tian, F. Observation and Identification of an Atomic Oxygen Structure on Catalytic Gold Nanoparticles. *Angew. Chem.* **2017**, *129*, 13132–13137.
- (646) Hoppe, S.; Li, Y.; Moskaleva, L. V.; Müller, S. How Silver Segregation Stabilizes 1D Surface Gold Oxide: A Cluster Expansion Study Combined with Ab Initio MD Simulations. *Phys. Chem. Chem. Phys.* **2017**, *19*, 14845–14853.
- (647) Sun, K.; Kohyama, M.; Tanaka, S.; Takeda, S. Theoretical Study of Atomic Oxygen on Gold Surface by Hückel Theory and DFT Calculations. *J. Phys. Chem. A* **2012**, *116*, 9568–9573.
- (648) Zambelli, T.; Barth, J. V.; Wintterlin, J.; Ertl, G. Complex Pathways in Dissociative Adsorption of Oxygen on Platinum. *Nature* **1997**, *390*, 495–497.
- (649) Fajin, J. L. C.; Cordeiro, M. N. D. S.; Gomes, J. R. B. DFT Study of the Au(321) Surface Reconstruction by Consecutive Deposition of Oxygen Atoms. *Surf. Sci.* **2008**, *602*, 424–435.
- (650) Min, B. K.; Deng, X.; Pinnaduwage, D.; Schalek, R.; Friend, C. M. Oxygen-Induced Restructuring with Release of Gold Atoms from Au(111). *Phys. Rev. B: Condens. Matter Mater. Phys.* **2005**, *72*, 121410.
- (651) Deng, X.; Min, B. K.; Guloy, A.; Friend, C. M. Enhancement of O₂ Dissociation on Au(111) by Adsorbed Oxygen: Implications for Oxidation Catalysis. *J. Am. Chem. Soc.* **2005**, *127*, 9267–9270.
- (652) Lytken, O.; Lew, W.; Campbell, C. T. Catalytic Reaction Energetics by Single Crystal Adsorption Calorimetry: Hydrocarbons on Pt(111). *Chem. Soc. Rev.* **2008**, *37*, 2172–2179.
- (653) Parker, D.; Bartram, M.; Koel, B. Study of High Coverages of Atomic Oxygen on the Pt (111) Surface. *Surf. Sci.* **1989**, *217*, 489–510.